Final Report

FDOT Contract No.: BDV24-977-24

DEVELOPMENT OF STATISTICAL MODELS TO PREDICT THE COMPRESSIBILITY OF FLORIDA'S SOILS

Prepared by:

Boo Hyun Nam, Ph.D. (Principal Investigator)

Ryan Shamet, M.S.

Yong Je Kim, M.S.

Petros Xanthopoulos, Ph.D.

Orestis Panagopoulos, Ph.D.

Department of Civil, Environmental and Construction Engineering

University of Central Florida

12800 Pegasus Drive, 442B, Engineering II

Orlando, FL 32816

Developed for the

FDOT Florida Department of **TRANSPORTATION**

Project Manager: David Horhota, P.E., Ph.D.

October 2019

DISCLAIMER

The opinions, findings, and conclusions expressed in this publication are those of the authors and not necessarily those of the Florida Department of Transportation or the U.S. Department of Transportation.

SI (MODERN METRIC) CONVERSION FACTORS (from FHWA)

Approximate Conversions to SI Units

Symbol	When You Know	Multiply By	To Find	Symbol
Length				
in	inches	25.4	millimeters	mm
ft	feet	0.305	meters	m
yd	yards	0.914	meters	m
mi	miles	1.61	kilometers	km
Area				
in^2	square inches	645.2	square millimeters	mm^2
ft^2	square feet	0.093	square meters	m^2
yd^2	square yard	0.836	square meters	m^2
ac	acres	0.405	hectares	ha
mi^2	square miles	2.59	square kilometers	km^2
Volume				
fl oz	fluid ounces	29.57	milliliters	mL
gal	gallons	3.785	liters	L
ft^3	cubic feet	0.028	cubic meters	m^3
yd^3	cubic yards	0.765	cubic meters	m^3
NOTE: volumes greater than 1000 L shall be shown in m^3				
Mass				
oz	ounces	28.35	grams	g
lb	pounds	0.454	kilograms	kg
T	short tons (2000 lb)	0.907	megagrams (or "metric ton")	Mg (or "t")
Temperature (exact degrees)				
°F	Fahrenheit	5 (F-32)/9 or (F-32)/1.8	Celsius	°C
Illumination				
fc	foot-candles	10.76	lux	lx
fl	foot-Lamberts	3.426	candela/m^2	cd/m^2
Force and Pressure or Stress				
lbf	poundforce	4.45	newtons	N
lbf/in^2	poundforce per square inch	6.89	kilopascals	kPa

Approximate Conversions from SI Units

Symbol	When You Know	Multiply By	To Find	Symbol
Length				
mm	millimeters	0.039	inches	in
m	meters	3.28	feet	ft
m	meters	1.09	yards	yd
km	kilometers	0.621	miles	mi
Area				
mm^2	square millimeters	0.0016	square inches	in^2
m^2	square meters	10.764	square feet	ft^2
m^2	square meters	1.195	square yards	yd^2
ha	hectares	2.47	acres	ac
km^2	square kilometers	0.386	square miles	mi^2
Volume				
mL	milliliters	0.034	fluid ounces	fl oz
L	liters	0.264	gallons	gal
m^3	cubic meters	35.314	cubic feet	ft^3
m^3	cubic meters	1.307	cubic yards	yd^3
Mass				
g	grams	0.035	ounces	oz
kg	kilograms	2.202	pounds	lb
Mg (or "t")	megagrams (or "metric ton")	1.103	short tons (2000 lb)	T
Temperature (exact degrees)				
°C	Celsius	1.8C+32	Fahrenheit	°F
Illumination				
lx	lux	0.0929	foot-candles	fc
cd/m^2	candela/m^2	0.2919	foot-Lamberts	fl
Force and Pressure or Stress				
N	newtons	02.225	poundforce	lbf
kPa	kilopascals	0.145	poundforce per square inch	lbf/in^2

* SI is the symbol for the International System of Units. Appropriate rounding should be made to comply with Section 4 of ASTM E380. (Revised March 2003)

TECHNICAL REPORT DOCUMENTATION PAGE

1. Report No.	2. Government Accession No.	3. Recipient's Catalog No.

4. Title and Subtitle	5. Report Date
Development of Statistical Models to Predict the Compressibility of Florida's Soils	September, 2019
	6. Performing Organization Code

7. Author(s)	8. Performing Organization Report No.
Boo Hyun Nam, Ryan Shamet, Yong Je Kim, Petros Xanthopoulos, and Orestis Panagopoulos	

9. Performing Organization Name and Address	10. Work Unit No. (TRAIS)
University of Central Florida 4000 Central Florida Blvd. Orlando, FL 32816-2450	
	11. Contract or Grant No.
	BDV24-977-24

12. Sponsoring Agency Name and Address	13. Type of Report and Period Covered
	$3/30/201 - 10/31/2019$
	14. Sponsoring Agency Code

15. Supplementary Notes

Dr. David Horhota of the State Materials Office at the Florida Department of Transportation served as the project manager for this project.

16. Abstract

The magnitude of the overall settlement depends on several variables such as compression index (C_c), recompression index (C_r), and secondary compression index (C_α), which are determined by a consolidation test. However, the test is time consuming and labor intensive. Correlations have been developed to approximate these compressibility indexes to supplement but not eliminate a geotechnical sampling and testing program. In this study, a data-driven approach has been employed to estimate C_c, C_r, C_α, and coefficient of consolidation (C_v). In this project, a support vector machine (SVM) classification technique was used to determine the number of distinct models to be developed. The statistical models were then constructed through a forward-selection stepwise regression procedure. Eight variables were used, and these variables included the moisture content, automatic hammer standard penetration test (SPT) blow count, overburden stress, fines content (-200), liquid limit, percent organic content, plasticity index, and specific gravity. The best performing statistical models of soil compressibility were constructed for the classified soil types. In addition, reduced models that minimize the number of variables were constructed for more practical usage. It is recommended that only the models with $R^2 > 0.5$ be used for engineering analysis. Lastly, the correlation between soil compressibility between CPT tip resistance (q_c) was checked. There is a general trend that C_c and C_r decrease as q_c increases; however, the correlation is not strong due to the limited dataset. Data collected under a controlled environment will be able to improve the correlation quality.

17. Key Word	18. Distribution Statement
Soil compressibility, Compression index (C_c), Recompression index (C_r), Support Vector Machine, and Cone Penetration Test(CPT)	

19. Security Classif. (of this report)	20. Security Classif. (of this page)	21. No. of Pages	22. Price
		120	

Form DOT F 1700.7 (8-72)   Reproduction of completed page authorized

ACKNOWLEDGEMENTS

EXECUTIVE SUMMARY

The settlement of soil is directly related to the compressibility of soil and is commonly defined by the compression index (C_c) and recompression index (C_r). However, consolidation testing for the C_c, C_r, C_v (coefficient of consolidation), and C_α (secondary compression index) is time consuming and there might be significant variability throughout a project site. There are two ways to determine soil compressibility: (1) direct measurement via lab test and (2) correlation to other soil data determined from lab tests. Many times, before confirming soil compressibility via laboratory testing, prediction models based on correlation analysis are useful for preliminary design and may also help to assess the variability of the site conditions. In addition, using those prediction models helps to select where the actual test samples should be obtained, which can help optimize the undisturbed sampling and performance-based testing.

The main goal of this project was to provide the best performing statistical models that predict the compressibility of Florida's soils. Three specific project objectives included: (1) to identify statistically significant affecting variables on soil compressibility (e.g., C_c and C_r), (2) to identify the most accurate prediction model of soil compressibility among existing correlations (from statistical analyses) for Florida's soils, and (3) to develop the best performing statistical models to predict soil compressibility (C_c, C_r, C_v, and C_α) for Florida's soils.

In order to achieve the objectives above, the following main work tasks were performed. It is important to note that data were collected throughout the state of Florida, but most data are from the Central Florida region. First, all existing models to predict C_c, C_r, C_v, and C_α were identified through a comprehensive literature review. Second, those identified models were evaluated with respect to their accuracy. The accuracy of the models was compared in terms of key goodness-of-fit characteristics, such as coefficient of determination (R^2) and root mean square error (RMSE). Third, the correlation between key index parameters and soil compressibility were evaluated. The key index parameters that were used include: effective overburden pressure in kips/ft^2 (ksf), wet density in lb/ft^3(pcf), dry density (pcf), natural moisture (w) (%), automatic hammer blow count, fines (-200) (%), liquid limit (LL), plasticity index (PI), initial void ratio (e_o), and specific gravity. The variables were ranked, and the top three variables (both positive and negative) were identified. Fourth, statistical prediction models for Florida's soils were constructed through a machine learning technique. The construction procedure involves the steps of data imputation, preprocessing, classification, and model development. The best performing statistical models were constructed for the following classified soil types: high plasticity clay (CH), low plasticity clay (CL), high plasticity silt (MH), high plasticity organic (OH), low plasticity organic (OL), and peat (Pt). However, due to limited data, the C_v and C_α models are available only for clay, organic, and peat. Lastly, the correlation of CPT data and soil compressibility was investigated.

Among existing correlations, in general, the C_r models seem more accurate than the C_c models for Florida's data. For C_c, Al-Khafaji and Andersland's model (1992), which is a function of e_o and LL, exhibited the highest accuracy. For C_r, the model proposed by Azzouz et al. (1976), which is a function of w, appears to be the best model. The results of the classification analysis indicated that the assumed soil classes are valid for C_c and C_r models. The C_c and C_r models for each soil type was constructed. All models exhibited higher accuracy associated with R^2 and RMSE when compared with the existing correlations. In addition, reduced models that minimize the number of variables without sacrificing the model accuracy were checked and constructed.

For the correlation between CPT tip resistance (q_c) and C_c or C_r, the general trend is that C_c and C_r decreases as CPT q_c increases, but there is no strong correlation. This is mainly due to the limited dataset. In addition, the matching of CPT and C_c or C_r was extremely difficult because of different times and locations of testing between the CPT and sampling for lab consolidation test.

TABLE OF CONTENTS

LIST OF FIGURES

LIST OF TABLES

LIST OF ABBREVIATIONS

CPT   -   Cone Penetration Test

CPTu   -   Piezocone Penetration Test

FDOT   -   Florida Department of Transportation

FHWA   -   Federal Highway Administration

LI   -   Liquidity Index

LL   -   Liquid Limit

PL   -   Plastic Limit

PI   -   Plasticity Index

SI   -   Shrinkage Index

SVM   -   Support Vector Machine

SPT   -   Standard Penetration Test

TSF   -   Tons per square foot ($2{,}000 \text{ lb/ft}^2$)

USGS   -   United States Geological Survey

USCS   -   Unified Soil Classification System

1. INTRODUCTION

1.1. Problem Statement

Soil settlement is directly related to the compressibility of soil. Hence, as compression index (C_c) and recompression index (C_r) increases, so does settlement. However, consolidation testing for the C_c, C_r, and C_v (coefficient of consolidation) is time consuming and there might be significant variability throughout a project site. On the other hand, the magnitude of primary soil settlement is dictated by a handful of variables (e.g., magnitude of loading, initial void ratio, thickness of soil layer, etc.), and most of these are relatively easy to obtain. Hence, there are two ways to determine C_c, C_r, and C_v: (1) direct measurement via lab test and (2) correlation to other soil data determined from lab tests. Many times, before confirming soil compressibility via laboratory testing, prediction models based on correlation analysis may be useful for preliminary design and may also help to assess the variability of the site conditions. In addition, using those prediction models help to select where the actual test samples should be obtained, which can help optimize the undisturbed sampling and performance-based testing.

There have been many studies on development of prediction models of soil compressibility such as C_c, C_r, and C_v. International, national, and state agencies (e.g., Federal Highway Admiration (FHWA) and state departments of transportation (DOTs)) may have their own recommendation; however, those models may not be accurate enough for Florida's soil conditions because the models are constructed based on local soils, and most existing models are based on a simple linear regression model. In addition, the level of uncertainty of the predicted C_c, C_r, and C_v is not available for the existing models.

1.2. Project Objectives

The goal of this study is to identify and develop the best statistical models that predict the compressibility of Florida's soils; thus, the models can be used as a preliminary design means and help to assess the variability of the site conditions prior to the collection of undisturbed samples and consolidation lab testing. The specific research objectives are as follows:

- To identify factors significantly affecting C_c and C_r and to evaluate their correlations,

- To identify the most accurate existing models of soil compressibility (from statistical analyses) for Florida's soils,

- To develop the best statistical models to predict C_c, C_r, C_v, and C_α for Florida's soils:
    - Using current state-of-the-art statistical techniques.
    - Developing models for specific soil types.

- To find a correlation between soil compressibility and Cone Penetration Test (CPT) data.

1.3. Project Description

To achieve the project objectives, the following main work tasks were performed. It is important to note that data were collected throughout the state of Florida but most data are from the central Florida region.

1) All existing models to predict C_c, C_r, C_v, and C_α were identified through a comprehensive literature review.

2) Those identified models were evaluated with respect to their accuracy. The accuracy of the models was compared in terms of key goodness-of-fit characteristics such as coefficient of determination (R^2) and root mean square error (RMSE).

3) The correlation between key index parameters and soil compressibility were evaluated. The key index parameters that were used include: effective overburden pressure in kips/ft^2 (ksf), wet density in lb/ft^3 (pcf), dry density (pcf), natural moisture (%), automatic hammer blow count, fines (-200) (%), liquid limit (LL), plasticity index (PI), initial void ratio (e), and specific gravity. The variables were ranked and the top three variables (both positive and negative) were identified.

4) Statistical prediction models for Florida's soils were constructed through a machine learning technique, with a support vector machine (SVM) classification and multi-variable regression. The construction procedure involves the steps of data imputation, preprocessing, classification, and model development. The best performing statistical models were constructed for the classified soil types: CH, CL, MH, OH, OL, and Pt. Due to limited data, the C_v and C_α models are available only for clay, organic, and peat.

5) The correlation of CPT data and soil compressibility was investigated.

1.4. Background

1.4.1. Consolidation Theory and Test

According to the widely accepted theory of 1-D consolidation (Terzaghi, 1925), dissipation of excess pore water pressure within a granular porous medium will result in a decrease in volume. For the case of soil, the volume change will result in a vertical settlement, identified as consolidation. Through the development and implementation of the consolidation test (or oedometer), Terzaghi determined that the consolidation of a soil specimen can be quickly characterized by two slopes from a e-logσ' plot; where σ' is the applied effective vertical stress to the sample, and e is the resulting void ratio of the sample. Shown in Figure 1-1, the resulting slopes of the virgin consolidation line and the laboratory rebound curve are taken as the compression index (C_c) and recompression index (C_r), respectively.
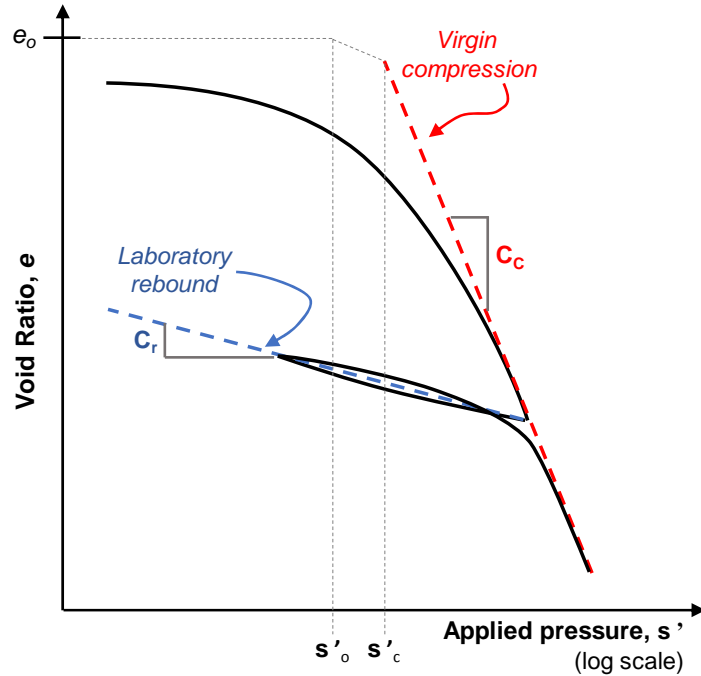
Figure 1-1. Typical consolidation curve of an over-consolidated clay

The compression indexes, C_c and C_r, can be measured via a consolidation test. The schematic diagram of oedometer is shown in Figure 1-2. A consolidation test consists of one-dimensional compression where lateral movement and strains are restricted. The undisturbed sample of soil is prepared and loaded into a confining apparatus, called an oedometer, such that soil strain and water flow are restricted to the vertical direction (Das, 2002).
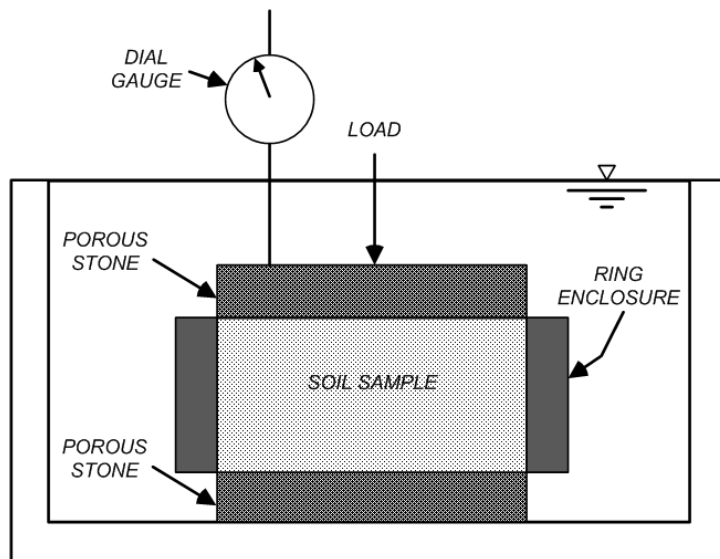
Figure 1-2. Schematic design of an oedometer

The soil sample is then subjected to a series of incremental loads with the resulting deformations recorded with time. In a typical consolidation test, the incremental loads are applied at 24-hour intervals and will have a magnitude of twice the previously applied load. Deformation readings are usually noted throughout the 24-hour loading period at times such that the interval between readings approximately doubles (Das, 2002). A commonly used deformation reading schedule is 2, 4, 8, and 24 hours after the application of the load.

As soils encountered in the field have a tendency to be over-consolidated, where the soil has experienced a higher stress in its history than what is currently being experienced, a common practice in a consolidation test is to run an unload-reload cycle. This will capture the behavior of the soil as the subjected stress is reduced and the sample is allowed to recover. Unloading intervals are taken at decreasing installments similar to loading intervals, such that the next interval will be decreased by half of the existing loading. Since each loading and unloading cycle takes 24 hours, a typical consolidation test will have approximately a two-week duration.

Consolidation test results are generally plotted in a graph that illustrates the sample's compressive behavior throughout the loading sequence. As the sample gets loaded, the air voids will slowly decrease, and water will escape. The graph is typically plotted showing the variation of the void ratio (e) with the corresponding changes in applied pressure, in kips per square foot, on a semilogarithmic graph in which void ratio is plotted on the arithmetic scale and pressure on the log scale.

Upon conclusion of the consolidation test, the engineer will usually note the compression indexes (C_c and C_r) and other descriptors of the sample such as the liquid and plastic limit of the soil, dry or moist density, moisture content, initial and final void ratios, USCS classification, location of undisturbed sample extraction (boring number and depth), sample description, and the maximum past pressure, σ'_c, that the soil has experienced.

The maximum past stress, σ'_c, also commonly referred to as the preconsolidation pressure, P_c, is normally interpreted from the void ratio-to-pressure relationship. Consolidation tests performed on samples taken from the field generally show a change in slope at the preconsolidation pressure (Sabatini, Bachus, Mayne, Schneider, & T.E., 2002). Sampling disturbance will usually lower the overall e-log(σ) curve relative to that of actual field conditions in the soil's natural state. As a result, the preconsolidation pressure is often underestimated from a routine testing. The Casagrande Method is used to reconstruct the e-log(σ) field curve to account for any disturbance during sample extraction from its natural state and during preparation for testing (Sabatini et al., 2002).

There are four primary steps to determining this value from the consolidation test results. They are as follows (NAVFAC, 1982):
1. Select the point of maximum curvature,
2. Draw a tangent line at the point of maximum curvature defined in Step 1,
3. Draw a horizontal line at the point of maximum curvature defined in Step 1,
4. Bisect the lines drawn in Steps 2 and 3,
5. Draw an extension of the line virgin compression zone.

The point of intersection between the bisector line in Step 4 and the extension line constructed, in Step 5, is the preconsolidation pressure, as noted in the Figure 1-3.
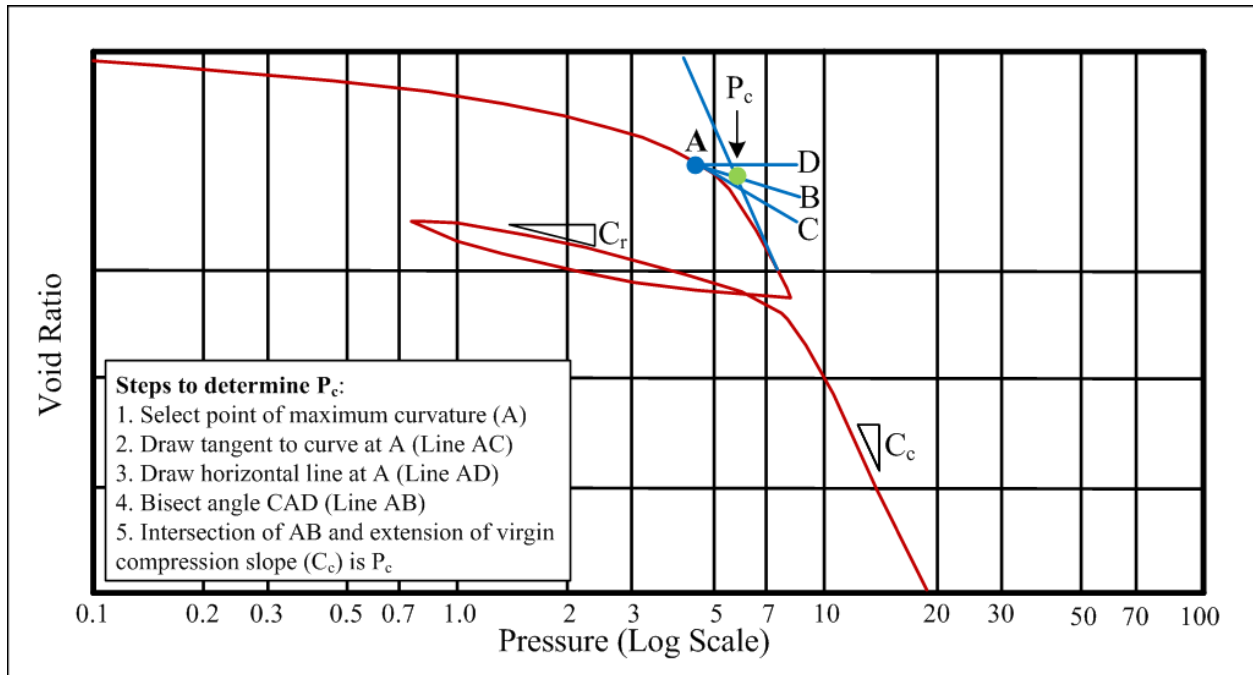
Figure 1-3. Determination of maximum past stress (Source: NAVFAC, 1982)

The compression indexes (C_c and C_r) can be determined from the slopes of various portions of the e-log(σ) curve. The Compression Index, C_c, is approximated as the slope of the e-log(σ) curve in the normally consolidated range. This is the behavior the soil exhibits when it's loaded to a stress beyond what it has been subjected to in its history. The Recompression Index, C_r, is computed as the slope of the curve in which the soil was unloaded and reloaded. This portion of the curve captures the behavior when a loading has been removed from the soil and then subsequently reloaded. This mimics field conditions when new construction with various loading conditions are applied to a previously loaded soil.

As can be seen in the settlement equations, the magnitude of the overall settlement depends on several variables such as the Compression Index, C_c, and Recompression Index, C_r. Due to the large amount of uncertainty for these parameters, engineers normally measure it directly via a consolidation test. This test is time consuming and can be relatively expensive. For this reason, correlations have been developed to approximate these compressibility indexes for preliminary design.

1.4.2. Settlement Prediction with Consolidation Theory

The magnitude of settlement is dependent on the soil's stress state, which can be either normally consolidated (NC) or over-consolidated (OC). Normally consolidated soils have never experienced a higher stress than the present stress; thus, are referred as "virgin" soils in their natural state. Over-consolidated soils have experienced a higher stress in the past than the present stress (Hough, 1957). The settlement of NC soils can be determined from Equation (1.1) and the settlement for OC soils can be determined from Equations (1.2) and (1.3) (Das, 2002).

$$S_c = \frac{C_c\ H_c}{1+e_o} \log\left(\frac{\sigma'_o + \Delta\sigma'}{\sigma'_o}\right) \tag{1.1}$$

Where S_c = settlement caused from the loading condition, C_c = compression index in the soil layer of interest, H_c = thickness of the soil layer of interest, e_o = initial void ratio in the soil layer of interest, σ'_o = initial vertical effective stress at the midpoint of the soil layer of interest, $\Delta\sigma'$ = change in vertical stress due to loading.

If a soil is over-consolidated, the computed settlement can be determined from one of two cases. If the initial stress, plus the change in stress from the loading, is less than the maximum past stress (σ'_c), the following settlement equation applies:

$$S_c = \frac{C_r\ H_c}{1+e_o} \log\left(\frac{\sigma'_o + \Delta\sigma'}{\sigma'_o}\right) \tag{1.2}$$

Where C_r = recompression index in the soil layer of interest.

If the initial stress, plus the change in stress from the loading, is greater than the maximum past stress (σ'_c), the following settlement equation applies:

$$S_c = \frac{C_r\ H_c}{1+e_o} \log\left(\frac{\sigma'_c}{\sigma'_o}\right) + \frac{C_c\ H_c}{1+e_o} \log\left(\frac{\sigma'_o + \Delta\sigma'}{\sigma'_c}\right) \tag{1.3}$$

For this study, the stress change in the settlement analysis will come in the form of a surcharge. The encountered stress change of the soil layer will be determined by the depth and spatial geometry in relation to the embankment surcharge dimensions (Das, 2002) and governed by the following equation:

$$\Delta\sigma = \frac{q_o}{\pi} * \left[\frac{B_1+B_2}{B_2} * (\alpha_1 + \alpha_2) - \frac{B_1}{B_2} * \alpha_2\right] \tag{1.4}$$

Where $\Delta\sigma$ = stress change in soil layer of interest, B_1 = horizontal distance from beginning of full height of surcharge to point of interest, B_2 = horizontal distance from toe of surcharge embankment to full height of surcharge, α_1 = angle from point of depth of interest to horizontal point B_1 at the

ground surface (in radians), and α_2 = angle from point of depth of interest to horizontal point B_2 at the ground surface (in radians).   The equations for α_1 and α_2 are defined below.

$$\alpha_1 = tan^{-1}((B_1 + B_2)/z) - tan^{-1}(B_1/z) \tag{1.5}$$

$$\alpha_2 = tan^{-1}(B_1/z) \tag{1.6}$$

Where z = depth to point of interest (ft).

$$q_o = \gamma H \tag{1.7}$$

Where γ = unit weight of embankment soil (pcf), and H = height of embankment (ft).

Figure 1-4 illustrates the meaning of these variables.
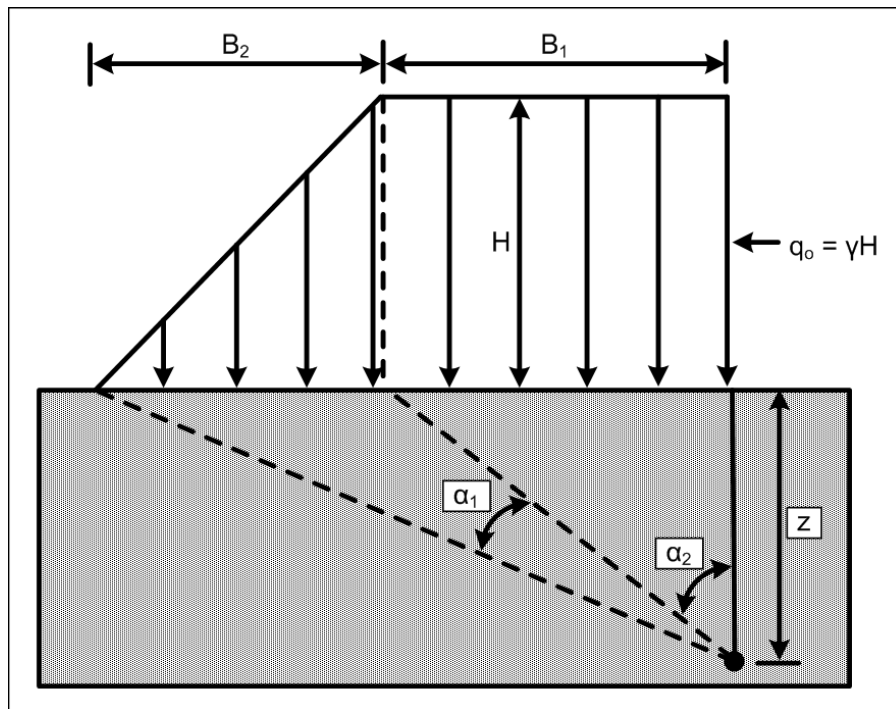
Figure 1-4. Embankment loading schematic

The initial vertical effective stress, σ'_o, is needed for each layer of interest. This is obtained by multiplying the height of the soil layer by its saturated unit weight (accounting for water table depth and hydrostatic water pressure) to the depth of interest and is governed by the Equation 1.8.

$$\sigma'_o = H(\gamma_{sat} - u) \tag{1.8}$$

7

Where σ'_o = initial vertical effective stress (psf), H = depth to point of interest (ft), γ_{sat} = saturated unit weight (pcf.), and u = hydrostatic porewater pressure (62.4 psf). The vertical effective stress will increase with depth.

Correlations for determining wet unit weight from SPT blow counts can be used to simplify the process (Teng, 1962). The following tables provide an estimate for wet unit weight to SPT blow counts for granular and cohesive soils.

Table 1-1. Granular soil correlation from SPT blow count to saturated unit weight

SPT Blow Count (N)	Compactness	Saturated unit weight (pcf)
0-4	Very Loose	Less than 100
5-10	Loose	101-110
11-30	Medium	111-130
31-50	Dense	131-140
Above 50	Very Dense	Greater than 140

Source: Teng, 1962

Table 1-2. Cohesive soil correlation from SPT blow count to saturated unit weight

SPT Blow Count (N)	Compactness	Saturated unit weight (pcf)
0-2	Very Soft	Less than 100
3-4	Soft	101-110
5-8	Medium	111-120
9-16	Stiff	121-130
17-32	Very Stiff	131-140
Above 32	Hard	Greater than 140

Source: Teng (1962)

2. EXISTING SOIL COMPRESSIBILITY MODELS

2.1. Existing Soil Compressibility Models

The research team reviewed numerous publications to identify existing prediction models of soil compressibility, including compression index (C_c), recompression index (C_r), coefficient of consolidation (C_v), and secondary compression index (C_α). C_c and C_r are used to predict the magnitude of settlement and C_v, as a rate parameter, is used to predict the rate of settlement. Existing prediction models are based on correlations between the consolidation properties and one or more physical or index properties of the soils. Those models provide a faster and more cost-effective estimate of these parameters than the consolidation test. The summary of the existing models along with reference information is presented in Table 2-1. Soil indices, as dependent variables in those models, include natural moisture content (w), initial void ratio (e_o), liquid limit (LL), plastic limit (PL), dry unit weight (γ_{dry}), activity (ACT), liquidity index (LI), plasticity index (PI), void ratio at the liquid limit (e_{LL}), and shrinkage index (SI).

There are numerous options for the correlations of consolidation parameters with different soil properties for different soils. The correlations of existing prediction models range from single parameter [e.g., void ratio (e), natural moisture content (w), plasticity index (PI)] to multiple parameters. The multiple parameter models incorporate a combination of different data from common lab tests for soil descriptors. The majority of C_c and all C_v prediction models were developed for clays, but several C_c and C_r models for peats and all soils also exist. It is important to note that some models are only applicable for specific soil types.

Table 2-1. Summary of existing correlations

Independent variable	Dependent variable	Equation	Reference	Soil Type
C_c	w	$C_c = 0.01w - 0.05$	Azzouz, Krizek, and Corotis (1976)	Not Specified (N/S)
		$C_c = 0.01w$	Koppula (1981)	Clays
		$C_c = 0.01w - 0.075$	Herrero (1983)	Clays
		$C_c = 0.013w - 0.115$	Park and Seung (2011)	Clays
		$C_c = 0.0075w$	Miyakawa (1960)	Peat
		$C_c = 0.011w$	Cook (1956)	Peat
	e_o	$C_c = 0.54e_o - 0.19$	Nishida (1956)	Clays
		$C_c = 0.43e_o - 0.11$	Cozzolino (1961)	Clays
		$C_c = 0.75e_o - 0.38$	Sowers and Sowers (1979)	Clays
		$C_c = 0.49e_o - 0.11$	Park and Seung (2011)	Clays
		$C_c = 0.4(e_o - 0.25)$	Azzouz et al. (1976)	(N/S)
		$C_c = 0.15e_o + 0.01077$	Bowles (1989)	Clays

Table 2-2. Continued. Summary of existing correlations (continued)

C_c	e_o	$C_c = 0.287e_o - 0.015$	Ahadiyan, Ebne, and Bajestan (2008)	Clays
		$C_c = 0.6e_o$	Sowers and Sowers (1979)	Peat
		$C_c = 0.3(e_o - 0.27)$	Hough (1957)	Clays
	LL	$C_c = 0.006(LL-9)$	Azzouz et al. (1976)	Clays
		$C_c = (LL-13)/109$	P. W. Mayne (1980)	Clays
		$C_c = 0.009(LL-10)$	Terzaghi and Peck (1967)	Clays
		$C_c = 0.014LL-0.168$	Park and Seung (2011)	Clays
		$C_c = 0.0046(LL-9)$	Bowles (1989)	Clays
		$C_c = 0.011(LL-16)$	McClelland (1967)	Clays
	w, LL	$C_c = 0.009w + 0.005LL$	Koppula (1981)	Clays
		$C_c = 0.009w + 0.002LL - 0.01$	Azzouz et al. (1976)	Clays
	e_o, w	$C_c = 0.4(e_o + 0.001w - 0.25)$	Azzouz et al. (1976)	(N/S)
	e_o, LL	$C_c = -0.156 + 0.411e_o - 0.00058LL$	Al-Khafaji and Andersland (1992)	Clays
		$C_c = -0.023 + 0.271e_o + 0.001LL$	Ahadiyan et al. (2008)	Clays
	e_o, w, LL	$C_c = 0.37(e_o + 0.003LL +).0004w - 0.34)$	Azzouz et al. (1976)	Clays
		$C_c = -0.404 + 0.341e_o + 0.006w + 0.004LL$	Yoon and Kim (2006)	Clays
	w, LL, e_o, γ_{dry}	$C_c = 0.1597(w^{-0.0187})(1 + e_o)^{1.592}(LL^{-0.0638})(\gamma_{dry}^{-0.8276})$	Ozer et al. (2008)	Clays
		$C_c = 0.151 + 0.001225w + 0.193e_o - 0.000258LL - 0.0699\gamma_{dry}$	Ozer et al. (2008)	Clays
C_r	e_o	$C_r = 0.156e_o + 0.0107$	Elnaggar and Krizek (1970)	Clays
		$C_r = 0.208e_o + 0.0083$	Peck and Reed (1954)	Clays
		$C_r = 0.14(e_o + 0.007)$	Azzouz et al. (1976)	(N/S)
	w	$C_r = 0.003(w + 7)$	Azzouz et al. (1976)	(N/S)
	LL	$C_r = 0.002(LL + 9)$	Azzouz et al. (1976)	(N/S)
	e_o, w	$C_r = 0.142(e_o - 0.009w + 0.006)$	Azzouz et al. (1976)	(N/S)
	w, LL	$C_r = 0.003w + 0.0006LL + 0.004$	Azzouz et al. (1976)	(N/S)
	e_o, LL	$C_r = 0.126(e_o + 0.003LL - 0.06)$	Azzouz et al. (1976)	(N/S)
	e_o, w, LL	$C_r = 0.135(e_o + 0.1LL-0.002w - 0.06)$	Azzouz et al. (1976)	(N/S)
C_v	LL	$C_v = 116.45LL^{-2.8784}$	US Navy (1971)	Clays
		$C_v = 4258LL^{-1.75}$ (m²/s)	Asma and Abbas (2011)	Clays
	ACT, LI, PI	$C_v = [9.09 \times 10^{-7}(1.192+ACT^{-1})^{6.993}(4.135LI+1)^{4.29}]/[PI(2.04LI+1.192+ACT^{-1})^{7.993}]$ (m²/s)	Carrier (1985)	Clays
	e_{LL}, σ_v	$C_v = [1+ e_{LL} (1.23-0.276\log\sigma_v)]/ e_{LL} \times [1/\sigma_v^{0.353}] \times 10^{-3}$ (cm²/s)	Narasimha, Pandian, and Nagaraj (1995)	Clays
	SI=LL-SL	$C_v = 3/[100(SI)^{3.54}]$ (m²/s)	Sridharan and Nagaraj (2004)	Clays
	PI	$C_v = 7.7525PI^{-3.1021}$ (cm²/s)	Solanki (2011)	Clays
C_α		$C_\alpha = 0.00168 + 0.00033PI$	Nakase, Kamei, and Kusakabe (1988)	(N/S)

Table 2-3. Continued. Summary of existing correlations (continued)

C_α	w	$C_\alpha = 0.0001w$	NAVFAC (1982)	(N/S)
		$C_\alpha = 0.00018w$	Simons and Menzies (2000)	(N/S)
	C_c	$C_\alpha = 0.032C_c$	G. Mesri and Godlewski (1977)	$0.025 < C_\alpha < 0.1$
		$C_\alpha = 0.06$ to $0.07C_c$	G. Mesri (1986)	Peats and organic soil
		$C_\alpha = 0.015$ to $0.03C_c$	G. Mesri, Feng, and Benak (1990)	Sandy clays
	C_c, LL, PL, w	$C_\alpha = 0.001C_c \cdot LL \cdot PL^{-1.571} \cdot w$	Anagnostopoulos and Grammatikopoulos (2011)	Silts and Clay

2.2. Accuracy Evaluation of the Existing Soil Compressibility Models

The accuracy of the existing correlations was investigated through analysis and regression of Florida-specific consolidation test results. Each correlation model was used with locally collected data to determine if the existing models were sufficiently accurate for Florida's soil conditions. The detailed description of the database used in this accuracy check analysis is presented in Section 3.2. Excluding data of coarse-grained soils, the total numbers of data points of C_c, C_r, C_v, and C_α are 551, 490, 440, and 113, respectively. It is important to note that only data corresponding to the specific soil type of existing correlations were used to evaluate the model accuracy.

The results of this analysis were then used to identify the most suitable models to be used for particular soil conditions in Florida. The accuracy of those existing models was compared in terms of key goodness of fit characteristics such as coefficient of determination (R^2) and root mean square error (RMSE). The coefficient of determination (R^2) is the square of the correlation between the response values and the predicted response values. It measures how successful the fit is in explaining the variation of the data, and takes on any value between 0 and 1, with a value closer to 1 indicating that a greater proportion of variance is accounted for by the model. The formula to determine the R^2 of a data-group is shown below in equation (2.1).

$$R^2 = 1 - \frac{SSE}{SSTO} \qquad (2.1)$$

where:
$SSE = \sum_{i=1}^{n}(y_i - \hat{y_i})^2$ (SSE is the "error sum of squares" and quantifies how much the data points, y_i, vary around the estimated regression line, $\hat{y_i}$)
$SSTO = \sum_{i=1}^{n}(y_i - \bar{y})^2$ (SSTO is the "total sum of squares" and quantifies how much the data points, y_i, vary around their mean)

The Root Mean Square Error (RMSE) is the standard deviation of the residuals (prediction errors). Residuals are a measure of how far from the regression line data points are and the RMSE is a measure of how spread out these residuals are. In other words, it tells you how concentrated the data is around the line of best fit. The formula is shown in equation (2.2).

$$RMSE = \sqrt{(f-o)^2} \qquad\qquad (2.2)$$

where f is forecasts (expected values or unknown results) and o is observed values (known results). Values closer to zero indicate a better fit.

It is important to note that R^2 is a relative measure of fit while RMSE is an absolute measure of fit. As the square root of a variance, RMSE can be interpreted as the standard deviation of the unexplained variance and has the usefu l property of being in the same units as the response variable. Lower values of RMSE indicate better fit. Therefore, RMSE was chosen in this analysis to rank the model accuracy.

A total of 551 consolidation test data were used for this analysis. The majority of the data collected is from the Florida Department of Transportation's (FDOT's) District Five, which includes the counties of Volusia, Seminole, Orange, Osceola, Brevard, Lake, Marion, Sumter, and Flagler. The soil types in Florida were assumed to fall into one of three categories, namely *fine-grained*, *organic peat*, and *organic silt,* and *organic clay*. *Fine-grained* soils are primarily composed of clays and silts. *Organic peat* soils compose of decaying plant life and other degradable materials containing large deposits of organics. *Organic silt* and *organic clay* type is fine-grained soils with traces of organic materials.

Table 2-2 shows the statistical strength of existing C_c and C_r correlation models. To search for the best prediction model for Florida's soil conditions, the RMSE values for each consolidation parameter were arranged in ranked order (smallest to largest) in Table 2-3, because the practical accuracy of a model is better determined by its RMSE than by the value of R^2.

Table 2-4. Accuracy check of existing C_c and C_r correlations

Consolidation parameter	Equation	Reference	Notes	R^2	RMSE
C_c	$C_c = 0.01w - 0.05$	Azzouz et al. (1976)	All soils	0.7448	0.8359
	$C_c = 0.01w$	Koppula (1981)	Clays	0.5202	0.4191
	$C_c = 0.01w - 0.075$	Herrero (1983)	Clays	0.5189	0.4336
	$C_c = 0.013w-0.115$	Park and Seung (2011)	Clays	0.6729	0.3953
	$C_c = 0.0075w$	Miyakawa (1960)	Peat	0.5784	1.5194
	$C_c = 0.011w$	Cook (1956)	Peat	0.6611	1.9601
	$C_c = 0.54e_o - 0.19$	Nishida (1956)	Clays	0.7236	0.3945
	$C_c = 0.43e_o - 0.11$	Cozzolino (1961)	Clays	0.6120	0.4046
	$C_c = 0.75e_o - 0.38$	Sowers and Sowers (1979)	Clays	0.7362	0.5552
	$C_c = 0.49e_o - 0.11$	Park and Seung (2011)	Clays	0.6847	0.3924
	$C_c = 0.4(e_o - 0.25)$	Azzouz et al. (1976)	All soils	0.5676	0.7501
	$C_c = 0.15e_o + 0.01077$	Bowles (1989)	Clays	0.3157	0.7536
	$C_c = 0.287e_o - 0.015$	Ahadiyan et al. (2008)	Clays	0.3847	0.7692

Table 2-5. Continued, Accuracy check of existing C_c and C_r correlations (continued)

C_c	$C_c = 0.6e_o$	Sowers and Sowers (1979)	Peat	0.6715	1.7876
	$C_c = 0.3(e_o - 0.27)$	Hough (1957)	Clays	0.4081	0.5425
	$C_c = 0.006(LL - 9)$	Azzouz et al. (1976)	Clays	0.2857	0.6213
	$C_c = (LL-13)/109$	Mayne (1980)	Clays	0.4323	0.5638
	$C_c = 0.009(LL -10)$	Terzaghi and Peck (1967)	Clays	0.4236	0.5641
	$C_c = 0.014LL - 0.168$	Park and Seung (2011)	Clays	0.5569	0.7921
	$C_c = 0.0046(LL-9)$	Bowles (1989)	Clays	0.2780	0.6989
	$C_c = 0.011(LL-16)$	McClelland (1967)	Clays	0.5094	0.5991
	$C_c = 0.009w + 0.005LL$	Koppula (1981)	Clays	0.5701	0.5518
	$C_c = 0.009w + 0.002LL - 0.01$	Azzouz et al. (1976)	Clays	0.5866	0.4875
	$C_c = 0.4(e_o + 0.001w - 0.25)$	Azzouz et al. (1976)	All soils	0.7057	0.7414
	$C_c = -0.156 + 0.411e_o - 0.00058LL$	Al-Khafaji and Andersland (1992)	Clays	0.5276	0.3881
	$C_c = -0.023 + 0.271e_o + 0.001LL$	Ahadiyan et al. (2008)	Clays	0.3400	0.4597
	$C_c = 0.37(e_o + 0.003LL +).0004w - 0.34)$	Azzouz et al. (1976)	Clays	0.5014	0.3888
	$C_c = -0.404 + 0.341e_o + 0.006w + 0.004LL$	Yoon and Kim (2006)	Clays	0.6805	0.4991
	$C_c = 0.1597(w^{-0.0187})(1 + e_o)^{1.592}(LL^{-0.0638})(\gamma_{dry}^{-0.8276})$	Ozer, Isik, and Orhan (2008)	Clays	0.6824	0.5886
	$C_c = 0.151 + 0.001225w + 0.193e_o - 0.000258LL - 0.0699\gamma_{dry}$	Ozer et al. (2008)	Clays	0.3006	0.5204
C_r	$C_r = 0.156e_o + 0.0107$	Elnaggar and Krizek (1970)	Clays	0.5330	0.2536
	$C_r = 0.208e_o + 0.0083$	Peck and Reed (1954)	Clays	0.5419	0.3643
	$C_r = 0.14(e_o + 0.007)$	Azzouz et al. (1976)	All soils	0.6016	0.3369
	$C_r = 0.003(w + 7)$	Azzouz et al. (1976)	All soils	0.5780	0.4415
	$C_r = 0.002(LL + 9)$	Azzouz et al. (1976)	All soils	0.5485	0.1682
	$C_r = 0.142(e_o - 0.009w + 0.006)$	Azzouz et al. (1976)	All soils	0.6089	0.1802
	$C_r = 0.003w + 0.0006LL + 0.004$	Azzouz et al. (1976)	All soils	0.5674	0.2344
	$C_r = 0.126(e_o + 0.003LL-0.06)$	Azzouz et al. (1976)	All soils	0.5808	0.2109
	$C_r = 0.135(e_o + 0.1LL-0.002w - 0.06)$	Azzouz et al. (1976)	All soils	0.5548	0.3131

Table 2-6. Statistical strength ranks by existing C_c correlations

Consolidation parameter	Equation	Reference	Notes	RMSE	Rank
C_c	$C_c = -0.156 + 0.411e_o - 0.00058LL$	Al-Khafaji and Andersland (1992)	Clays	0.3881	1
	$C_c = 0.37(e_o + 0.003LL + 0.0004w - 0.34)$	Azzouz et al. (1976)	Clays	0.3888	2
	$C_c = 0.49e_o - 0.11$	Park and Seung (2011)	Clays	0.3924	3
	$C_c = 0.54e_o - 0.19$	Nishida (1956)	Clays	0.3945	4
	$C_c = 0.013w - 0.115$	Park and Seung (2011)	Clays	0.3953	5
	$C_c = 0.43e_o - 0.11$	Cozzolino (1961)	Clays	0.4046	6
	$C_c = 0.01w$	Koppula (1981)	Clays	0.4191	7
	$C_c = 0.01w - 0.075$	Herrero (1983)	Clays	0.4336	8
	$C_c = -0.023 + 0.271e_o + 0.001LL$	Ahadiyan et al. (2008)	Clays	0.4597	9
	$C_c = 0.009w + 0.002LL - 0.01$	Azzouz et al. (1976)	Clays	0.4875	10
	$C_c = -0.404 + 0.341e_o + 0.006w + 0.004LL$	Yoon and Kim (2006)	Clays	0.4991	11
	$C_c = 0.151 + 0.001225w + 0.193e_o - 0.000258LL - 0.0699\gamma_{dry}$	Ozer et al. (2008)	Clays	0.5204	12
	$C_c = 0.3(e_o - 0.27)$	Hough (1957)	Clays	0.5425	13
	$C_c = 0.009w + 0.005LL$	Koppula (1981)	Clays	0.5518	14
	$C_c = 0.75e_o - 0.38$	Sowers and Sowers (1979)	Clays	0.5552	15
	$C_c = (LL-13)/109$	Mayne (1980)	Clays	0.5638	16
	$C_c = 0.009(LL -10)$	Terzaghi, Peck (1967)	Clays	0.5641	17
	$C_c = 0.1597(w^{-0.0187})(1 + e_o)^{1.592}(LL^{-0.0638})(\gamma_{dry}^{-0.8276})$	Ozer et al. (2008)	Clays	0.5886	18
	$C_c = 0.011(LL-16)$	McClelland (1967)	Clays	0.5991	19
	$C_c = 0.006(LL - 9)$	Azzouz et al. (1976)	Clays	0.6213	20
	$C_c = 0.0046(LL-9)$	Bowles (1989)	Clays	0.6989	21
	$C_c = 0.4(e_o + 0.001w - 0.25)$	Azzouz et al. (1976)	All soils	0.7414	22
	$C_c = 0.4(e_o - 0.25)$	Azzouz et al. (1976)	All soils	0.7501	23
	$C_c = 0.15e_o + 0.01077$	Bowles (1989)	Clays	0.7536	24
	$C_c = 0.287e_o - 0.015$	Ahadiyan et al. (2008)	Clays	0.7692	25
	$C_c = 0.014LL - 0.168$	Park and Seung (2011)	Clays	0.7921	26
	$C_c = 0.01w - 0.05$	Azzouz et al. (1976)	All soils	0.8359	27
	$C_c = 0.0075w$	Miyakawa (1960)	Peat	1.5194	28
	$C_c = 0.6e_o$	Sowers and Sowers (1979)	Peat	1.7876	29
	$C_c = 0.011w$	Cook (1956)	Peat	1.9601	30

Table 2-7. Statistical strength ranks by existing C_r correlations

Consolidation parameter	Equation	Reference	Notes	RMSE	Rank
C_r	$C_r = 0.002(LL + 9)$	Azzouz et al. (1976)	All soils	0.1682	1
	$C_r = 0.142(e_o - 0.009w + 0.006)$	Azzouz et al. (1976)	All soils	0.1802	2
	$C_r = 0.126(e_o + 0.003LL-0.06)$	Azzouz et al. (1976)	All soils	0.2109	3
	$C_r = 0.003w + 0.0006LL + 0.004$	Azzouz et al. (1976)	All soils	0.2344	4
	$C_r = 0.156e_o + 0.0107$	Elnaggar and Krizek (1970)	Clays	0.2536	5
	$C_r = 0.135(e_o + 0.1LL-0.002w - 0.06)$	Azzouz et al. (1976)	All soils	0.3131	6
	$C_r = 0.14(e_o + 0.007)$	Azzouz et al. (1976)	All soils	0.3369	7
	$C_r = 0.208e_o + 0.0083$	Peck and Reed (1954)	Clays	0.3643	8
	$C_r = 0.003(w + 7)$	Azzouz et al. (1976)	All soils	0.4415	9

Table 2-8. Statistical strength ranks for the existing C_v correlations

Consolidation parameter	Equation	Reference	Soil type	RMSE	Rank
C_v	$C_v = 4258LL^{-1.75}$ (m²/s)	Asma and Abbas (2011)	Clays	0.819	1
	$C_v = 116.45LL^{-2.8784}$	US Navy (1971)	Clays	0.837	2
	$C_v = [1+ e_{LL} (1.23-0.276\log\sigma_v)]/ e_{LL} \times[1/\sigma_v^{0.353}]\times10^{-3}$ (cm²/s)	Narasimha et al. (1995)	Clays	0.850	3
	$C_v = [9.09\times10^{-7}(1.192+\ldots \ldots+ACT^{-1})^{6.993}(4.135LI+1)^{4.29}] /[PI(2.04LI+1.192+ACT^{-1})^{7.993}]$ (m²/s)	Carrier (1985)	Clays	0.860	4
	$C_v = 7.7525PI^{-3.1021}$ (cm²/s)	Solanki (2011)	Clays	0.868	5
	$C_v = 3/[100(SI)^{3.54}]$ (m²/s)	Sridharan and Nagaraj (2004)	Clays	n/a	n/a

Table 2-9. Statistical strength ranks for the existing C_α correlations

Consolidation parameter	Equation	Reference	Soil type	RMSE	Rank
C_α	$C_\alpha = 0.0001w$	NAVFAC (1982)	All soils	0.0049	1
	$C_\alpha = 0.00018w$	Simons and Menzies (2000)	All soils	0.0101	2
	$C_\alpha = 0.00168 + 0.00033PI$	Nakase et al. (1988)	All soils	0.0245	3

As discussed above, RMSE was used to rank the accuracy of the existing models because the practical usefulness of a model is better determined by its RMSE than by the value of R^2. The analysis results are presented in Tables 2-2 through 2-6. These tables summarize the accuracy of the models and the ranking of the Cc, Cr, Cv, and Cα models. According to the RMSE values, in general, the C_r models seem more accurate than the C_c models for Florida's data. For C_c, Al-Khafaji, Andersland's model (1992), which is a function of e_o and LL, exhibited the highest accuracy. For C_r, the model propsed by Azzouz et al. (1976), which is a function of w, appears to be the best model. For C_v, Asma and Abba's model (2011) seems more accurate than the others, but the RMSE is quite high at 0.8193. Therefore, the authors recommended that none of models are suitable for Florida's soil conditions. For C_α, NAVFAC's model (1982), which is a function w, exhibits the highest accuracy. This model exhibits a very low RMSE value (0.0049), but one should note that the number of data points were limited (about 20 data points).

2.3. Statewide Survey

A statewide survey was sent to consultants to identify the most commonly used correlations for estimating the soil compressibility among the professional community. The team conducted the first survey in January 2018; however, insufficient number of responses was received. Thus, a second-round survey (with web-based survey link) was conducted. A summary of the two survey results is presented in Tables 2-7 through 2-10. According to the survey result, the most used correlation is (Eq. 2.3) Terzaghi and Peck (1967) and the second one is (Eq. 2.2) Koppula (1981). The two correlations are presented below.

$$C_c = 0.009(LL-10) \text{ (Terzaghi and Peck, 1967)} \tag{2.3}$$

$$C_c = 0.009w + 0.005LL \text{ (Koppula, 1981)} \tag{2.4}$$

For other correlations, several consultants responded with following models.

$$C_r = 0.003w + 0.0006LL + 0.004 \quad \text{(Azzouz et al., 1976)} \tag{2.5}$$

$$C_v = 116.45LL^{-2.8784} \quad \text{(US Navy, 1971)} \tag{2.6}$$

$$C_\alpha = 0.06 \text{ to } 0.07C_c \quad \text{(G. Mesri, 1986)} \tag{2.7}$$

16

Table 2-10. Results of survey responses – C_c

Independent variable	Dependent variable	Equation	Reference	Notes	# of Responses
C_c	w	$C_c = 0.01w - 0.05$	Azzouz et al. (1976)	All soils	1
		$C_c = 0.0054(2.6w - 35)$	Nishida (1956)	Clays	1
		$C_c = 0.01w$	Koppula (1981)	Clays	2
		$C_c = 0.01w - 0.075$	Herrero (1983)	Clays	
		$C_c = 0.013w - 0.115$	Park and Seung (2011)	Clays	
		$C_c = 0.0075w$	Miyakawa (1960)	Peat	1
		$C_c = 0.011w$	Cook (1956)	Peat	2
		$C_c = 0.0102(w - 9.15)$	Hough (1957)	Clays	1
		$C_c = 0.0074w - 0.007$	Kalantary and Kordnaeij (2012)	Clays	
	e_o	$C_c = 0.54e_o - 0.19$	Nishida (1956)	Clays	1
		$C_c = 0.5217(e_o - 0.2)$	Nishida (1956)	Clays	1
		$C_c = 0.43e_o - 0.11$	Cozzolino (1961)	Clays	
		$C_c = 0.75e_o - 0.38$	Sowers and Sowers (1979)	Clays	
		$C_c = 0.49e_o - 0.11$	Park and Seung (2011)	Clays	
		$C_c = 0.4(e_o - 0.25)$	Azzouz et al. (1976)	All soils	1
		$C_c = 0.15e_o + 0.01077$	Bowles (1989)	Clays	2
		$C_c = 0.287e_o - 0.015$	Ahadiyan et al. (2008)	Clays	
		$C_c = 0.6e_o$	Sowers and Sowers (1979)	Peat	1
		$C_c = 0.3(e_o - 0.27)$	Rendon-Herrero (1980)	Clays	1
		$C_c = 0.4049(e_o - 0.3216)$	Hough (1957)	Clays	1
		$C_c = 0.3608e_o - 0.0713$	Kalantary and Kordnaeij (2012)	Clays	
	LL	$C_c = 0.006(LL-9)$	Azzouz et al. (1976)	Clays	2
		$C_c = (LL-13)/109$	Mayne (1980)	Clays	1
		$C_c = 0.009(LL-10)$	Terzaghi and Peck (1967)	Clays	10
		$C_c = 0.014LL-0.168$	Park and Seung (2011)	Clays	1
		$C_c = 0.0046(LL-9)$	Bowles (1989)	Clays	2
		$C_c = 0.011(LL-16)$	McClelland (1967)	Clays	
	w, LL	$C_c = 0.009w + 0.005LL$	Koppula (1981)	Clays	4
		$C_c = 0.009w + 0.002LL - 0.01$	Azzouz et al. (1976)	Clays	2
	e_o, w	$C_c = 0.4(e_o + 0.001w - 0.25)$	Azzouz et al. (1976)	All soils	1

Table 2-11. Continued, Results of survey responses – C_c (continued)

C_c	e_o, LL	$C_c = -0.156 + 0.411e_o - 0.00058LL$	Al-Khafaji and Andersland (1992)	Clays	1
		$C_c = -0.023 + 0.271e_o + 0.001LL$	Ahadiyan et al. (2008)	Clays	
	e_o, w, LL	$C_c = 0.37(e_o + 0.003LL +).0004w - 0.34)$	Azzouz et al. (1976)	Clays	1
		$C_c = -0.404 + 0.341e_o + 0.006w + 0.004LL$	Yoon and Kim (2006)	Clays	
	w, LL, e_o, γ_{dry}	$C_c = 0.1597(w^{-0.0187})(1 + e)^{1.592}(LL^{-0.0638})(\gamma_{dry}^{-0.8276})$	Ozer et al. (2008)	Clays	
		$C_c = 0.151 + 0.001225w + 0.193e_o - 0.000258LL - 0.0699\gamma_{dry}$	Ozer et al. (2008)	Clays	
	Gs, PI	$C_c = 0.5Gs*[PI(\%)]/100$	Wroth and Wood (1978)	Clays	1

Table 2-12. Results of survey responses – C_r

Independent variable	Dependent variable	Equation	Reference	Notes	# of Responses
C_r	e_o	$C_r = 0.156e_o + 0.0107$	Elnaggar and Krizek (1970)	Clays	
		$C_r = 0.208e_o + 0.0083$	Peck and Reed (1954)	Clays	2
		$C_r = 0.14(e_o + 0.007)$	Azzouz et al. (1976)	All soils	1
	w	$C_r = 0.003(w + 7)$	Azzouz et al. (1976)	All soils	2
		$C_r = w/1,000$	Samtani and Nowatzki (2006)	All soils	2
	LL	$C_r = 0.002(LL + 9)$	Azzouz et al. (1976)	All soils	1
	e_o, w	$C_r = 0.142(e_o - 0.009w + 0.006)$	Azzouz et al. (1976)	All soils	1
	w, LL	$C_r = 0.003w + 0.0006LL + 0.004$	Azzouz et al. (1976)	All soils	3
	e_o, LL	$C_r = 0.126(e_o + 0.003LL - 0.06)$	Azzouz et al. (1976)	All soils	1
	e_o, w, LL	$C_r = 0.135(e_o + 0.1LL-0.002w - 0.06)$	Azzouz et al. (1976)	All soils	1
	Cc	$C_r = (0.05 \text{ to } 0.2)* C_c$	No reference?	All soils?	1
	PI	$C_r = PI/370$	Kulhawy and Mayne (1990)	Clays	1

Table 2-13. Results of survey responses – C_v

Independent variable	Dependent variable	Equation	Reference	Notes	# of Responses
C_v	LL	$C_v = 116.45LL^{-2.8784}$	US Navy (1971)	Clays	2
		$C_v = 4,258LL^{-1.75}$ (m²/s)	Asma and Abbas (2011)	Clays	1
	ACT, LI, PI	$C_v = [9.09\times10^{-7}(1.192+ACT^{-1})^{6.993}(4.135LI+1)^{4.29}]/[PI(2.04LI+1.192+ACT^{-1})^{7.993}]$ (m²/s)	Carrier (1985)	Clays	1
	e_{LL}, σ_v	$C_v = [1+ e_{LL} (1.23-0.276\log\sigma_v)]/ e_{LL} \times[1/\sigma_v^{0.353}]\times10^{-3}$ (cm²/s)	Narasimha et al. (1995)	Clays	
	SI=LL-SL	$C_v = 3/[100(SI)^{3.54}]$ (m²/s)	Sridharan and Nagaraj (2004)	Clays	
	PI	$C_v = 7.7525PI^{-3.1021}$ (cm²/s)	Solanki (2011)	Clays	

Table 2-14. Results of survey responses – C_α

Independent variable	Dependent variable	Equation	Reference	Notes	# of Responses
C_α	PI	$C_\alpha = 0.00168 + 0.00033PI$	Nakase et al. (1988)	All soils?	2
	w	$C_\alpha = 0.0001w$	NAVFAC (1982)	All soils?	3
		$C_\alpha = 0.00018w$	Simons and Menzies (2000)	All soils?	
	C_c	$C_\alpha = 0.032C_c$	Mesri and Godlewski (1977)	$0.025 < C_a < 0.1$	
		$C_\alpha = 0.06$ to $0.07C_c$	Mesri (1986)	Peats and organic soil	3
		$C_\alpha = 0.015$ to $0.03C_c$	Mesri et al. (1990)	Sandy clays	1
		$C_\alpha = (0.03$ to $0.09)*C_c$	No reference?	All soils?	1
	C_c, LL, PL, w	$C_\alpha = 0.001C_c\cdot LL\cdot PL^{-1.571}\cdot w$	Anagnostopoulos, Grammatikopoulo (2011)	Silts/Clay	

2.4. Summary and Conclusion

The goals of this chapter were to first, to identify the accuracy of the existing correlations used internationally to estimate soil compressibility parameters using the Florida soil consolidation database (discussed in more detail in Chapter 3) and, second, to determine the most popularly used correlations in the Florida geotechnical consultant community. When comparing the information presented in this chapter, it is interesting to note that the model with the highest accuracy for the Florida soils database (i.e., Azzouz et al. 1976) did not have a majority of responses from the survey. Rather, the overwhelmingly most used correlation was from Terzaghi and Peck's famous Theoretical Soil Mechanics textbook from 1967. With the capability now to statistically develop models using a Florida specific database of soils, empirical models will be developed in the following chapters, relating compressibility parameters to soil index parameters obtained from split spoon samples in the lab.

3. DATA COLLECTION AND PARAMETER CORRELATION ANALYSIS

3.1. Florida's Geological Formation

Florida's geology is unique from the Panhandle in the north, to the Central Highlands and Coastal Lowlands in the south. The Panhandle contains much of Florida's clayey sands and gravels, while the Central Highlands and Coastal Lowlands are composed mainly of medium to fine sands and silts, shelly sands and clays, and large deposits of limestone, as noted in Figure 3-1. A large portion of Florida's soils are clayey sands, defined as SC in the USCS. Due to the compressive nature of clay particles in this particular soil and the sand particle's propensity for rearrangement during loading, there is a high settlement potential for these soils; however, the project mainly focused on clay, organic, and peat soils.
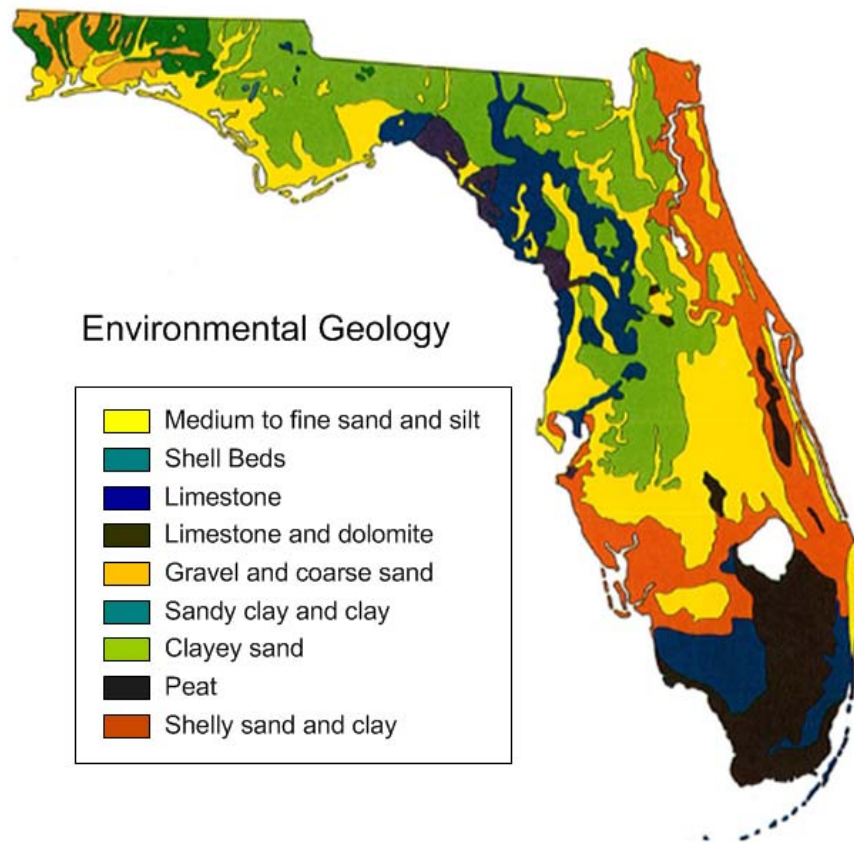

Figure 3-1: Map outlining environmental geology of Florida

source: Anderson, Krafft, and Remington (1981)

Over-consolidation of soil can be observed due to several reasons. It could be that a greater depth of past overburden has eroded away over the course of time, commonly due to land shifts over many years and glacial movements. Cycles of wetting and drying could subject the soil to shrinkage and swelling (Bowles, 1989). As Florida has very wet and dry seasons, moisture intrusion/drying is very likely. The soil could also be exposed to cycles of wetting and drying in the presence of certain sodium, calcium, and magnesium salts, and there could be effective pressure changes from water table fluctuations (Bowles, 1989).

A brief look into Florida's geologic history will illustrate how unique the state really is. Florida's history begins out of the break-up of a supercontinent called Rodinia around 700 Ma (million years ago) into a new land mass called Gondwana. This process is composed of two parts: rifting and seafloor spreading. Rifting is the initial splitting apart of the continental mass and seafloor spreading is the formation of a new ocean basin (Hine, 2013). What is now North America was a separate land mass that collided with Gondwana approximately 350 Ma. When this occurred, it formed what we know as Florida today. The shifting and movement that occurred throughout this process displaced what is now Florida from the South Pole to its present location (Hine, 2013).

If one examines the topography of the state, the presence of numerous former beaches, scarps (steep slopes), and shorelines can be observed. This suggests that sediment movement was very likely (Hine, 2013). This occurred from the north to south orientation from peninsular Florida and must have occurred by breaking waves transporting soils from one location to another, much like how sand is moved in modern beaches today. This transport occurred when sea levels were at a higher elevation. When sea levels were lower, local streams and small rivers probably eroded into the former shorelines and moved various amounts of sediments from the east to west (Hine, 2013).

During the peak of the Middle Miocene era (18 Ma), approximately 300 feet of water covered south-central Florida, linking the Gulf of Mexico with the northern Straits of Florida (Hine, 2013). During this time, sea levels fluctuated with great regularity, leaving portions of Florida to become shallower and, at times, were emergent, which allowed rivers to flow overland to estuaries and coastlines. There were, however, many time periods during this time in which Florida was high and dry. This provided an environment where land animals and terrestrial creatures thrived due to the rich soils left behind from receding oceans. This sea level history of repeated flooding and exposing of land created one of the great fossil hunting locations in the world, mixing the remains of an abundance of land and marine organisms (Hine, 2013).

Given the geologic history of Florida, it is reasonable to assume that much of Florida's soils are over-consolidated to some degree, as large portions of Florida have been subjected to rising and lowering water tables and sediment transport, and there have been thousands of cycles of wetting and drying throughout the state's history. For this reason, when the soil is subjected to a change in stress and settlement ensues, it is reasonable to assume that a portion of the soil's behavior can be described by the unload-reload cycle of the consolidation curve. When this occurs, the recompression index, C_r, will be a factor in the primary consolidation settlement. Existing correlations for the recompression index, C_r, are not as abundant as for the compression index, C_c, particularly for fine-grained and coarse-grained soils.

The existing correlations utilize soil descriptors such as liquid limit (LL), initial void ratio (e_o), moisture content (w), and dry unit weight (γ_{dry}). While these soil descriptors are useful and relatively easy to obtain, there are several other parameters that also meet these criteria and could have as much, if not more, influence on the parameters that are influencing primary consolidation settlement. These parameters include the saturated unit weight (γ_{sat}), automatic hammer SPT blow count (N), overburden stress (σ), plasticity index (PI), and fine content (-200). Having a full spectrum of soil parameters to develop new correlations could yield stronger predictions of settlement.

3.2. Data Collection

A total of 644 consolidation test data conducted on soils throughout the state of Florida was collected. The status of data collection is shown in Table 3-1. Each consolidation test has an accompanying SPT boring to provide a description of the soil's stiffness. The majority of the data collected is from the Florida Department of Transportation's (FDOTs) District Five which includes the counties of Volusia, Seminole, Orange, Osceola, Brevard, Lake, Marion, Sumter, and Flagler.

Table 3-1. Data collection numbers

Soil type		# of Data points	
		C_c	C_r
Fine-grained	clays	396	380
	silts	31	21
Organic soils		124	89
Coarse-grained*		93	93
	Total	644	583

*Not included in model development for this study

Stress Level	Stress Range (psf)	# of Data points	
		C_v	C_α
Low	< 2000	150	38
Intermediate	2000 ≤ σ ≤ 4000	147	38
High	> 4000	143	37
	Total	440	113

The soil types are assumed to fall into one of four categories. The first category is "fine-grained" materials, which is primarily composed of clays and silts. Fine-grained materials are classified by having over half of the sample's particle diameter smaller than 0.074 mm, or the #200 sieve. Fine-grained materials are then broken into separate classes of silts and clays. These will be analyzed separately from the fine-grained classification. The next category is assumed to be soils with large deposits of organics and is called "Organic Peat". These fibrous soils are composed of decaying plant life and other degradable materials that are classified by visual inspection. They are often referred to as "muck" and are normally over-saturated with water. The last category is coarse-grained materials, which is primarily composed of sands with varying amounts of clays and silts

intermingled. Coarse-grained materials are classified by having more than half of the sample's particle diameter larger than 0.074 mm, or the #200 sieve. For this study, however, the coarse-grained material data will not be included in any model development presented in Chapter 4 due to the concerns regarding consolidation test results because of sample disturbance when retrieving Shelby tubes.

The value of the coefficient of consolidation (C_v) and coefficient of secondary consolidation (C_α), are contingent on experienced stress. As there are a variety of different stressors that can be encountered on a roadway construction project (surcharge, live load, construction equipment, structural footings, etc.), it was decided to model different stress levels for examination, these being the low stress range (less than 2,000 psf), intermediate stress range (between 2,000 and 4,000 psf), and high stress range (over 4,000 psf). Each stress range will be examined to determine if a reliable correlation can be developed for C_v and C_α.

Table 3-2 shows an example data set of C_c and C_r and Table 3-3 shows an example data set of C_v and C_α. A Microsoft Access database was created to store and sort the existing data for quick analysis. This database houses the general information of where the sample was taken (project numbers and description, FDOT District and County, etc.), specific information of where the sample was taken (latitude and longitude, boring number, sample depth), sample description (soil type, USCS Classification, fines content (-200), moisture content (w), initial void ratio (e_o), Atterberg limits (LL and PL), SPT automatic hammer blow count (N), and specific gravity (G_s)), and stress state of the soil (compression index (C_c), recompression index (C_r), coefficient of consolidation (C_v), coefficient of secondary consolidation (C_α), effective overburden pressure (σ'_o), and preconsolidation pressure (P_c)).

Overburden pressure was computed using the correlation for SPT blow count to saturated unit weight of soil (Teng, 1962). This is determined for each soil strata above the depth from which the sample was taken and each unit weight is then multiplied by the height of each respective soil strata, taken from the SPT boring. The seasonal high-water table was used to account for the effective overburden pressure computation.

The SPT borings were also used to help identify some of the missing data from the consolidation test report. If the moisture content (*w*) or fines content (-200) were not included on the consolidation test report, they were accounted for via lab tests within the same soil strata and close proximity to where the undisturbed sample was taken.

Table 3-2. Example data set of C_c and C_r

Project	County	Soil Type	USCS	Natural Moisture (%)	γ_{dry} (pcf)	γ_{sat} (pcf)	Gs	Fines (-200) (%)	Liquid Limit (LL)	Plasticity Index (PI)	Organic Content (%)	Initial void Ratio (e_o)	σ'_o (ksf)	Cc	Cr
SR 223 over CR 100A and CSX RR	Bradford	Fine-grained	CH	82	50.3	91.6	2.64	98	133	99		2.28	2.28	1.05	0.24
SW 42nd St. Flyover	Marion	Fine-grained	CH	55	67.0	103.9	2.66	95	157	118		1.48	3.08	0.35	0.10
SR 10 at Little Pottsburg Creek	Duval	Organic Peat	PT	414	12.7	65.4	2.19	1			87	9.76	1.85	6.41	0.63

Table 3-3. Example data set of C_v and C_a

Soil Type	(USCS)	σ'_o (ksf)	γ_{dry} (pcf)	γ_{sat} (pcf)	Natural Moisture (%)	Fines (-200) (%)	Liquid Limit (LL)	Plasticity Index (PI)	Initial Void Ratio (e)	Specific Gravity	Cv	C_α	Stress Range
Fine-grained	CH	1.12	71.6	104.6	46.1	58	61	44	1.35	2.7	0.01	0.009	High
Fine-grained	CH	1.12	71.6	104.6	46.1	58	61	44	1.35	2.7	0.05	0.003	Intermediate
Fine-grained	CH	1.49	52.8	95.3	80.4	88	108	75	2.24	2.74	0.11	0.001	Low
Organic Peat	PT	0.09	11.3	62.8	456	59	-	-	8.08	1.64	0.07	0.024	Intermediate
Organic Peat	PT	0.15	5.4	55.8	934	94	-	-	12.68	1.18	0.0001	0.015	Low

3.3. Correlation Between Index Parameters and Soil Compressibility

The research team evaluated the correlation between key index parameters and soil compressibility, which include C_c, C_r, C_v, and C_α. The key index parameters that were used include Effective Overburden Pressure (ksf), Wet Density (pcf), Dry Density (pcf), Natural Moisture (%), Automatic Hammer Blow Count, Fines (-200) (%), Liquid Limit (LL), Plasticity Index (PI), Initial Void Ratio (e_o), and Specific Gravity.

The soil types that were evaluated include fine-grained and organic soils. The fine-grained soils were subdivided into silt, high plasticity clay, and low plasticity clay. Tables 3-4 through 3-13 contain the calculated Pearson's Correlation Coefficient values, Coefficient of Determination (R^2) values and Root Mean Square Error values (RMSE) for the above soil types. Pearson's Correlation Coefficient analysis was used to identify "better" performing parameters in predicting the C_c and C_r of specific soil. A high (positive) correlation coefficient indicates that there is a strong uphill relationship between key index parameters and soil compressibility (C_c and C_r). Such a relationship implies that as an index parameter increases, the C_c and C_r of a specific soil will increase as well. On the contrary, a low (negative) correlation coefficient indicates that there is a strong downhill relationship between key index parameters and soil compressibility. Such a relationship indicates that as an index parameter increases, the C_c and C_r of a specific soil will decrease and vice versa. Coefficient of Determination and Root Mean Square Error values were calculated to quantify the performance level of the key index parameters. A perfect correlation yields an R^2 value of 1.0, and an RMSE value of zero.

The analysis results for the fine-grained soils including silts and clays are shown in Tables 3-4 and 3-5. The subdivision of fine-grained soils (the results of silts, low plasticity clays, and high plasticity clays) are summarized in Tables 3-6 through 3-11. The analysis results of organic soils are presented in Tables 3-12 and 3-13. Within the following tables, Pearson's Correlation Coefficients highlighted in red denote the three largest negative correlations (i.e., the most inverse proportional). Adversely, the cells highlighted in green represent the three highest correlation coefficients (i.e., the most directly proportional), for each soil type data group analyzed.

Table 3-4. Correlation of C_c for fine-grained soils

Type	Var1	Var2	Pearson's Correlation Coefficient	R-Squared	RMSE
Fine-grained	C_c	Effective Overburden Pressure (ksf)	0.051	0.003	0.621
	C_c	Wet Density (pcf)	-0.629	0.395	0.484
	C_c	Dry Density (pcf)	-0.689	0.474	0.451
	C_c	Natural Moisture (%)	0.765	0.585	0.401
	C_c	Automatic Hammer Blow Count	-0.235	0.055	0.605
	C_c	Fines (-200) (%)	0.057	0.003	0.621
	C_c	Liquid Limit (LL)	0.533	0.284	0.526
	C_c	Plasticity Index (PI)	0.454	0.206	0.554
	C_c	Initial Void Ratio (e_o)	0.764	0.584	0.401
	C_c	Specific Gravity	-0.075	0.006	0.620

26

Table 3-5. Correlation of C_r for fine-grained soils

Type	Var1	Var2	Pearson's Correlation Coefficient	R-Squared	RMSE
Fine-grained	C_r	Effective Overburden Pressure (ksf)	-0.066	0.004	0.085
	C_r	Wet Density (pcf)	-0.426	0.182	0.077
	C_r	Dry Density (pcf)	-0.476	0.227	0.075
	C_r	Natural Moisture (%)	0.576	0.332	0.069
	C_r	Automatic Hammer Blow Count	-0.131	0.017	0.084
	C_r	Fines (-200) (%)	-0.062	0.004	0.085
	C_r	Liquid Limit (LL)	0.491	0.241	0.074
	C_r	Plasticity Index (PI)	0.395	0.156	0.078
	C_r	Initial Void Ratio (e_o)	0.524	0.274	0.072
	C_r	Specific Gravity	-0.129	0.017	0.084

Table 3-6. Correlation of C_c for silts

Type	Var1	Var2	Pearson's Correlation Coefficient	R-Squared	RMSE
Silts	C_c	Effective Overburden Pressure (ksf)	0.057	0.003	0.886
	C_c	Wet Density (pcf)	-0.568	0.323	0.730
	C_c	Dry Density (pcf)	-0.611	0.373	0.702
	C_c	Natural Moisture (%)	0.739	0.546	0.598
	C_c	Automatic Hammer Blow Count	-0.057	0.003	0.886
	C_c	Fines (-200) (%)	-0.670	0.450	0.658
	C_c	Liquid Limit (LL)	0.747	0.558	0.590
	C_c	Plasticity Index (PI)	0.735	0.540	0.602
	C_c	Initial Void Ratio (e_o)	0.570	0.325	0.729
	C_c	Specific Gravity	-0.715	0.512	0.620

Table 3-7. Correlation of C_r for silts

Type	Var1	Var2	Pearson's Correlation Coefficient	R-Squared	RMSE
Silts	C_r	Effective Overburden Pressure (ksf)	0.004	0.000	0.197
	C_r	Wet Density (pcf)	-0.551	0.303	0.165
	C_r	Dry Density (pcf)	-0.575	0.331	0.162
	C_r	Natural Moisture (%)	0.718	0.515	0.138
	C_r	Automatic Hammer Blow Count	-0.268	0.072	0.190
	C_r	Fines (-200) (%)	-0.635	0.403	0.153
	C_r	Liquid Limit (LL)	0.616	0.379	0.156
	C_r	Plasticity Index (PI)	0.634	0.401	0.153
	C_r	Initial Void Ratio (e_o)	0.538	0.289	0.166
	C_r	Specific Gravity	-0.743	0.551	0.132

Table 3-8. Correlation of C_c for low plasticity clays

Type	Var1	Var2	Pearson's Correlation Coefficient	R-Squared	RMSE
Clays – (CL)	C_c	Effective Overburden Pressure (ksf)	0.180	0.033	0.424
	C_c	Wet Density (pcf)	-0.489	0.239	0.376
	C_c	Dry Density (pcf)	-0.551	0.304	0.360
	C_c	Natural Moisture (%)	0.617	0.380	0.339
	C_c	Automatic Hammer Blow Count	-0.207	0.043	0.422
	C_c	Fines (-200) (%)	0.146	0.021	0.426
	C_c	Liquid Limit (LL)	0.155	0.024	0.426
	C_c	Plasticity Index (PI)	0.008	0.000	0.431
	C_c	Initial Void Ratio (e_o)	0.645	0.417	0.329
	C_c	Specific Gravity	0.036	0.001	0.431

Table 3-9. Correlation of C_r for low plasticity clays

Type	Var1	Var2	Pearson's Correlation Coefficient	R-Squared	RMSE
Clays – (CL)	C_r	Effective Overburden Pressure (ksf)	0.032	0.001	0.049
	C_r	Wet Density (pcf)	-0.233	0.054	0.048
	C_r	Dry Density (pcf)	-0.324	0.105	0.047
	C_r	Natural Moisture (%)	0.381	0.145	0.046
	C_r	Automatic Hammer Blow Count	-0.089	0.008	0.049
	C_r	Fines (-200) (%)	0.050	0.003	0.049
	C_r	Liquid Limit (LL)	0.221	0.049	0.048
	C_r	Plasticity Index (PI)	0.091	0.008	0.049
	C_r	Initial Void Ratio (e_o)	0.374	0.140	0.046
	C_r	Specific Gravity	0.064	0.004	0.049

Table 3-10. Correlation of C_c for high plasticity clays

Type	Var1	Var2	Pearson's Correlation Coefficient	R-Squared	RMSE
Clays – (CH)	C_c	Effective Overburden Pressure (ksf)	-0.021	0.000	0.716
	C_c	Wet Density (pcf)	-0.702	0.494	0.510
	C_c	Dry Density (pcf)	-0.789	0.622	0.441
	C_c	Natural Moisture (%)	0.815	0.664	0.415
	C_c	Automatic Hammer Blow Count	-0.336	0.113	0.675
	C_c	Fines (-200) (%)	-0.116	0.013	0.712
	C_c	Liquid Limit (LL)	0.460	0.212	0.636
	C_c	Plasticity Index (PI)	0.361	0.130	0.668
	C_c	Initial Void Ratio (e_o)	0.829	0.687	0.401
	C_c	Specific Gravity	-0.047	0.002	0.716

Table 3-11. Correlation of C_r for high plasticity clays

Type	Var1	Var2	Pearson's Correlation Coefficient	R-Squared	RMSE
Clays – (CH)	C_r	Effective Overburden Pressure (ksf)	-0.079	0.006	0.089
	C_r	Wet Density (pcf)	-0.423	0.179	0.081
	C_r	Dry Density (pcf)	-0.467	0.218	0.079
	C_r	Natural Moisture (%)	0.454	0.206	0.079
	C_r	Automatic Hammer Blow Count	-0.167	0.028	0.088
	C_r	Fines (-200) (%)	-0.131	0.017	0.088
	C_r	Liquid Limit (LL)	0.439	0.193	0.080
	C_r	Plasticity Index (PI)	0.255	0.065	0.086
	C_r	Initial Void Ratio (e_o)	0.436	0.190	0.080
	C_r	Specific Gravity	-0.099	0.010	0.088

Table 3-12. Correlation of C_c for organic soils

Type	Var1	Var2	Pearson's Correlation Coefficient	R-Squared	RMSE
Organic Peat	C_c	Effective Overburden Pressure (ksf)	-0.261	0.068	2.116
	C_c	Wet Density (pcf)	-0.374	0.140	2.033
	C_c	Dry Density (pcf)	-0.602	0.363	1.750
	C_c	Natural Moisture (%)	0.706	0.499	1.552
	C_c	Automatic Hammer Blow Count	-0.162	0.026	2.163
	C_c	Fines (-200) (%)	-0.187	0.035	2.154
	C_c	Organic Content (%)	0.436	0.190	1.973
	C_c	Initial Void Ratio (e_o)	0.716	0.513	1.530
	C_c	Specific Gravity	-0.197	0.039	2.149

Table 3-13. Correlation of C_r for organic soils

Type	Var1	Var2	Pearson's Correlation Coefficient	R-Squared	RMSE
Organic Peat	C_r	Effective Overburden Pressure (ksf)	-0.222	0.049	0.297
	C_r	Wet Density (pcf)	-0.273	0.074	0.293
	C_r	Dry Density (pcf)	-0.467	0.218	0.269
	C_r	Natural Moisture (%)	0.541	0.293	0.256
	C_r	Automatic Hammer Blow Count	-0.182	0.033	0.300
	C_r	Fines (-200) (%)	-0.181	0.033	0.300
	C_r	Organic Content (%)	0.255	0.065	0.295
	C_r	Initial Void Ratio (e_o)	0.823	0.677	0.173
	C_r	Specific Gravity	-0.007	0.000	0.305

The team also evaluated the correlation between key index parameters and coefficient of consolidation (C_v) and secondary compression index (C_α). The key index parameters that were used include effective overburden pressure (ksf), wet density (pcf), dry density (pcf), natural moisture (%), sutomatic hammer blow count (N), fines (-200) (%), organic content (%), liquid limit (LL), plasticity index (PI), initial void ratio (e_o), and specific gravity. The soil types that were evaluated are, fine-grained soils, organic soils. Since C_v and C_α are a function of stress level, three categories of stress levels were selected: (1) low stress level in the range of 500-1,000 psf, (2) mid-stress level in the range of 2,000-3,000 psf, and (3) high stress level in the range of 5,000-6,000 psf. Thus, a total of nine data sets were prepared. Tables 3-14 through 3-25 contain the calculated Pearson's Correlation Coefficient values, Coefficient of Determination (R^2) values and Root Mean Square Error values (RMSE) for the above soil types.

Table 3-14. Correlation of C_v for fine-grained soil (at high stress level)

Type	Var1	Var2	Pearson's Correlation Coefficient	R-Squared	RMSE
Fine-grained (High)	C_v	Effective Overburden Pressure (ksf)	-0.323	0.104	0.294
	C_v	Wet Density (pcf)	0.053	0.003	0.311
	C_v	Dry Density (pcf)	0.106	0.011	0.309
	C_v	Natural Moisture (%)	-0.159	0.025	0.307
	C_v	Automatic Hammer Blow Count	-0.020	0.000	0.311
	C_v	Fines (-200) (%)	-0.180	0.033	0.306
	C_v	Liquid Limit (LL)	-0.047	0.002	0.311
	C_v	Plasticity Index (PI)	-0.107	0.012	0.309
	C_v	Initial Void Ratio (e_o)	-0.140	0.020	0.308
	C_v	Specific Gravity	-0.047	0.002	0.311

Table 3-15. Correlation of C_α for fine-grained soil (at high stress level)

Type	Var1	Var2	Pearson's Correlation Coefficient	R-Squared	RMSE
Fine-grained (High)	C_α	Effective Overburden Pressure (ksf)	-0.202	0.041	0.016
	C_α	Wet Density (pcf)	-0.592	0.351	0.013
	C_α	Dry Density (pcf)	-0.670	0.449	0.012
	C_α	Natural Moisture (%)	0.787	0.619	0.010
	C_α	Automatic Hammer Blow Count	-0.270	0.073	0.015
	C_α	Fines (-200) (%)	-0.254	0.065	0.015
	C_α	Liquid Limit (LL)	0.740	0.548	0.010
	C_α	Plasticity Index (PI)	0.726	0.527	0.011
	C_α	Initial Void Ratio (e_o)	0.675	0.456	0.012
	C_α	Specific Gravity	-0.672	0.451	0.012

Table 3-16. Correlation of C_v for fine-grained soil (at intermediate stress level)

Type	Var1	Var2	Pearson's Correlation Coefficient	R-Squared	RMSE
Fine-grained (intermediate)	C_v	Effective Overburden Pressure (ksf)	0.296	0.088	0.438
	C_v	Wet Density (pcf)	0.100	0.010	0.457
	C_v	Dry Density (pcf)	0.154	0.024	0.454
	C_v	Natural Moisture (%)	-0.182	0.033	0.451
	C_v	Automatic Hammer Blow Count	0.068	0.005	0.458
	C_v	Fines (-200) (%)	-0.100	0.010	0.457
	C_v	Liquid Limit (LL)	-0.077	0.006	0.458
	C_v	Plasticity Index (PI)	-0.096	0.009	0.457
	C_v	Initial Void Ratio (e_o)	-0.157	0.025	0.453
	C_v	Specific Gravity	-0.014	0.000	0.459

Table 3-17. Correlation of C_α for fine-grained soil (at intermediate stress level)

Type	Var1	Var2	Pearson's Correlation Coefficient	R-Squared	RMSE
Fine-grained (intermediate)	C_α	Effective Overburden Pressure (ksf)	-0.299	0.089	0.004
	C_α	Wet Density (pcf)	-0.625	0.391	0.003
	C_α	Dry Density (pcf)	-0.678	0.459	0.003
	C_α	Natural Moisture (%)	0.708	0.502	0.003
	C_α	Automatic Hammer Blow Count	-0.201	0.041	0.004
	C_α	Fines (-200) (%)	0.010	0.000	0.004
	C_α	Liquid Limit (LL)	0.559	0.313	0.004
	C_α	Plasticity Index (PI)	0.533	0.284	0.004
	C_α	Initial Void Ratio (e_o)	0.668	0.446	0.003
	C_α	Specific Gravity	-0.516	0.267	0.004

Table 3-18. Correlation of C_v for fine-grained soil (at low stress level)

Type	Var1	Var2	Pearson's Correlation Coefficient	R-Squared	RMSE
Fine-grained (low)	C_v	Effective Overburden Pressure (ksf)	0.341	0.116	0.424
	C_v	Wet Density (pcf)	0.075	0.006	0.450
	C_v	Dry Density (pcf)	0.104	0.011	0.449
	C_v	Natural Moisture (%)	-0.106	0.011	0.449
	C_v	Automatic Hammer Blow Count	0.026	0.001	0.451
	C_v	Fines (-200) (%)	-0.095	0.009	0.449
	C_v	Liquid Limit (LL)	-0.020	0.000	0.451
	C_v	Plasticity Index (PI)	-0.044	0.002	0.451
	C_v	Initial Void Ratio (e_o)	-0.090	0.008	0.449
	C_v	Specific Gravity	-0.009	0.000	0.451

Table 3-19. Correlation of C_α for fine-grained soil (at low stress level)

Type	Var1	Var2	Pearson's Correlation Coefficient	R-Squared	RMSE
Fine-grained (low)	C_α	Effective Overburden Pressure (ksf)	-0.191	0.036	0.003
	C_α	Wet Density (pcf)	-0.303	0.092	0.003
	C_α	Dry Density (pcf)	-0.388	0.151	0.003
	C_α	Natural Moisture (%)	0.450	0.203	0.003
	C_α	Automatic Hammer Blow Count	-0.298	0.089	0.003
	C_α	Fines (-200) (%)	0.097	0.010	0.003
	C_α	Liquid Limit (LL)	0.071	0.005	0.003
	C_α	Plasticity Index (PI)	0.089	0.008	0.003
	C_α	Initial Void Ratio (e_o)	0.332	0.110	0.003
	C_α	Specific Gravity	-0.435	0.189	0.003

Table 3-20. Correlation of C_v for organic peat (at high stress level)

Type	Var1	Var2	Pearson's Correlation Coefficient	R-Squared	RMSE
Organic peat (high)	C_v	Effective Overburden Pressure (ksf)	-0.152	0.023	0.707
	C_v	Wet Density (pcf)	0.007	0.000	0.715
	C_v	Dry Density (pcf)	-0.028	0.001	0.715
	C_v	Natural Moisture (%)	0.042	0.002	0.715
	C_v	Automatic Hammer Blow Count	-0.203	0.041	0.701
	C_v	Fines (-200) (%)	-0.270	0.073	0.689
	C_v	Organic Content (%)	0.411	0.169	0.652
	C_v	Initial Void Ratio (e_o)	0.251	0.063	0.693
	C_v	Specific Gravity	0.250	0.063	0.693

Table 3-21. Correlation of C_α for organic peat (at high stress level)

Type	Var1	Var2	Pearson's Correlation Coefficient	R-Squared	RMSE
Organic peat (high)	C_α	Effective Overburden Pressure (ksf)	-0.853	0.728	0.006
	C_α	Wet Density (pcf)	-0.316	0.100	0.010
	C_α	Dry Density (pcf)	-0.517	0.267	0.009
	C_α	Natural Moisture (%)	0.206	0.043	0.010
	C_α	Automatic Hammer Blow Count	-0.923	0.852	0.004
	C_α	Fines (-200) (%)	-0.927	0.859	0.004
	C_α	Organic Content (%)	-0.308	0.095	0.010
	C_α	Initial Void Ratio (e_o)	0.409	0.167	0.010
	C_α	Specific Gravity	0.555	0.308	0.009

Table 3-22. Correlation of C_v for organic peat (at intermediate stress level)

Type	Var1	Var2	Pearson's Correlation Coefficient	R-Squared	RMSE
Organic peat (intermediate)	C_v	Effective Overburden Pressure (ksf)	0.040	0.002	1.140
	C_v	Wet Density (pcf)	-0.092	0.009	1.137
	C_v	Dry Density (pcf)	-0.124	0.016	1.132
	C_v	Natural Moisture (%)	0.089	0.008	1.137
	C_v	Automatic Hammer Blow Count	-0.020	0.000	1.141
	C_v	Fines (-200) (%)	-0.374	0.140	1.059
	C_v	Organic Content (%)	0.416	0.173	1.038
	C_v	Initial Void Ratio (e_o)	0.235	0.055	1.109
	C_v	Specific Gravity	0.102	0.010	1.135

Table 3-23. Correlation of C_α for organic peat (at intermediate stress level)

Type	Var1	Var2	Pearson's Correlation Coefficient	R-Squared	RMSE
Organic peat (high)	C_α	Effective Overburden Pressure (ksf)	-0.853	0.728	0.006
	C_α	Wet Density (pcf)	-0.316	0.100	0.010
	C_α	Dry Density (pcf)	-0.517	0.267	0.009
	C_α	Natural Moisture (%)	0.206	0.043	0.010
	C_α	Automatic Hammer Blow Count	-0.923	0.852	0.004
	C_α	Fines (-200) (%)	-0.927	0.859	0.004
	C_α	Organic Content (%)	-0.308	0.095	0.010
	C_α	Initial Void Ratio (e_o)	0.409	0.167	0.010
	C_α	Specific Gravity	0.555	0.308	0.009

Table 3-24. Correlation of C_v for organic peat (at low stress level)

Type	Var1	Var2	Pearson's Correlation Coefficient	R-Squared	RMSE
Organic peat (low)	C_v	Effective Overburden Pressure (ksf)	-0.141	0.020	2.522
	C_v	Wet Density (pcf)	-0.091	0.008	2.537
	C_v	Dry Density (pcf)	-0.142	0.020	2.522
	C_v	Natural Moisture (%)	0.078	0.006	2.540
	C_v	Automatic Hammer Blow Count	-0.095	0.009	2.536
	C_v	Fines (-200) (%)	-0.411	0.169	2.322
	C_v	Organic Content (%)	0.380	0.144	2.357
	C_v	Initial Void Ratio (e_o)	0.204	0.042	2.494
	C_v	Specific Gravity	0.205	0.042	2.493

Table 3-25. Correlation of C_α for organic peat (at low stress level)

Type	Var1	Var2	Pearson's Correlation Coefficient	R-Squared	RMSE
Organic peat (low)	C_α	Effective Overburden Pressure (ksf)	-0.949	0.900	0.003
	C_α	Wet Density (pcf)	-0.592	0.351	0.007
	C_α	Dry Density (pcf)	-0.785	0.616	0.005
	C_α	Natural Moisture (%)	0.534	0.286	0.007
	C_α	Automatic Hammer Blow Count	-0.969	0.939	0.002
	C_α	Fines (-200) (%)	-0.722	0.522	0.006
	C_α	Organic Content (%)	-0.022	0.001	0.008
	C_α	Initial Void Ratio (e_o)	0.732	0.536	0.006
	C_α	Specific Gravity	0.455	0.207	0.007

3.4. Summary

The information presented in this chapter is crucial in the development of the regression models presented in Chapter 4. The provided datasets were analyzed for authenticity and application for the model development, and the following conclusions and data exclusions were drawn before model development commenced.

1) Coarse-grained material data set was not included in the final data set. Although the coarse-grained data set (i.e., fines < 50%) accounted for nearly 16% of both the collected C_c and C_r database, the utilization of coarse-grained material in the models were deemed not applicable. Coarse-grained material will generally be governed by elastic settlement and developed pore-water pressures will dissipate much quicker, therefore not following the mechanisms of consolidation settlement. Therefore, developing models for this soil group will inherently be inaccurate due to the inaccuracy of the input variables. Also, truly "undisturbed" sample retrieval of coarse-grained material is much more difficult causing concerns regarding the quality of the lab test results. Due to these factors, the authors did not include any coarse-grained models in this presented study.

2) Generally, within the provided datasets, natural moisture content ($w\%$) and initial void ratio (e_o) showed the strongest Pearson correlation to the consolidation parameters. This finding is apparent when comparing the information presented in Tables 3-4 through 3-25. This is also somewhat expected since both parameters can be directly related to the mechanics of consolidation settlement (i.e., dissipation of water pressure and subsequent decrease in void ratio). However, since the void ratio cannot be measured through simple index testing, and within the dataset was either determined through consolidation testing or correlations, it will be excluded from the models developed in the next chapter. This is again due to the overall goal of this research to bypass the reliance on high-quality sample retrieval and time-exhausting consolidation testing.

Although the authors believe each of the conclusions above may warrant additional study to fully characterize the effects of each, they are not included in the scope of this study. The following chapter presents the methodology implemented to create the statistical models to be used in prediction of consolidation parameters specific for Florida soils.

4. DEVELOPMENT OF SOIL COMPRESSIBILITY MODELS

4.1. Methodology

The application of a machine learning approach was implemented to develop soil compressibility prediction models for Florida's soil data. The concept of machine learning, in the form of classification, is the process of estimating the category of a previously unknown object, out of a finite set of predefined categories based on a set of objects whose category is known (Bishop, 2006). A pool of objects that are pre-labeled, are used as the training set for machine learning algorithms. The training set is used to infer a mapping function. The mapping function is then used to predict the category of new objects/observations (O. P. Panagopoulos, Pappu, Xanthopoulos, & Pardalos, 2016; Pappu, Panagopoulos, Xanthopoulos, & Pardalos, 2015).

Applications of machine learning in civil engineering include but are not limited to: the prediction of tunnel support stability using artificial neural networks (Leu, Chen, & Chang, 2001), predicting the remaining service life of bridge decks (Melhem & Cheng, 2003), predicting the ground surface settlement induced by deep excavation using artificial neural networks (Sou-Sen & Hsien-Chuang, 2004), optimizing the energy efficiency of buildings and their cooperation (Alam, Panagopoulos, Rogers, Jennings, & Scott, 2014; A. A. Panagopoulos, Alam, Rogers, & Jennings, 2015; A. A. Panagopoulos, Jennings, Maleki, Rogers, & Venanzi, 2017), and predicting and optimizing building-integrated renewable energy resources.

The data was assumed to fall into different classifications and was tested to determine if different models for each soil type was necessary. In addition to the correlated parameters summarized in Tables 3-2 and 3-3, this study accounted for other soil descriptors such as automatic hammer Standard Penetration Test (SPT) blow count (N), plasticity index (PI), overburden stress (σ), and fines content (-200) of the soil, defined as the portion of the soil sample that has a particle diameter smaller than 0.074 mm (Bowles, 1989). Including these parameters may increase the predictive capability of models generated. As part of the study, existing correlations were tested to determine their predictive capability and compared to the new models that were generated from the data collected.

4.2. Model Development Procedure

In this chapter, the procedure to develop the soil compressibility prediction models is explained in detail, including the theoretical background of the model development, and the model validation procedure and results.

Figure 4-1 presents an overview of the methodology used for the data analysis. First, the collected data was evaluated for completeness. The difference in number between the total dataset (with some missing parameters) and the full dataset is significant. For example, the total and full datasets of clay contain 396 and 254 data points, respectively. The total and full datasets of silts are 31 and 16 data points, respectively. Thus, data will be brought to a form that has no missing values through

data imputation, which will also reduce the effect of outliers. During the preprocessing step, data is normalized and prepared for the next step, which is classification. In this stage, the number of distinct groups of soil that exist is determined for classification purposes. A regression model was then developed for each distinct group during the model development phase. Details of each step are presented below.

4.2.1. Data Imputation

The total number of C_c and C_r data points collected throughout the state of Florida are 551 and 490, respectively. The full dataset includes values of specific soil and site conditions such as: effective overburden pressure (s_o' in ksf), wet density (γ in pcf), dry density (γ_d in pcf), natural moisture content (w in %), automatic hammer blow count (N in blows/ft), fine content (-200 in %), initial void ratio (e_o), specific gravity (G_s), and Atterberg plasticity testing (LL, PI, in %). Also with each data point includes the results from a consolidation test, thus providing a corresponding value for compression index (C_c), recompression index (C_r), coefficient of consolidation (C_v), and coefficient of secondary compression (C_α). It is important to note that safety SPT N-values were converted to an automatic hammer blow count by the conversion factor of 1.24, as recommended by the FDOT's Soil and Foundation Handbook (Florida Department of Transportation, 2019). In addition, the initial void ratio was not included in the model because it is obtained directly from the consolidation test. Both wet and dry density values were estimated by either Standard Penetration Test blow count or moisture-related equations, thus both will also not be included in the models.

Figure 4-1. Standard methodology used for data analysis

Not all individual datasets had complete information. Some of the information (referred as descriptors or attributes in the statistical analysis) was missing and those are referred to as "missing dataset" herein. The numbers of missing datasets for C_c and C_r were 551 and 490, respectively. Therefore, the issue of missing attributes was addressed using two different approaches. Any missing descriptor values was substituted with the best-approximated values. The samples for which some of the soil compressibility parameters were missing were planned to be discarded. However, this time the samples for which some of the descriptors were missing will be completed with approximation values. Several methods were trialed to approximate the missing attributes, including: mean value imputation, interpolation, and k-Nearest Neighbor imputation. It was

determined that the *k-nearest neighbor imputation* method achieved the best results. The steps for this method are below.

Missing values are imputed from samples with similar characteristics to the incomplete samples. If an incomplete sample had a missing value of a particular attribute, the missing value (*k*) was determined from other samples which had a value present on that of that attribute with values more similar (in terms of their Euclidean distance, shown in equation 4.1) to that incomplete sample. The missing value of the incomplete sample was calculated as the result of average the values of the missing attribute from the *k* of the nearest neighbors to the incomplete sample.

$$D(a,b) = \sqrt{\sum_{i=1}^{n}(x_i - y_i)^2} \qquad (4.1)$$

Figure 4-2 and Table 4-1 show an arbitrary example of the aforementioned steps. The sample that appears in red has a missing value on specific gravity. The values of all samples as well as their distances to the red sample appear in Table 4-1. We set the value of *k* equal to three. We will then seek to find three other samples (highlighted by red circle), which have a value present on Specific Gravity with values closest to that incomplete sample (i.e., wet density and dry density) without missing values. The missing value for specific gravity of the incomplete sample (red in Figure 4-2) will be calculated as the result of averaging the values of specific gravity from the three nearest neighbors to the incomplete sample. The calculated missing value appears in Table 4-2.
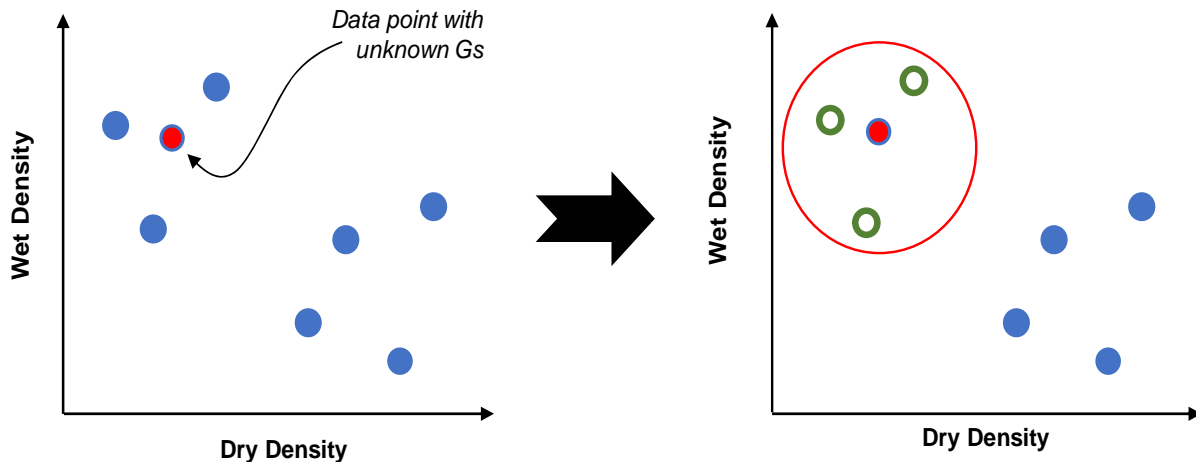
Figure 4-2. Illustrative example of samples with three variables and using Euclidean distance to estimate missing variable of one data point.

Table 4-1. Numerical example of imputation processes calculating Euclidean distance (from Figure 4-2).

	Specific Gravity	Wet Density (pcf)	Dry Density (pcf)	Euclidean Distance, D
Green Sample	2.71	97.0	61.0	$\sqrt{(97-91.2)^2+(61-53)^2}=9.88$
Green Sample	2.69	85.94	59.9	8.67
Green Sample	2.55	96.84	47.0	8.23
Blue Sample	1.90	88.03	95.0	42.11
Blue Sample	2.89	90.5	93.0	40.00
Blue Sample	2.20	93.9	85.0	32.11
Blue Sample	1.95	79.9	89.9	38.59
Blue Sample	2.35	78.0	91.0	40.22
Red Sample	?	91.2	53.0	

Table 4-2. Numerical example of imputation and interpolation of missing G_s parameter from values with smallest Euclidean distance (shown with *).

	Specific Gravity	Wet Density (pcf)	Dry Density (pcf)	Euclidean Distance
Green Sample	**2.71**	97.0	61.0	*9.88
Green Sample	**2.69**	85.94	59.9	*8.67
Green Sample	**2.55**	96.84	47.0	*8.23
Blue Sample	1.90	88.03	95.0	42.11
Blue Sample	2.89	90.5	93.0	40.00
Blue Sample	2.20	93.9	85.0	32.11
Blue Sample	1.95	79.9	89.9	38.59
Blue Sample	2.35	78.0	91.0	40.22
Red Sample	$= \dfrac{2.71+2.69+2.55}{3}$ $= \mathbf{2.65}$	91.2	53.0	

When *k-nearest neighbor* imputation is applied the dimensionality of the dataset will be higher than that of the samples shown in the previous illustrative example. For instance, a clay will have a dimensionality of ten since it has the following ten descriptors: pressure, wet density, dry density, natural moisture, automatic hammer blow count, fines, liquid limit, plasticity index, initial void ratio, and specific gravity. Since the algorithm uses distance to learn, data will be rescaled through normalization before *k-nearest neighbor* is applied.   An example of the calculated missing value and distances for a normalized clay sample is shown in Table 4-3. The missing value for pressure of the incomplete sample (sample 4) is calculated as the result of averaging the values of pressure from the three nearest neighbors that appear in bold.

The Euclidean distance (D) of all samples to sample 4 for this example was calculated as:

$$D = \sqrt{\begin{array}{l}(WD1 - WD2)^2 + (DD1 - DD2)^2 + (w1 - w2)^2 + (N1 - N2)^2 \ldots \\ + (F1 - F2)^2 + (LL1 - LL2)^2 + \ldots (PI1 - PI2)^2 + (e_o1 - e_o2)^2 + (G_s1 - G_s2)^2\end{array}}$$

Table 4-3. Arbitrary example of how to calculate missing parameter with ten attributes, using Euclidean distance equation above.

	Pressure	*WD*	*DD*	*w*	*N*	*F*	*LL*	*PI*	*e_o*	*G_s*	*D*
Sample 1	**0.06**	0.15	0.42	0.02	0.76	0.01	0.85	0.98	0.74	0.13	0.76
Sample 2	**0.04**	0.19	0.92	0.05	0.74	0.06	0.82	0.22	0.45	0.13	0.80
Sample 3	**0.02**	0.30	0.45	0.02	0.85	0.03	0.45	0.32	0.89	0.47	0.24
Sample 4	$\frac{1}{3}(0.04 + 0.06 + 0.02)$ $= 0.04$	0.36	0.49	0.09	0.88	0.07	0.64	0.42	0.90	0.50	

After applying the *k-Nearest Neighbor imputation* method, the resulting dataset has the same number of attributes as the full dataset (i.e., the samples without missing values). High values of parameter *k* are chosen when using the method to make it more robust and to decrease the effect of outliers on the dataset.

4.3. Theoretical Background

An automatic classification approach called Support Vector Machines (SVM) was employed to determine the number of distinct groups of soil that exist and require separate statistical models. A theoretical explanation of the SVM data processing process is presented herein.

4.3.1. Support Vector Machine (SVM)

The classification model was developed such that it assisted in determining the number of distinct groups of soil that exist. Through this process, the goal was to confirm or reject the hypothesis that each soil type requires a different statistical model. The data were divided into two sets: the training set and the testing set. The training set is composed of data used to teach the supervised learning algorithm, while the testing set will remain a set of unclassified data used to evaluate the accuracy and predictability of the trained algorithm. The collected data indicate that the classes are highly variant in terms of size. The discrepancy in size between the classes has the potential to affect the efficient training of our model and thus needs to be taken into consideration. To that end, when building the model, a class weighting scheme was utilized in the optimization process. This was done to address the issue of having a different number of samples from each soil type. The class weighting scheme that was followed is a one-verse-all approach of SVM. The multiclass problem will be decomposed into four binary classification scenarios. In particular, four binary classifiers were built where the nth classifier separates the nth class from the rest. The class of a new point is then determined according to a majority voting principle. The trained model is then evaluated using the remaining data, which encompasses the test set. The classification results of the test set will aid in the confirmation or rejection of the hypothesis that each soil type requires a different statistical model.

If data can be separated with a hyperplane or decision surface in the trained SVMs, that will be an early indication that a regression model is needed for each distinct classification (e.g., fine-grained vs. organic peat). Figure 4-3 demonstrates instances of trained SVMs. The straight line represents the two-dimensional decision surface. The figure depicts an instance in which data are separable, and thus, a regression model will need to be developed for each classification of data (i.e., blue filled circle vs. green empty).
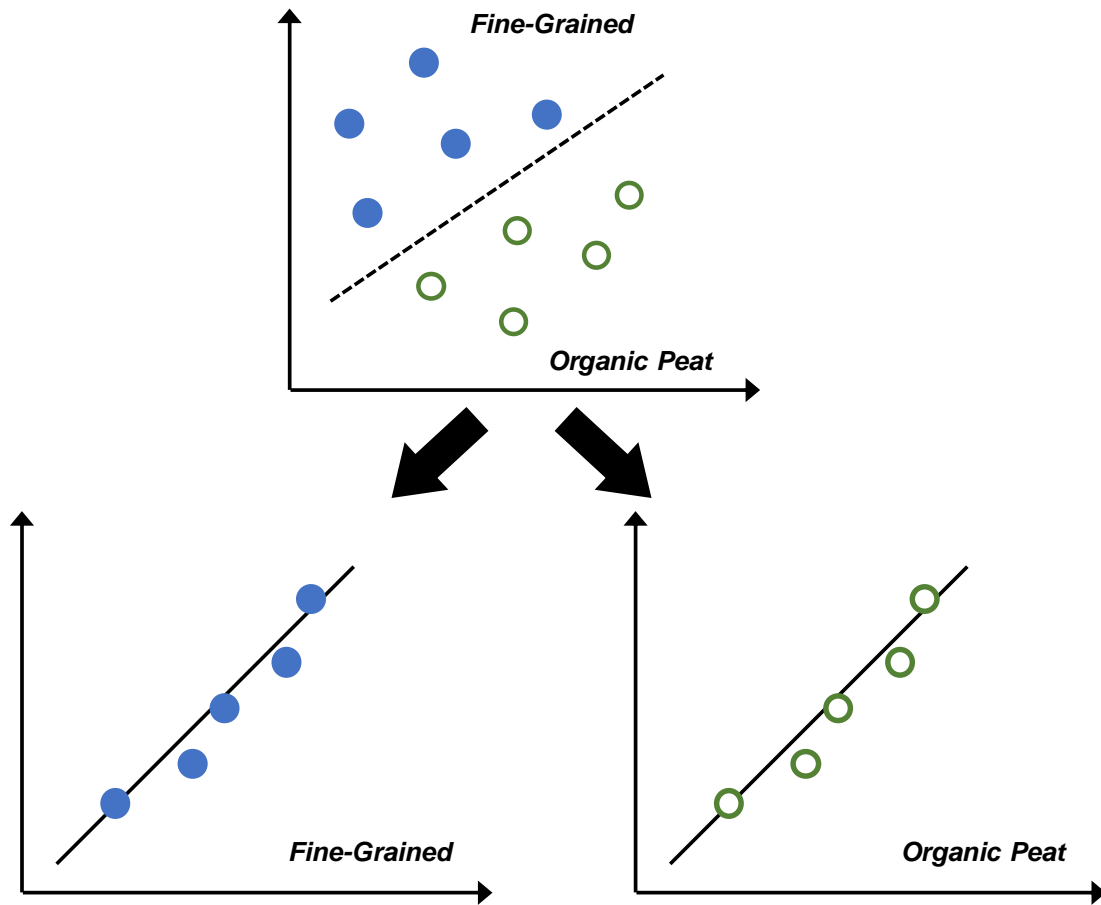
Figure 4-3. Theoretical example of regression model development for two distinct classifications of data.

Figure 4-4, on the other hand, demonstrates an inseparable dataset. This example suggests that the organic silt/clay class and fine-grained class will need to be grouped together when it comes to the development of the regression models. That is, there lacks a significant differentiation between the two data sets and a single regression model should be developed to represent the group of samples that encompasses both organic silt/clay and fine-grained samples. Once the necessary number of distinct groups were determined, the corresponding C_c, C_r, C_v, and C_α models were developed for each classification group; presented in Section 4.4.
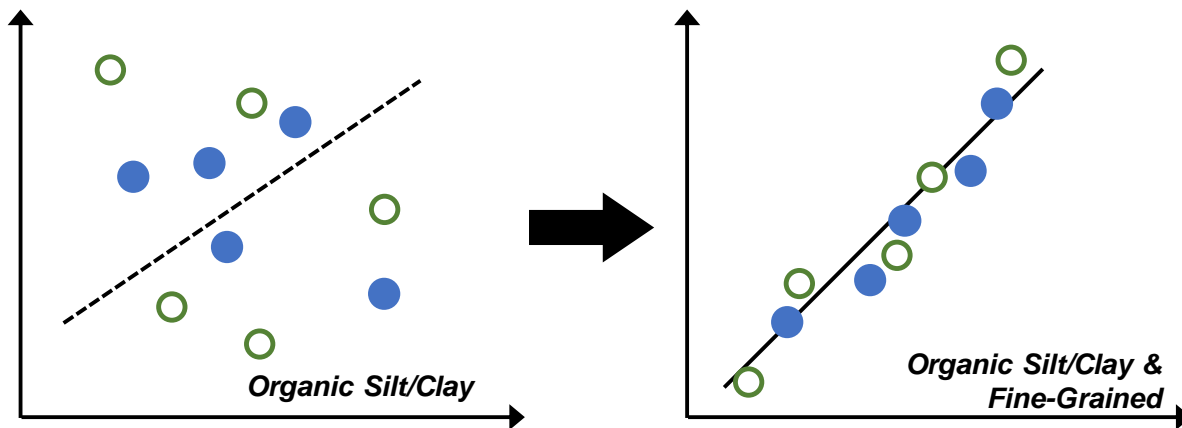
Figure 4-4. Theoretical example of an inseparable dataset. Suggesting that datasets of organic silt/clay and fine-grained will need to be grouped together for accurate regression model.

4.3.2. Multi-Variate Regression Model

The forward selection stepwise regression procedure was used to minimize the term-trusted "goodness of fit" measure Bayesian Information Criterion (BIC). The variable selection procedure used during the forward selection stepwise regression takes into consideration the correlation coefficients of the participating variables to minimize multicollinearity. At the first step of the process, the initial regression model for every group of samples will contain no variables. At each iteration, the present independent variable in the equation will be help fixed and only the variable that is the most highly correlated with the response variable (i.e., C_c, C_r, C_v and C_α) enters the regression model. This procedure leads to the most parsimonious model while trying to eliminate multicollinearity. The multicollinearity refers to the problems that arise in regression models when some of the predictors are highly correlated with each other. Although multicollinearity by itself does not affect the predictive performance of the model, it may negatively influence the determination of which factors are the most significant. Multicollinearity essentially obstructs the effective choosing of the right predictors to include in the predictive model, making it hard to obtain a parsimonious model. Parsimony is an essential property of every effective prediction model. We obtain more insight into the influence of the predictors in models with few parameters. Moreover, using predictors that are uncorrelated with the response variable may result in instability

of the developed regression. That in turn might influence the ability of the model to generalize correctly. In practice, this means that we cannot make accurate predictions with data that was not used to train the model, neglecting the whole purpose for these statistically developed prediction models. The *forward selection stepwise regression* procedure that was used in this study leads to models that are based only on the most influential parameters, thus bypassing the previously mentioned limitations.

4.4. Soil Compressibility Models

Eight variables were analyzed to determine their potential impact on the correlations to the four soil compressibility characteristic parameters (i.e., C_c, C_r, C_v and C_α) for CH, CL, MH, OH, OL, and Pt soil classification types. It is noted that the data for the ML classification was not sufficient for the model development. These parameters include the moisture content (w), automatic hammer SPT blow count (N), overburden stress (σ), fines content (-200), liquid limit (LL), Percent organic content (OC %), plasticity index (PI), and specific gravity (G_s).

Strength of correlation parameters, such as root mean square error values, coefficient of determination and adjusted coefficient of determination values, were noted. A perfect correlation yields an R^2 value of 1.0 and an RMSE value of 0.0. Models with an R^2_{adj} value of 0.5 or higher were used for predictions.

It is important to note that some of the datasets had limited number of data points (less than 20). These limited datasets included the MH and OL models for C_c and C_r, and the organic soil model for C_α. High R^2 values are shown for the MH and C_c, OL and C_r, and Organic and C_α models. Therefore, it is recommended that the MH and OL models need additional validation.

4.4.1. C_c Models

Table 4-4 presents the developed C_c models for the classified soil types of CH, CL, MH, OH, OL, Pt. The table includes the information of model equation, soil type, input variables, the model accuracy (e.g., R^2 and RMSE). Both full and reduced models were constructed and the CH, CL, OH, OL, and Pt models have the same results. The reduced models include minimum number of required variables but have similar prediction accuracy from a statistical point of view.

Table 4-4. Statistical strength of developed correlations – C_c

Equation	Notes	Input variables	R^2	R^2_{adj}	RMSE
C_c = - 1.4045 + 0.0155 * w + 0.0005 * LL + 0.398 * Gs - 0.00003 * [(w - 68.837) * (LL -105.48)] - 0.00002 * [(w - 68.837) * (w - 68.837)]	CH	w, LL, Gs	0.731	0.726	0.375
Reduced C_c -> Same as C_c	CH	w, LL, Gs			
C_c = - 1.6912 + 0.0118 * w + 0.5919 * Gs	CL	w, Gs	0.525	0.495	0.174
Reduced C_c -> Same as C_c	CL	w, Gs			
C_c = - 8.4424 + 0.0077 * w + 0.0085 * Fines (-200) + 0.0143 * PI + 2.7149 * Gs + 0.0828 * [(w - 89.8) * (Gs – 2.664)]	MH	w, Fines, PI, Gs	0.984	0.975	0.075
Reduced C_c = - 9.2573 + 0.0087 * w + 0.009 * PI + 3.337 * Gs + 0.1095 * [(w - 89.8) * (Gs – 2.6635)]	MH	w, PI, Gs	0.935	0.906	0.145
C_c = -0.4799 + 0.076 * σ_o'(ksf) + 0.0098 * w + 0.0046 * PI + 0.0005 * [(σ_o'(ksf) – 1.445) * (w – 123.02)] + 0.0036 * [(σ_o'(ksf) – 1.445) * (PI – 81.879)]	OH	σo', PI, w	0.793	0.779	0.439
Reduced C_c -> Same as C_c	OH	σo', PI, w			
C_c = 0.8164 + 0.0096 * w - 0.0145 * Fines (-200)	OL	w, Fines	0.488	0.428	0.564
Reduced C_c -> Same as C_c	OL	w, Fines			
Cc = - 10.7737 + 0.0078 * w + 0.0772 * OC + 2.8672 * Gs + 0.0074 * [(w – 481.673) * (Gs - 1.5677)] - 0.2644 * [(OC – 83.0208) * (Gs - 1.5677)] + 0.0075 * [(OC – 83.0208)²]	Pt	w, OC, Gs	0.795	0.765	1.284
Reduced C_c -> Same as C_c	Pt	w, OC, Gs			

4.4.2. C_r Models

Table 4-5 presents the developed C_r modes for each respective soil classification. Both full and reduced models were constructed. The CL and Pt models have the same results.

Table 4-5. Statistical strength of developed correlations – C_r

Equation	Notes	Input variables	R^2	R^2_{adj}	RMSE
C_r = - 0.0057 - 0.00069 * σo' (ksf) + 0.0012 * w + 0.0015 * N + 0.00007 * LL - 0.0196 * LI - 0.0014 * [(σo'(ksf) -1.986) * (w - 68.175)] + 0.0009 * [(σo'(ksf) -1.986) * (LL - 105.323)] + 0.0603 * [(σo'(ksf) -1.986) * (LI – 0.520)] + 0.00008 * [(w - 68.175) * (N - 5.473)] + 0.000009 * [(w - 68.175) * (LL - 105.323)] + 0.0005 * [(w - 68.175) * (LI – 0.520)]	CH	σo', w, N, LL, LI	0.608	0.590	0.069
Reduced C_r = - 0.0136 - 0.0023 * σo'(ksf) + 0.0014 * w + 0.0001 * LL - 0.0004 * [(σo'(ksf) -1.986) * (w - 68.175)] + 0.0002 * [(σo'(ksf) -1.986) * (LL- 105.323)] + 0.000007 * [(w - 68.175) * (LL- 105.323)]]	CH	σo', w, LL	0.527	0.516	0.076
C_r = - 0.05 + 0.0021 * w + 0.0018 * N	CL	w, N	0.312	0.269	0.047
Reduced C_r -> Same as C_r	CL	w, N			
C_r = - 3.5505 + 0.0014 * w - 0.009 * N + 0.0006 * PI + 1.324 * Gs - 0.00002 * [(w – 100.99) * (PI – 48.0397)] + 0.0254 * [(w – 100.99) * (Gs – 2.656)]	MH	w, N, PI, Gs,	0.100	0.999	0.002
Reduced C_r = -3.0434 + 0.0014 * w -0.0063 * N + 1.1368 * Gs + 0.0244 * [(w – 100.99) * (Gs – 2.656)]	MH	w, N, Gs	0.940	0.892	0.022
C_r = -0.1101 + 0.0485 * σo'(ksf) + 0.0019 * w - 0.0042 * N - 0.0000002 * LL - 0.0022 * OC + 0.0004 * PI + 0.0051 * [(σo'(ksf) - 1.4864) * (OC-21.652)] - 0.0008 * [(N - 3.05) * (OC -21.6517)] -0.00003 * [(LL - 150.138) * (OC - 21.6517)]	OH	σo', w, N, LL, OC, PI	0.742	0.703	0.077
Reduced C_r = -0.0667 + 0.0326 * σo'(ksf) + 0.002 * w - 0.0036 * OC + 0.0029 * [(σo'(ksf) – 1.4864) * (OC – 21.6517)]	OH	σo', w, OC	0.565	0.538	0.096
Cr = 0.8808 + 0.0346 * σo'(ksf) + 0.0002 * w + 0.0048 * OC − 0.048 * PI + 0.0121 * [(σo'(ksf) - 1.015) * (PI - 20.2964)] - 0.0069 * [(OC – 17.8) * (PI - 20.2964)] - 0.0188 * [(σo'(ksf) - 1.015) * (σo'(ksf) - 1.015)] + 0.0006 * [(OC – 17.8)²]	OL	σo', w, OC, PI	0.100	0.998	0.002

Equation	Notes	Input variables	R^2	R^2_{adj}	RMSE
Reduced Cr = 2.3651 + 0.0039 * σo'(ksf) + 0.011 * OC − 0.1212 * PI + 0.0586 * [(σo'(ksf) - 1.015) * (PI − 20.2964)] - 0.0167 * [(OC − 17.8) * (PI − 20.2964)] - 0.0263 * [(σo'(ksf) - 1.015) * (σo'(ksf) - 1.015)] + 0.0009 * [(OC − 17.8)²]	OL	σo', OC, PI	0.991	0.961	0.008
Cr = - 0.5938 + 0.0009 * w + 0.3356 * Gs + 0.5344 * [(Gs - 1.4373)²] + 0.0017 * [(w - 472.835) * (Gs - 1.4373)]	Pt	w, Gs	0.768	0.739	0.182
Reduced C$_r$ -> Same as C$_r$	Pt	W, Gs			

4.4.3. C$_v$ Models

Table 4-6 presents the developed C_v models for the classified soil types. Due to the limited number of data points, the models are constructed on three soil types of clay, organic, and peat. Both full and reduced models were constructed. Overall R^2 values are low and the models with $R^2 > 0.5$ are recommended and considered to have reasonable accuracy.

Table 4-7. Statistical strength of developed correlations – C_v

Equation	Notes	Input variables	R^2	R^2_{adj}	RMSE
C$_v$ = - 3.3179 + 0.121 * σo'(ksf) + 0.0023 * w − 0.0283 * N - 0.0099 * Fines − 0.8108 * Gs − 0.00003 * Stress Level - 0.0592 * [(σo'(ksf) - 1.5932) * (N − 4.5071)] + 0.0024 * [(w - 57.1574) * (N − 5.5071)] - 0.0074 * [(N − 4.5071)) * (Fines(-200) − 82.1046)] + 0.151 * [(σo'(ksf) - 1.5932) * (σo'(ksf) - 1.5932)] + 0.0000000009 * [(Stress Level − 4,909.97 * (Stress Level − 4,909.97)]	Clay	σo', w, N, Fines, Gs, Stress level	0.226	0.215	0.914
Reduced C$_v$ = 0.788 + 0.1213 * σo'(ksf) − 0.02 * N - 0.0058 * Fines(-200) − 0.0718 * [(σo'(ksf) - 1.5932) * (N − 4.5071)] - 0.0043 * [(N − 4.5071)) * (Fines(-200) − 82.1046)] + 0.1231 * [(σo'(ksf) - 1.5932)²]	Clay	σ$_o$', N, Fines	0.146	0.139	0.957
C$_v$ = 1.1395 − 0.0022 * w + 0.0556 * N + 0.0018 * PI + 0.00001 * Stress Level − 0.4432 * Gs	Organic	w, N, PI	0.090	0.047	0.333
Reduced C$_v$ = 1.1959 − 0.0625 * N + 0.002 * PI + 0.000009 * Stress Level	Organic	N, PI, Stress level	0.068	0.042	0.334

Equation	Notes	Input variables	R^2	R^2_{adj}	RMSE
C_v = 11.7596 + 0.0815 * N - 0.0762 * Fines(-200) + 0.0317 * OC - 3.1765 * Gs - 0.0002 * Stress Level - 0.0024 * [(Fines(-200) - 56.9176) * (OC – 59.522)] - 0.1156 * [(OC - 59.522) * (Gs – 1.9426)] - 0.00001 * [(OC - 59.522) * (Stress Level – 2391.88)] - 0.0005 * [(Gs - 1.9426) * (Stress Level – 2391.88)] - 0.4487 * [(N - 2.1618)^2] − 0.0004 * [(Fines (-200) - 56.9176)^2]	Peat	N, Fines, OC, Gs, Stress level,	0.522	0.491	1.519
Reduced C_v = 7.7106 + 0.0644 * N - 0.0647 * Fines (-200) + 0.0415 * OC - 2.014 * Gs - 0.0019 * [(Fines (-200) - 56.9176) * (OC – 59.522)] − 0.1051 * [(OC - 59.522) * (Gs – 1.9426)] - 0.3782 * [(N - 2.1618)^2] - 0.0005 * [(Fines(-200) - 56.9176)^2]	Peat	N, Fines, OC, Gs	0.433	0.407	1.640

*Note: Stress level = lb/ft^2 (psf)

4.4.4. C_a Models

Table 4-7 presents the developed C_α models for the soil types of clay, organic and peat. Both full and reduced models were constructed. The clay and peat models have the same results.

Table 4-9. Statistical strength of developed correlations – C_α.

Equation	Notes	Input variables	R^2	R^2_{adj}	RMSE
C_α = - 0.0077 + 0.0001 * w + 0.000002 * PI + 0.0000006 * Stress Level - 0.000000009 * [(w - 60.3376) * (Stress Level – 10,084.8)] + 0.000004 * [(PI - 70.5461)^2] - 0.000000000002 * [(Stress Level – 10,084.8)^2]	Clay	w, PI, Stress level	0.545	0.525	0.007
Reduced C_α -> Same as C_α	Clay	w, PI, Stress level			
C_α = - 0.09 + 0.0001 * w + 0.0002 * Fines(-200) + 0.0001 * PI + 0.0185 * Gs + 0.000002 * Stress Level + 0.00000002 * [(w - 95.9455) * (Stress Level – 5,674.24)] + 0.00000003 * [(Fines(-200) - 60.0606) * (Stress Level – 5,674.24)] + 0.00000004 * [(PI - 92.455) * (Stress Level - 5674.24)] + 0.000008 * [(Gs - 2.4) * (Stress Level – 5,674.24)]	Organic	w, Fines, PI, Gs, Stress level	0.952	0.933	0.005

Table 4-10. Continued, Statistical strength of developed correlations – C_α (continued)

Correlation	Soil	Variables			
Reduced C_α = - 0.0436 + 0.0002 * PI + 0.0097 * Gs + 0.000001 * Stress Level + 0.00000006 * [(PI - 92.455) * (Stress Level - 5674.24)] + 0.000004 * [(Gs - 2.4) * (Stress Level - 5674.24)]	Organic	PI, Gs, Stress level	0.840	0.810	0.008
C_α = - 0.0660 + 0.00005 * w + 0.0006 * OC + 0.000008 * Stress Level + 0.00000002 * [(w − 575.783) * (Stress Level − 2,020.6)] + 0.0000004 * [(OC (%) − 64.933) * (Stress Level − 2,020.6)]	Peat	w, OC, Stress level	0.778	0.732	0.009
Reduced C_α -> Same as C_α	Peat	w, OC, Stress level			

*Note: Stress level = lb/ft^2 (psf)

4.5. Delineation Analysis

A specific range of input variables may have a higher influence on the soil compressibility parameters. A process to develop segmented regression models was introduced that was able to capture and express the variations of C_c and C_r and their corresponding model input variables. The breakpoints of influential factors (e.g., LL, PI, OC) on C_c and C_r from the dataset were determined so that the prediction accuracy of the proposed correlation models was evaluated.

4.5.1. Methodology

The overall process framework is shown in Figure 4-5. For the segmented regression models, the first step is the discovery of a particular value (or breakpoint) of a parameter for which its influence on the response variable (C_c or C_r) drastically changes. Secondly, two regression models were developed that fit the two different segments of data. The publicly-available computer program (SegReg) was used to perform the calculations and to find the breakpoint. A regression model was fit to the entire dataset and its resulting R^2 value was recorded.

Data was then sorted in increasing order with respect to the influential parameter of interest and split into two groups. The first group consisted of a small number (k) of data points which present a low-value influential parameter while the second group contained those data points having a high-value influential parameter (i.e., the rest $n - k$ data points). The two regression models were fit to the two groups and their R^2 values were recorded.

Data were then split into two new groups at a different breakpoint such that the first group had $k + 1$ data points, while the second contained $n - k - 1$ data points. The data point that was transferred to from the second group to the first one was that with the lowest value influential parameter among the data points of the second group. Two new regression models were fit to the two groups and their R^2 values were recorded. The aforementioned process was repeated until the first group contained $k + n - l$ points and the second group contained a small number of points.

50

The values of k and l are chosen by the user, are dataset specific, and depend on the number of samples one has access to.

The highest achieved R^2 value was identified and compared to the R^2 that was recorded when a regression model was fit to the entre dataset at the beginning of the process. If any of the coefficients of determination values of the regression lines that were fit to the segmented data were higher than the R^2 value of the regression line that was fit to the entire dataset then the corresponding breakpoint was recorded. That particular recorded value (breakpoint) of the influential parameters for which its influence on the response changes, was used in the second step of the process.

At the second step of the process, a piecewise regression model was developed that fit the two different segments of data. At this step, the developed models considered all the attributes (variables) of the dataset as potential predictors for the response.
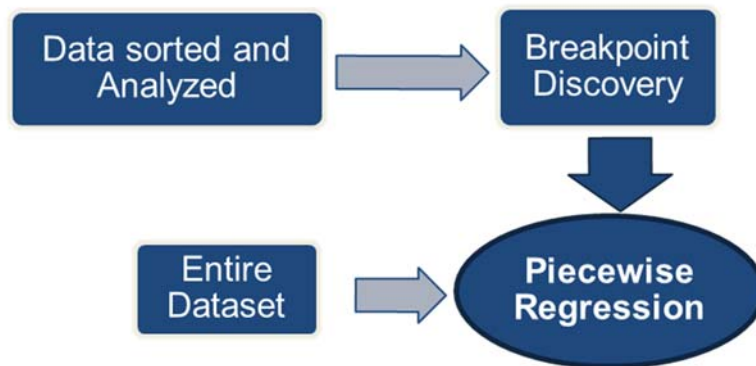
Figure 4-5. Process utilized for development of piecewise regression and delineation determination.

4.5.2. Delineation Analysis Results

For clays and silts, the Atterberg limits (LL, PL, and PI) were used to check the breakpoints. For the organic soil data group, the organic content (OC) of soil was used. Tables 4-8 and 4-9 present the analysis results and respective breakpoints and resulting R^2_{adj} factor for each range of data shown (i.e., breakpoint). In this way, the accuracy of the model in segmented data was checked. For some cases, (e.g., organic soils with C_c model) the resulting R^2_{adj} values were virtually the same, meaning the model accuracy was similar through the whole range of data (diverse). Other cases (e.g., silt model with C_c in Table 4-8) showed that the developed model (see Table 4-4) had a higher accuracy when the LL value was less than 69.8%.

An interesting conclusion from the breakpoint analysis was that the organic soils seem to show a significant change in C_r-model accuracy when the breakpoint is at roughly 75% organic content (OC). This supports the suggested classification differentiation between "Peat" soils and "Organic" soils, as suggested in the FDOT's Soils and Foundation Handbook (Florida Department of Transportation, 2019). All other *fine-grained soils* (i.e., clays and silts) showed little change in model accuracy for between the breakpoint values, suggesting that the specific degree of LL and PI does not affect the soils resulting compressibility indices. This initial finding suggests that the dataset of Florida soils tested may not strictly adhere to the traditional classification of the soils' level of plasticity that is Casagrande's plasticity chart (i.e., LL=50%) (1948). The initial statistics (albeit based on limited dataset) suggests there may be a different *break-point* to distinguish between soils following a "high" and "low" plasticity characteristic, which in turn would provide to better way of estimating compressibility parameters through correlations. . Although the breakpoints determined for clays and silts are near the suggested threshold of plasticity (i.e., LL = 50%) for both Cr and Cc models, the resulting $R^2_{adj.}$ shows little change in model. This finding, however, could simply be a result of insufficient number of data points in the lower plasticity ranges, and additional data collection and analysis would be required to draw further conclusions.

Table 4-11. Delineation analysis results for C_c models

Notes	Breakpoint	R^2_{adj}
C_c Models – See Table 4-4		
Clays	LL < 85.6	0.482
Clays	LL > 85.6	0.427
Clays	PI < 33.3	0.155
Clays	PI > 33.3	0.386
Organic	OC < 66.9	0.794
Organic	OC > 66.9	0.763
Silts	LL < 69.8	0.855
Silts	LL > 69.8	0.689
Silts	PI - No Breakpoint was found	N/A

Table 4-12. Delineation analysis results for C_r models

Notes	Breakpoint	R^2_{adj}
Clays	LL - No Breakpoint was found	N/A
Clays	PI < 70.4	0.129
Clays	PI > 70.4	0.236
Organic	OC < 74.6	0.632
Organic	OC > 74.6	0.840
Silts	LL < 92.9	0.619
Silts	LL > 92.9	0.625
Silts	PI < 48.0	0.558
Silts	PI > 48.0	0.665

C_r Models – See Table 4-5

4.6. Summary

This chapter of the report presents the background and results of the statistical regression models used to estimate the soils compressibility characteristic parameters (C_c, C_r, C_v, and C_α) through simple lab index parameters or site characteristics (i.e., overburden pressure). The benefit of these models (presented in Tables 4-4 through 4-7) is that 1) they are developed specifically from a database of Florida soils, and 2) the consolidation characteristics can be estimated quickly without obtaining *undisturbed* samples via Shelby tube or other methods. Although the models are lengthy equations, they can quickly be input into a spreadsheet for quick analysis during preliminary design. However, the authors stress that discretion should always be employed when using the proposed models. Even though the accuracy of each model is presented (i.e., R^2, $R^2_{adj.}$, and RMSE), it is important to remember these models are only as accurate as their input variables (e.g., moisture content, Atterberg limits, organic content, etc.). Individual test error will add error to the model due to the testing procedure and subsequent input error, particularly the determination of moisture and material-related properties such as LL, PI and OC. Therefore, careful lab testing and soil sample retrieval and handling must be employed for the accuracy of the proposed statistical models.

5. CORRELATION BETWEEN CONE PENETRATION TEST (CPT) and SOIL COMPRESSIBILITY

The models presented in the previous chapters are functions of laboratory-determined soil index properties and are designed to be used in conjunction with the standard penetration test (SPT) and split spoon sampling. Although the SPT is considered to be the most popular subsurface exploration method for geotechnical engineers, its inherent limitations in soft soils and thinly stratified soil making it less than ideal in all geologic settings. Therefore, the cone penetration test (CPT) is becoming more popular as its technology and applications techniques have diversied in the recent decade.

Unlike the SPT, the standard CPT process does not allow for retrieval of physical soil samples, enabling further index testing in a lab setting. Rather, the CPT records the soil's response to the penetrating of a cone through the soil matrix, measuring the tip resistance (q_c) and sleeve friction (f_s) along the probe every 0.8 inches (2 cm). Although the lack of physical sample is a significant limitation, the CPT benefits from its ability to detect discrete soil stiffness changes and better characterize stiffness of relatively softer soil matrices, such as clays, silts, and organics. Therefore, if correlations can be drawn between CPT output parameters and soil compressibility, a much better understanding of the compressibility characteristics of the entire soil layer in question can be made. This chapter explores the application of CPT to estimate the consolidation parameters discussed earlier (i.e., C_c and C_r) through a presentation of existing models and a preliminary empirical study of Florida soils.

5.1. Review of Previous Studies

An extensive literature review of existing models and techniques implementing the CPT to estimate soil consolidation behavior parameters was performed. The researchers briefly present two of the fundamental theories and practices when relating such parameters. To best understand the methods used to estimate consolidation, a brief overview of the cone penetration test, dissipation test, behavior of clay, and consolidation is presented.

The CPT is a method used to determine the geotechnical properties of soils by pushing a conically-tipped probe (i.e., penetrometer) into the earth and recording the resulting tip resistance and sleeve friction. Specialized techniques can also be used for the measurement of excess pore water pressure, shear wave velocity, and various other parameters at designated intervals of depth. The general CPT provides continuous and repeatable data which can be related to many important soil parameters, including soil behavior type. The CPT has strong theoretical interpretations because it very closely follows cavity expansion theory (Vesić, 1972).

Consolidation is a time-dependent settlement mode which occurs in cohesive material (clay). Cohesive material has a nonlinear stress-strain relationship, a visco-elastic response, both recoverable and unrecoverable deformation, as well as a memory of previous stress. It is important to understand that this material does not abide by elastic theory. Consolidation is the process of stress transfer from pore pressure to the soil skeleton via the dissipation of water from the voids.

This release of water allows the soil to compress into a denser configuration which is seen as settlement on the surface. This dissipation depends on the soil properties, which through extensive research, may be predicted from a cost effective and continuous in-situ test.

5.1.1. Theoretical Background:

Deformation characteristics of soils are generally expressed by one-dimensional constrained modulus (M), undrained Young's modulus in compression loading (E_u), and small-strain shear modulus (G_o). One-dimensional consolidation settlement is based on the assumption that the lateral strain is equal to zero. Hence, the appropriate parameter to define the deformation characteristics of soils in the consolidation process is the one-dimensional constrained modulus, M. One-dimensional constrained modulus is defined in equation (5.1)

$$M = \frac{d\sigma_v'}{d\varepsilon_v} = \frac{1}{m_v} \tag{5.1}$$

In which σ_v' is the vertical effective stress, ε_v is the vertical strain, and m_v is the coefficient of volume compressibility. The settlement due to consolidation (S_c) can then be calculated through the relationships of the change of influence of stress and constrained modulus. Hence, the following equation can be formulated (5.2), where $\Delta\sigma'$ represents the increase in effective stress at target soil layer depth, and H is the thickness of soil layer in question.

$$S_c = \frac{1}{M} * \Delta\sigma' * H \tag{5.2}$$

5.1.2. Estimation of Constrained Modulus using CPT

The estimated constrained modulus (M) can be estimated for a given soil layer through correlation with the soil behavior type index (I_c), presented by Robertson (1990). The constrained modulus is the inverse of the coefficient of volume change, which can quantify how susceptible a soil is to compressibility. Robertson's contribution of the I_c makes it simple to determine the soils behavior and transition zones from the CPT. The SBTn chart also allows the soil behavior type to be used when relating CPT data to soil parameters, in this case the constrained modulus. It is important to note that the normalization factor is used to convert parameters between SBTn graph and un-normalized cone tip resistance and sleeve friction. The process Robertson follows to relate the CPT and constrained modulus is as follows. First, a relation between CPT and shear wave velocity is determined, which is related directly to the small shear modulus. The small shear modulus is then related to the constrained modulus.

A set of normalized shear wave velocity (V_{s1}) contours is plotted on the SBTn chart from over 100 SCPT profiles. Then a function that best approximates the V_{s1} contours is used to relate shear wave velocity to cone tip resistance and soil type. Shear wave velocity is the first soil stiffness parameter in this process determined from the CPT because shear wave velocity and cone tip resistance are both dependent on the soil's relative density, effective stress state, age and cementation.

The small strain shear modulus (G_o) is a soil stiffness parameter that describes the materials response to shear stress. The shear modulus is directly related to the shear wave velocity. Using this direct relationship, normalized G_o can be contoured on the SBT$_n$ chart and become a function of tip resistance, sleeve friction ratio and soil type. Since the shear modulus is a stiffness parameter for elastic materials, there could be small error in the results when these contours are extended into the plastic region of the SBT$_n$ chart.

Mayne (2006) suggested the small strain shear modulus is related to constrained modulus through a simple ratio of net cone tip resistance (i.e., $q_t - \sigma_{vo}$). Using a similar method as above the constrained modulus can be contoured on the SBTn chart and be written as a function of tip resistance, sleeve friction ratio, and soil type. This equation is shown below (5.3), where α_M is a constrained modulus cone factor, q_t is the cone tip resistance and σ_{vo} is the in-situ total vertical stress at the depth at which q_t is measured (in same units as q_t).

$$M = \alpha_M(q_t - \sigma_{vo})$$ (5.3)

The constrained modulus calculated from the CPT has a strong correlation to the constrained modulus determined in the laboratory. The accuracy of this relationship is apparent in Figure 5-1, recreated from data presented by Robertson (2009). Through accumulation of CPT and lab data from 13 soft clay sites, Robertson developed guidelines for estimating α_M with CPT normalized tip resistance (Q_{tn}) and soil behavior type index (I_c); which is a function of Q_{tn} and normalized Friction Ratio, F_R (Robertson & Wride, 1998).
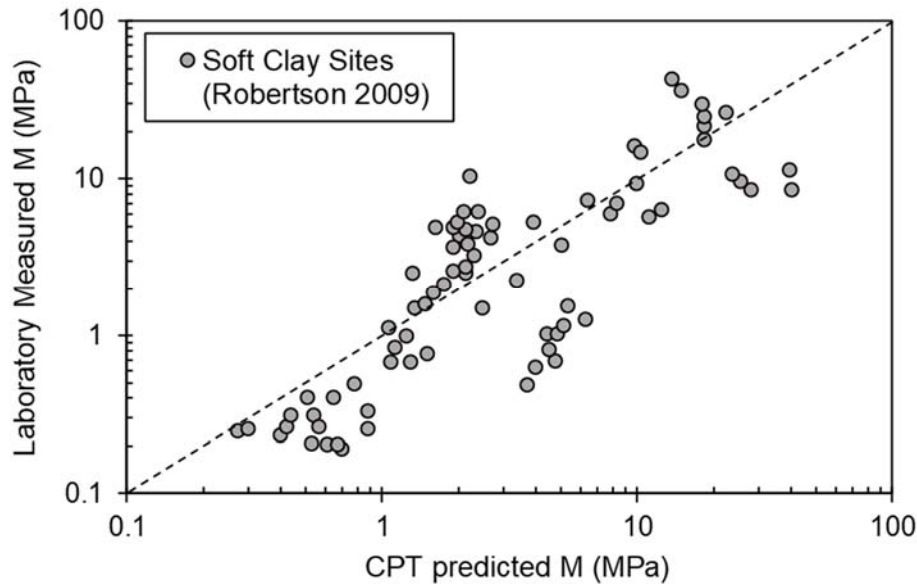
Figure 5-1. Predicted 1D constrained modulus (*M*) derived from Q$_{tn}$ and α_M

[Modified from Robertson 2009]

56

5.1.3. Mathematical Derivation from Elastic Theory

The method discussed in this section is a mathematical derivation based on assumptions to relate compressibility and cone tip resistance. This was most notably first performed by Buisman (1936), whom expanded upon the Dutch's work focused on estimating the compressibility constant (C). This research resulted in the well-known semi-empirical Terzaghi-Buismans settlement equation, shown in equation (5.4). Where, $\Delta h/h$ is taken as the relative settlement, $\Delta\sigma$ is the increase in stress due to loading at the specified depth, and σ_o represents the in situ vertical stress at the target depth at which the settlement is being investigated.

$$\frac{\Delta h}{h} = \frac{1}{C}\ln\left(1 + \frac{\Delta\sigma}{\sigma_o}\right) \tag{5.4}$$

Buisman's derivation is founded upon several assumptions. These assumptions are that the volume decrease occurring at the point of the penetrometer q_c is only a function of soil compression, as well as the oedometric modulus is constant due to the small loading area and the shape of cone tip being half a sphere. Another assumption is that stress at a certain distance from the cone can be calculated from Bousinesq's method to estimate the increase in stress at a given depth (z). Finally, Buisman also assumes that the soil is elastic because this derivation was initially for loose sands. The solution when tested with actual results, for sands, was proven to be the upper bounds of settlement and is a conservative estimation, shown in equation (5.5).

$$C = \frac{3}{2} * \frac{q_c}{\sigma_o} \tag{5.5}$$

Sanglerat (1972) proposed altering Buisman's solution for cohesive soils by replacing 3/2 with a constant dependent on soil type, denoted as alpha (see Equation 5.6). Therefore, the compressibility coefficient is a function of cone tip resistance and soil type. This alteration still assumes that the soil is elastic. It is also important to note that the equation is only valid within the virgin region on the consolidation curve. The National Institute of Applied Sciences of Lyons (NIASL) determined the values of alpha for different types of soils through extensive data collection.

$$C = \alpha\left(\frac{q_c}{\sigma_o}\right) \tag{5.6}$$

5.1.4. Relationship Between CPT (q_c) and Soil Compressibility (C_c)

NIASL followed a reliable process to recommend appropriate alpha values for soil types. The institute determined the compressibility constant from consolidation tests and the tip resistance from the cone penetration test. An alpha for the corresponding soil type is then assigned by using the above equation, since alpha is now the only unknown. The Institute's research used 600 comparative couples for fine-grained soils (>50% fines) to create tables of alpha values for different soil types, which also includes information on water content.

The NIASL database was also used to graph tip resistance versus measured compressibility index. The data was categorized based on the range of water content measured (*w*) and the results can be found in the recreated scatter plot in Figure 5-2. From these results, there is no recommended function to accurately describe this relation, but two hyperbolic boundary curves can be fitted (shown in the figure as the dashed lines). Also, the results show that regions of weak q_c (less than 10 bars) reveal that the compression index is highly dependent on moisture content. This was not the main purpose of the research by the NIASL, and therefore does not receive extensive analysis of results.

Figure 5-3 presents the averaged data of each water content soil range. Also shown by the error bars of each data point are the respective standard deviation ranges in C_c values and q_c values. Through plotting the data in this format, the 600 data points can be easily viewed along with their trend of moisture content. To compare the data presented in Sanglerat (1972) with the database collected in this study for Florida sites, the theoretical data limits and water content dividing lines were constructed on the figure. These lines are strictly for comparison purposes and no statistical regression was used in their development.
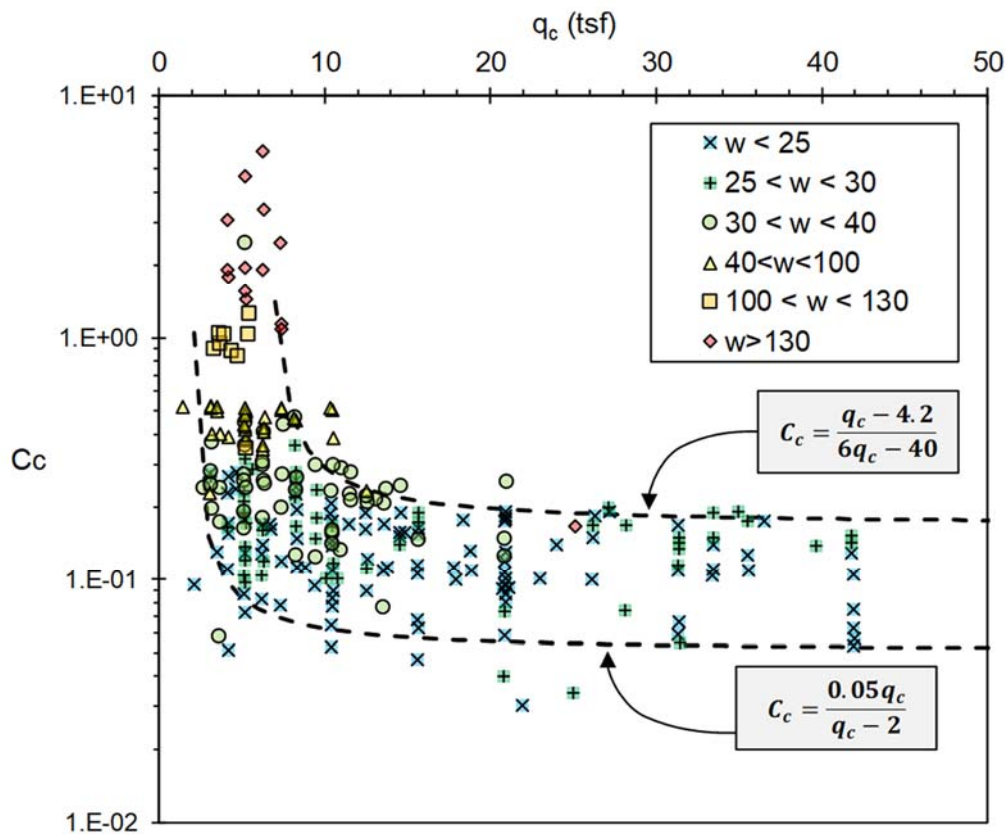
Figure 5-2. Empirical relationship of CPT cone tip resistance (q_c), C_c, and soil moisture content (*w*)

[Modified from Sanglerat 1972]

58
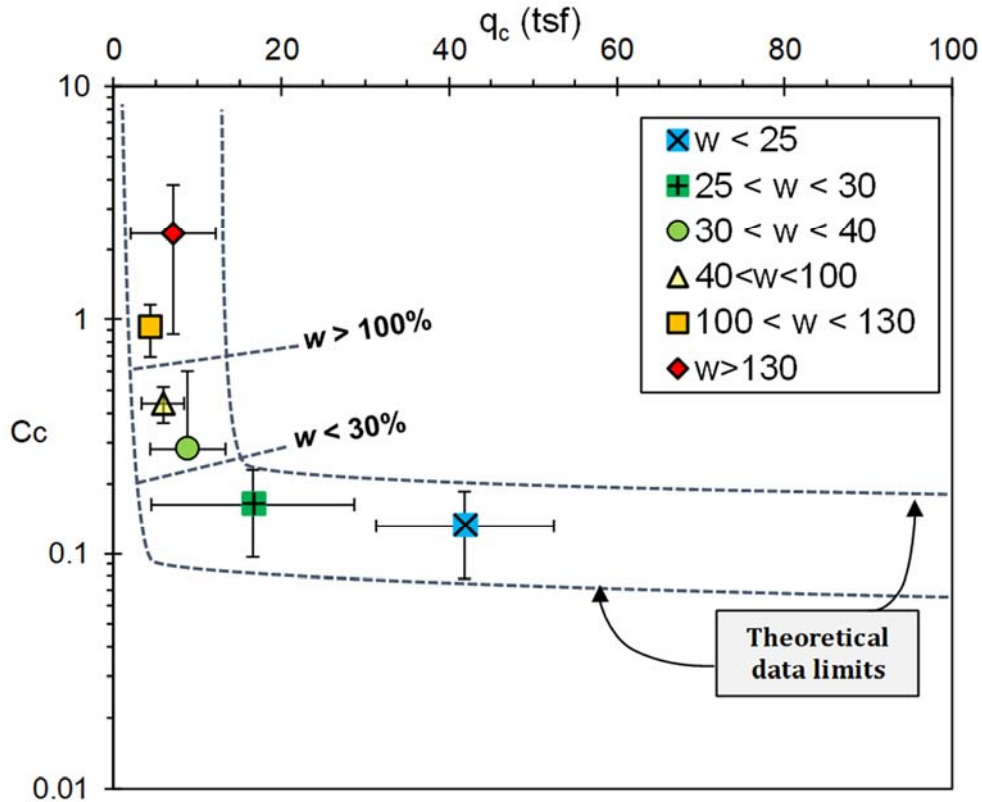
Figure 5-3. Summary of Sanglerat (1972) data with theoretical data limits and conceptual soil moisture content (*w*) trends used for comparison in this study.

5.2. Correlation Between Soil Compressibility and CPT – Florida Case Study

5.2.1. Methodology for Collection of Florida Soil Data

To achieve the tasks of this section, a database for Florida soil and consolidation testing was developed. Corresponding cone penetration testing data was collected to identify which CPT parameters (if any) can be used to develop a correlation to the respective soil consolidation indices. The researchers have accumulated a database of CPT soundings performed near borings with Shelby tube samples used for consolidation testing. Several sites were also chosen for additional CPTs to be performed to collect resistance data within layers with previous consolidation testing results. The oedometer tests will determine the compressible constant and the cone penetrometer will determine the corresponding cone tip and friction resistance. The following section will present the data collection and filtering process used to obtain the database of Florida CPT and consolidation parameters.

Couples of consolidation data and cone penetrometer data were formed. The couples were then filtered based on location, time and soil stratum between the standard penetration test used to obtain the sample and the cone penetration test, as well as the quality of the consolidation test. Soil profiles from the two in-situ tests are compared and checked for similar stratum, especially within the Shelby tube area. The next step was to select an appropriate tip resistance and friction ratio from the Cone Penetration Test to represent the soil type in the Shelby tube, used for the consolidation test. Once this data collection has been completed, the data sets (i.e., q_c, f_s, R_f, C_c, C_r, index parameters) was added to the comprehensive data base. The total database used in this study consisted of 14 sites and is presented in Tables 5-1 and 5-2. A total of thirteen excess pore-water pressure dissipation tests were also performed in 7 of the CPTu locations. However, due to inconsistencies in data and anticipated error in test performance, the resulting tests yielded inconclusive results. The CPTu resistance profiles and dissipation results are shown in the Appendix.

Example of Data Processing

This section will provide an example of the filtering process mentioned above for one of the accepted data points. The site used in this example is SR-46 (TB-12). The Shelby tube sample was obtained in 2012 and the cone penetration test was performed in 2018. A fill was added in between the two points, which is why the cone penetration test is located far north of the standard penetration test. An outline of the general data processing steps is visualized in Figure 5-4.
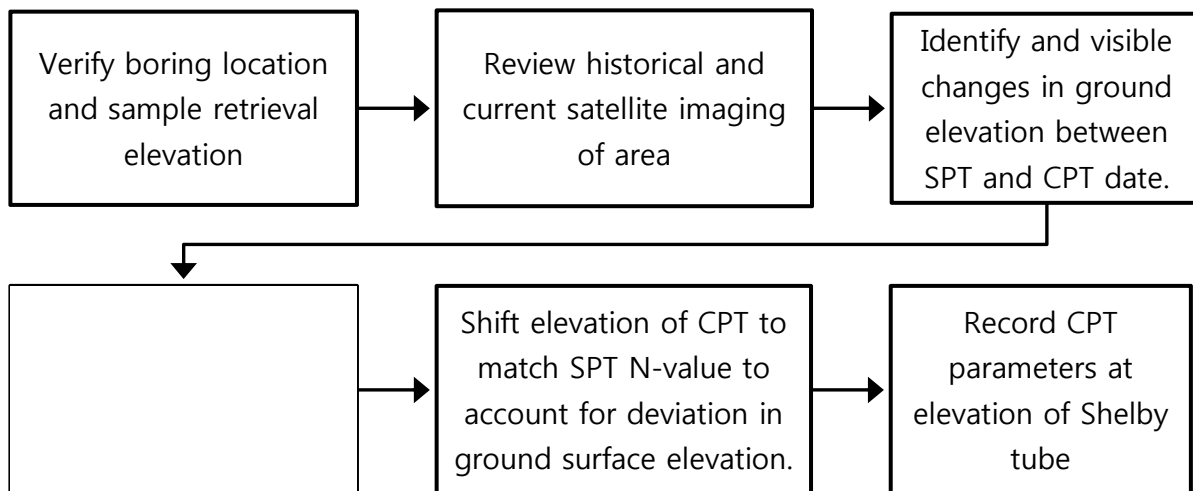
Figure 5-4. Flow chart outlining data processing steps

Step 1) Check the boring locations for excessive distance, changes in the area due to construction, and borings performed in a probable muck area or elevated zones. Google satellite imaging was utilized in this step, with the ability to view images from previous years. When google imaging was inconclusive, a site visit and roadway plan comparison was performed. When it could be verified that no significant change in ground surface elevation or other geologic and hydrologic deviations had occurred since the retrieval of the Shelby tube, then a CPT was performed at the site within 3 meters of the original boring location.

Step 2) Compare in-situ soil data obtained from the Standard Penetration Test and Cone Penetration Test: the soil boring log and blow counts will be compared to soil type (Robertson 1990) and the tip and sleeve friction resistance. Figure 5-5 shows the soil boring log, blow counts, tip resistance, friction resistance and soil type. The initial fitting method used was to relate the blow count and tip resistance profiles. Therefore, depths of high blow counts should match areas of high tip resistances and sleeve frictions, and vice-versa. This initial matching, combined with site information above, allowed for slight manipulation of the CPT "zero depth" datum to account for differences in locations and profiles over time. In this example about 4 feet of fill was added after the SPT but before the CPT, and this additional soil was accounted for by "shifting" the CPT data up 4 feet. If the effects of space and time have been properly accounted for, the layer in which the Shelby tube was taken should match up to a clay soil on the soil behavior type. In this case the shifting of 4 feet up causes the Shelby tube layer to correspond to a clay soil type above the refusal layer. This is noted as a good match and no further manipulation or filtering of data was needed.

Step 3) The consolidation test performed on the Shelby tube sample must be checked for quality. If the test is poor-quality then the compressibility coefficients obtained won't be representative of the soil and the data couple was removed. Since previous checks removed most of the data points, this step was not performed; otherwise, there would have been too few data points available for comparison.
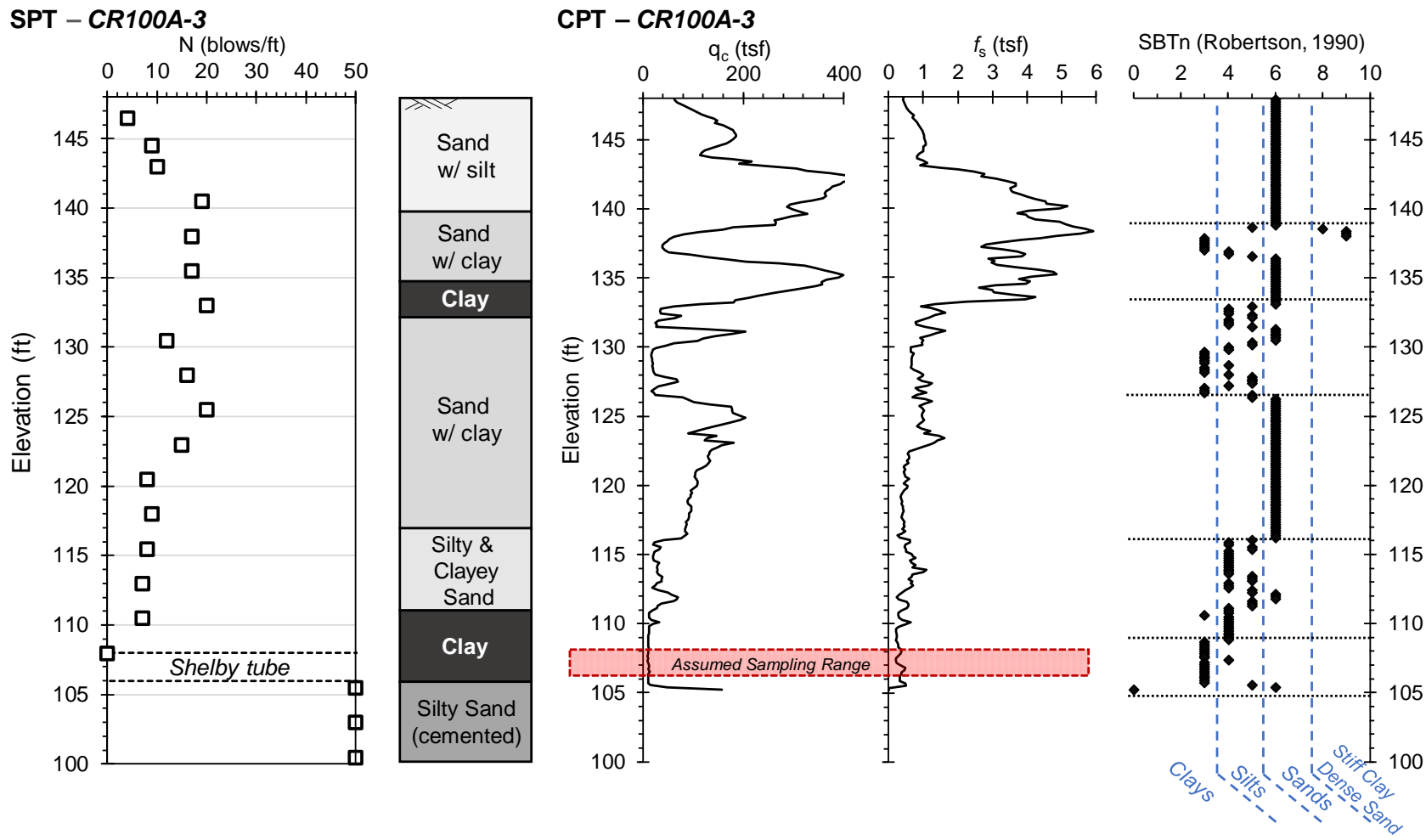
Figure 5-5. Comparison of SPT and CPT to determine depth at which CPT data range will correlate with consolidation test

Table 5-1. Summary of consolidation test data used for this study

Project I.D.	Sample Type (USCS)	Depth (ft)	-200 (%)	w (%)	LL (%)	PI (%)	s' (tsf)	Pc (tsf)	OCR	e_o	C_c	C_r
WPV_S1	CH	40 - 42	96	50	98	79	1.38	4.75	3.4	1.35	0.420	0.070
WPV_S2	SM	55 - 57	13	38	NP	NP	1.81	1.01	-	1.08	0.200	0.020
SR-100A	CH	30 - 32	99	68	117	96	0.96	6.10	6.4	2.52	0.940	0.130
i4 Ult_B204-2	CH	57 - 59	96	72	58	37	1.10	3.85	3.5	2.08	0.820	0.075
i4 Ult_B201-2	CH	40 - 42	97	67	89	61	1.01	3.45	3.4	1.84	1.000	0.138
i4 Ult B204-2*	OH (44%)	30 - 32	96	123	61	22	0.96	3.63	3.8	2.17	1.390	0.060
SR415_TB6	CH	5.5	91	51	110	29	0.14	1.00	7.0	1.40	0.490	0.100
SR44_Dep1	MH	66	76	105	184	121	2.14	0.32	-	7.60	3.070	0.110
HospVill_2	CL	50.5	56	68	48	24	1.75	1.47	0.8	1.87	0.730	0.150
UCF_ST1	CL-ML	40 - 42	67	40	22	5	0.99	2.72	2.7	1.09	0.400	0.044
SR46_TB1	CH*	50 - 52	50	59	81	33	2.50	0.52	-	1.33	0.251	0.027
SR46_TB10	SC	42 - 45	48	58	64	34	2.35	0.25	-	1.16	0.144	0.033
SR46_TB12	CH	32 - 35	74	65	126	64	1.90	2.85	1.5	1.90	1.247	0.016
CR-100 A-3	CH	40 - 42	77	97	140	103	1.24	2.05	1.7	2.84	1.360	0.050

Table 5-2. Summary of CPT data from layer corresponding to consolidation data

Project I.D.	Data count	Tip Resistance, q_c (tsf)		Sleeve Friction, f_s (tsf)		Friction Ratio, R_f (%)	
		Avg.	Std. dev.	Avg.	Std. dev.	Avg.	Std. dev.
WPV_S1	6	15.84	8.81	1.07	0.20	7.04	1.53
WPV_S2	5	71.22	16.28	0.54	0.09	0.80	0.11
SR-100A	8	5.15	3.07	0.11	0.08	2.28	1.13
i4 Ult_B204-1	8	36.81	7.05	N/A	N/A	N/A	N/A
i4 Ult_B201-2	8	54.56	4.09	0.31	0.10	0.58	0.23
i4 Ult B204-2	7	13.86	1.26	0.28	0.03	2.00	0.11
SR415_TB6	12	4.87	0.72	0.30	0.05	6.18	0.51
SR44_Dep.	10	7.93	2.81	0.29	0.19	3.79	1.52
HospVill_2	6	31.48	16.95	0.43	0.14	1.48	0.29
UCF_ST1	6	10.15	6.26	0.16	0.08	1.69	0.14
SR46_TB1	14	20.91	6.82	0.61	0.06	2.99	0.95
SR46_TB10	13	14.60	7.94	0.49	0.24	3.11	0.43
SR46_TB12	15	16.77	2.12	0.34	0.09	1.81	0.32
CR-100 A-3	13	11.07	0.89	0.34	0.09	2.99	0.50

5.3. Analysis Results

Figure 5-6 shows the 14 datasets from the Florida sites, overlain on the resulting thresholds of data presented by Sanglerat (1972). Each data point shows the average value of q_c with their respective C_c value. Since q_c is measured every 0.8 inches (2 cm), and the exact depth of sample taken for the consolidation test was not known, the average was taken over the entire depth at which the Shelby tube was obtained from (~2 ft). Therefore, the standard deviation of q_c was also calculated and is presented in Figure 5-6 as error bars for each data point. Also shown above each point is the soil samples' respective measured natural moisture content; obtained when preparing the samples for the consolidation testing. Although the tip resistance data does not fall within the threshold lines of the Sanglerat's data, a similar trend in moisture content can be identified (i.e., moisture content increases as q_c decreases and C_c increases). Figures 5-7 through 5-12 presents the dataset comparison of C_c and C_r with CPT determined q_c, f_s, and R_f.
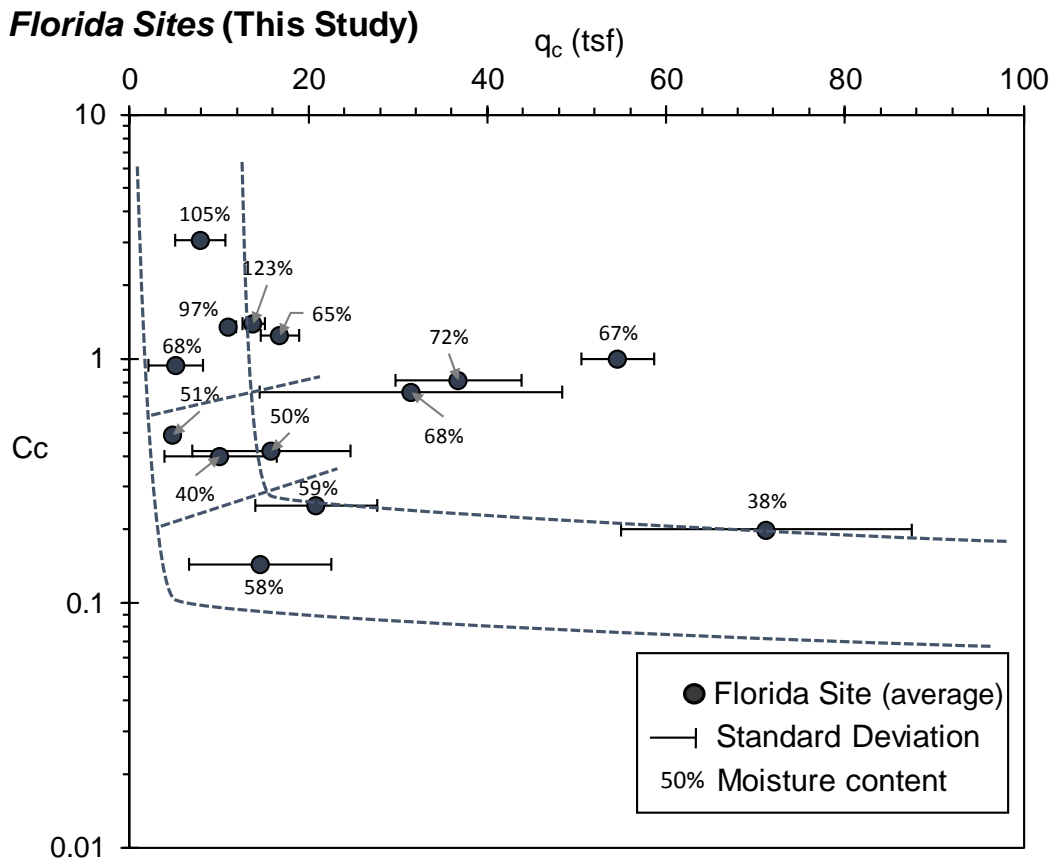
Figure 5-6. CPT (q_c) and consolidation (C_c) data presented on the trends derived from Sanglerat data (see figure 5-3)

64
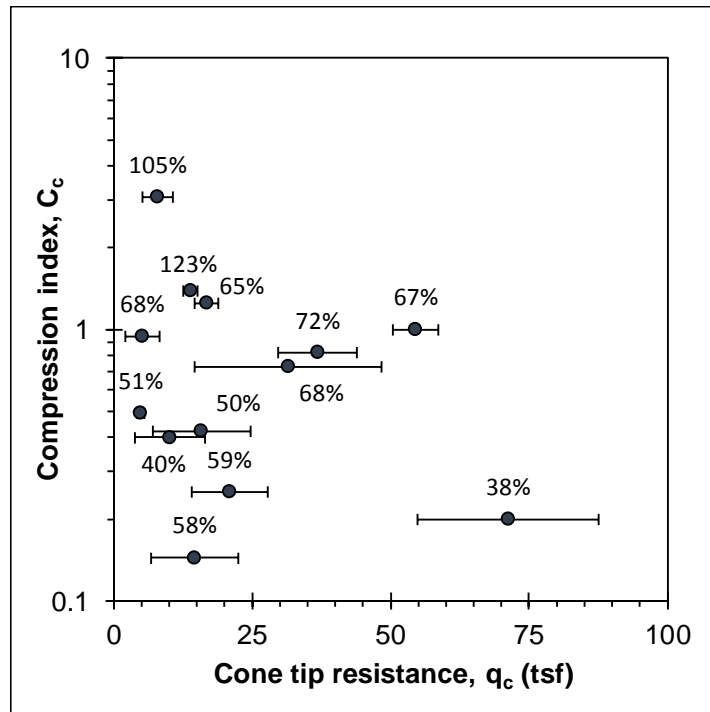
Figure 5-7. Comparison of C_c and CPT tip resistance values
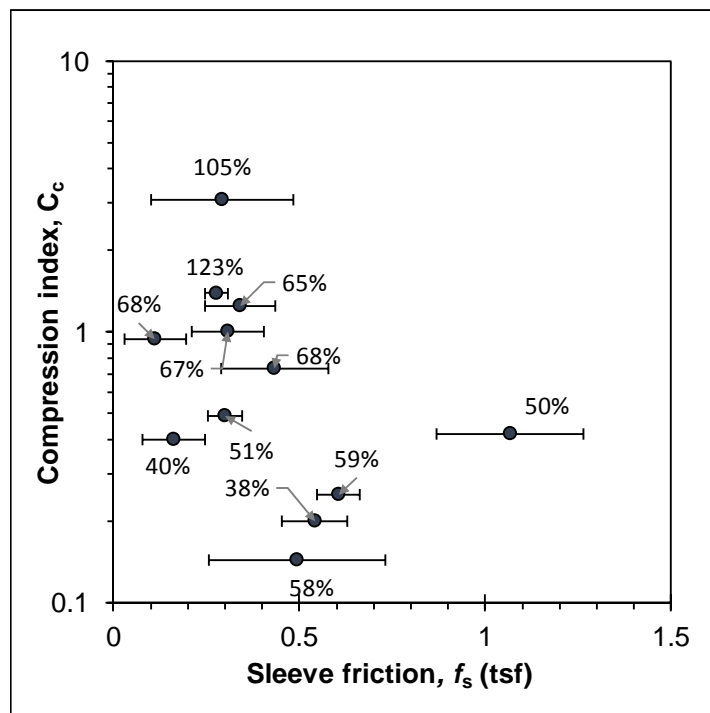
Figure 5-8. Comparison of C_c and CPT sleeve friction values
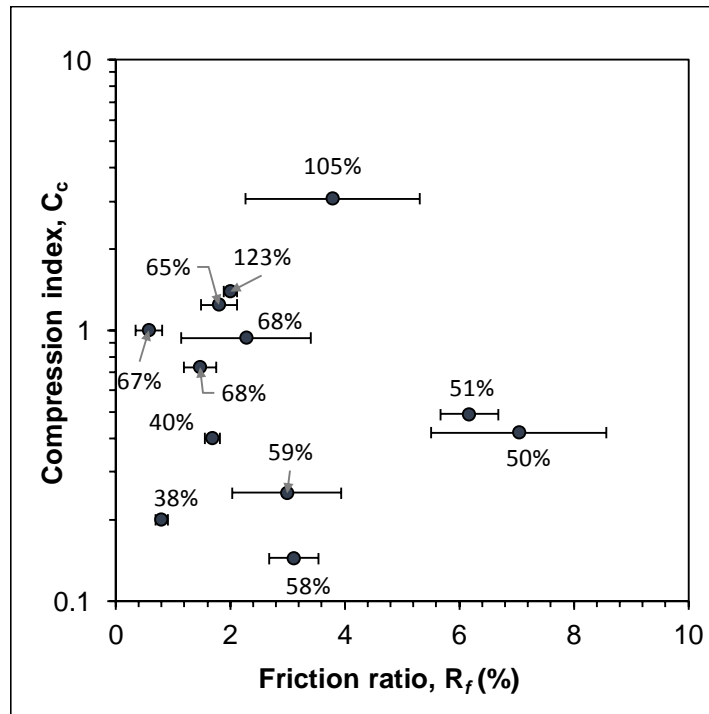
Figure 5-9. Comparison of C_c and CPT friction ratio values
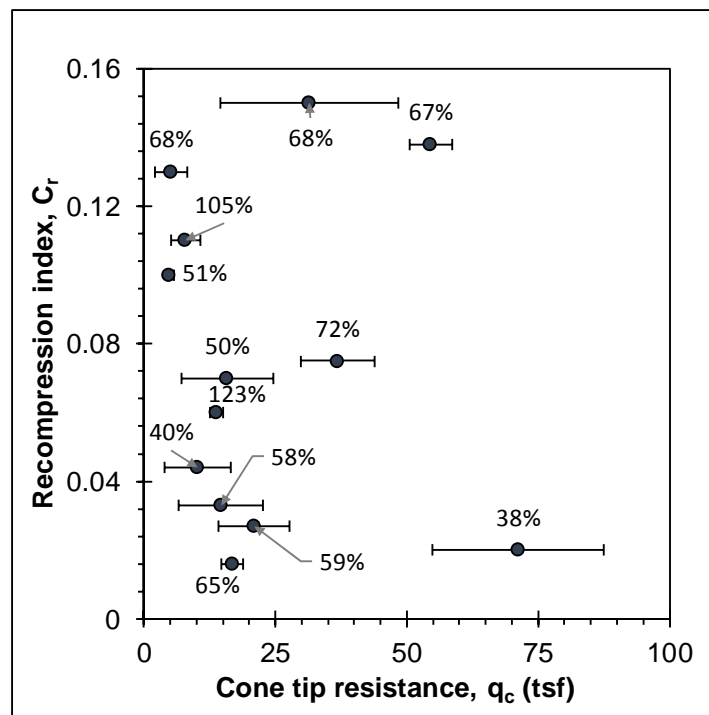
Figure 5-10. Comparison of C_r and CPT tip resistance values
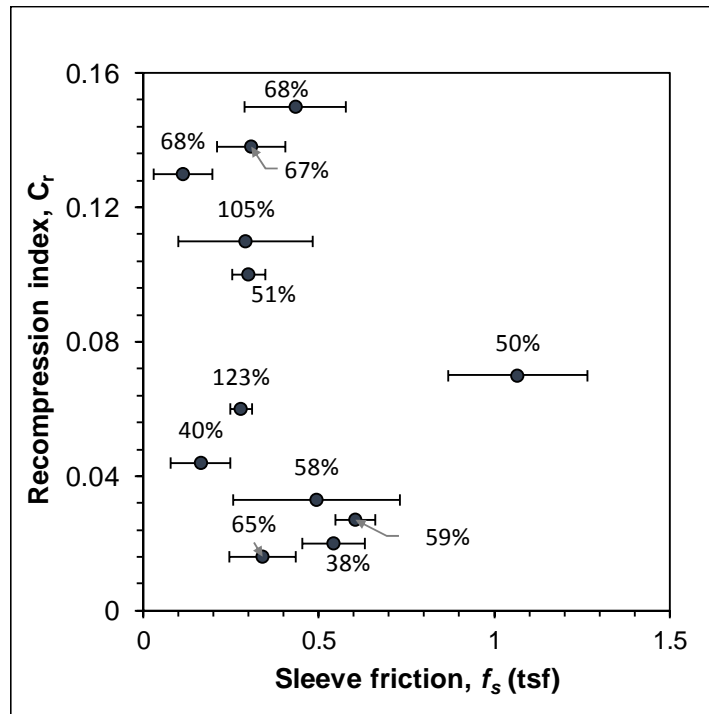
Figure 5-11. Comparison of C_r and CPT sleeve friction values
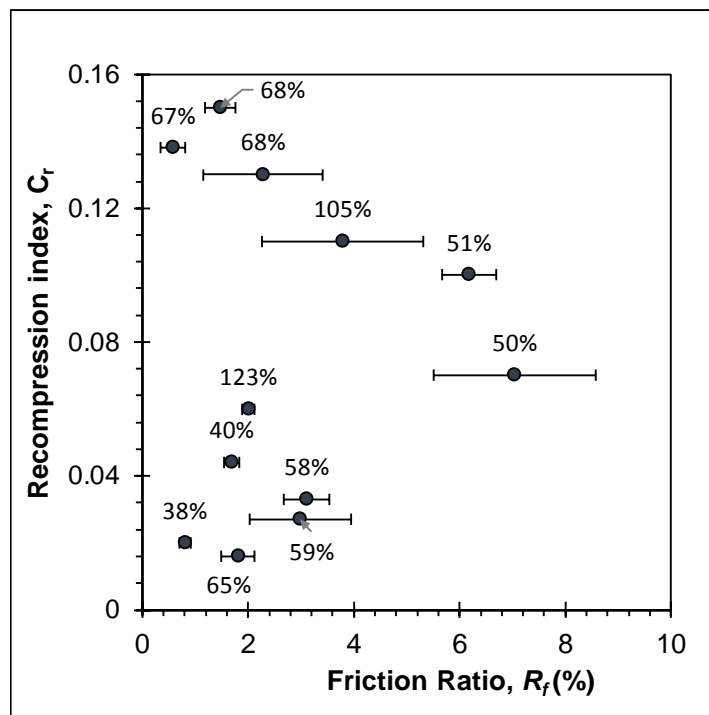
Figure 5-12. Comparison of C_r and CPT friction ratio values

67

5.4. Discussion

According to Terzaghi's consolidation theory, the soil compressibility is not directly related to soil resistance (or stiffness and strength). However, the elasticity theory can explain the correlation between constrained modulus and soil compressibility. According to the literature review analysis (see Figure 5-3), there seems a general trend that qc increases as the soil compressibility decreases. Using this general correlation trend is not accurate enough to predict the soil compressibility from CPT tests.

From the limited dataset and preliminary analysis performed with Florida's data, it appears there is no strong correlation between CPT resistance parameters and C_c or C_r variables (see Figures 5-7 through 5-12). However, the authors could attribute this poor correlation to multiple factors. The database was of insufficient quality due to the magnitude of variables present in the data collection heavily impacting the results. More specifically, first, the limited number of data points available are of concern. Second, the soil samples used for the consolidation tests and the CPTs were performed at different times. Although the CPTs were performed in virgin ground away from any construction which may have occurred post-sample retrieval it is still likely in situ stress conditions may have deviated over time through natural consolidation or through other unanticipated anthropogenic affects. Third, changes in the ground surface elevations were also encountered, making it extremely difficult to prescribe the correct CPT parameters to the exact depths at which the soil was obtained for use in the consolidation test. Therefore, the researchers believe higher quality data collected from controlled sites (i.e., no time gap between consolidation test and CPT) will greatly increase the reliability of the results.

This analysis was conducted for preliminary purposes and the authors are aware that the reliability of data must be improved upon for any conclusive remarks. However, the researchers checked the relationship between C_c, C_r and the calculated moisture content (w) for the dataset used in this task and can verify that there is a strong correlation between w and compression index (C_c) for clay and silt soil. The complete dataset used in this study consists of soils classified as silty fine sands (SM), clayey fine sands (SC), and organic silts (OH). The relationship between the complete dataset can be seen in Figure 5-13A, with the data points highlighted in red being a soil type which may not follow the conventional consolidation theory mechanics. Once these points are filtered out, there is a very strong correlation between w and C_c (Figure 5-13B). Interestingly, the correlation between C_r and w showed very low accuracy ($R^2 < 0.2$) for the filtered and non-filtered case.

The authors should note that the relationship shown in Figure 5-13 is not a recommended model for actual analysis due to the limited data points used in its creation (n = 9). Rather, the point is to reinforce the controlling factor of natural moisture content on a soil's respective compression index value, for silts and clays in Florida. Therefore, using a specialized CPT probe to estimate soil moisture content or directly measure soil moisture content (such as CPTu or probe equipped with a dielectric reflectometer or resistivity) may greatly increase the ability to directly estimate the compression index values of a soil layer with high resolution.
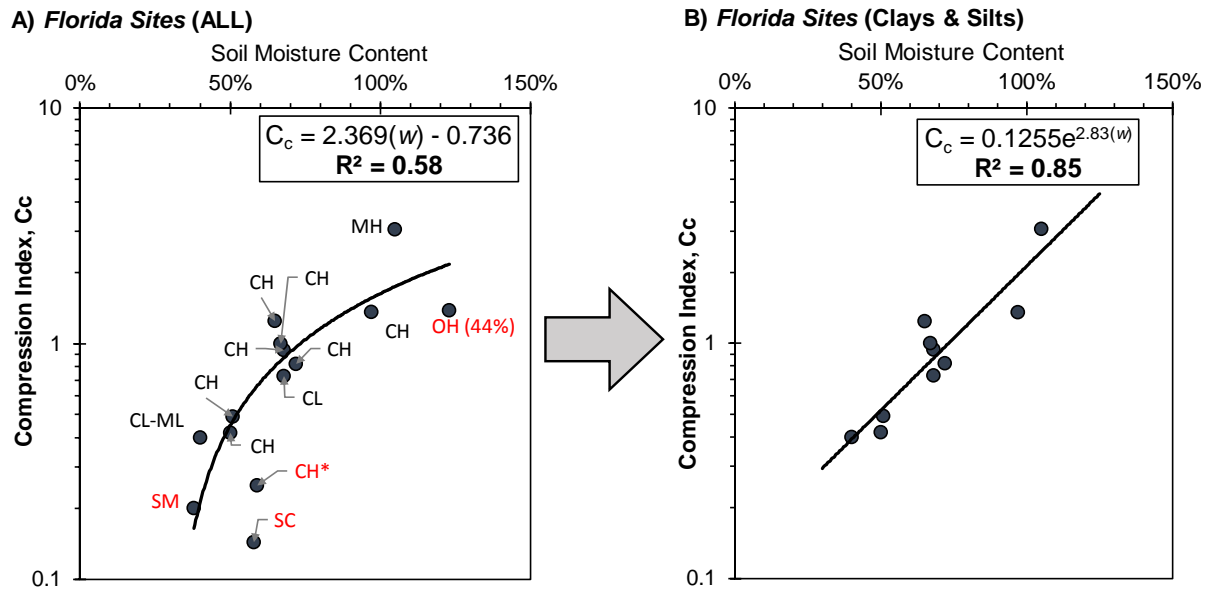
Figure 5-13. Relationship between C_c and soil moisture content for: A) all Florida sites (14), and B) clays and silts (10)

6. CONCLUSION

6.1. Summary of Proposed Correlation Models

The primary result of this project was the development of several statistical models correlating consolidation parameters (i.e., C_c, C_r, C_v and C_α) to various soil index properties (e.g., moisture content, liquid limit, fines content, etc.). These models were developed using a database of 551 consolidation test results and were categorized based on the soils' USCS (Unified Soil Classification System) classification (e.g., CH, CL, MH, OH, OL, Pt). The following section presents the best performing models to be used for each soil type. As previously discussed in Chapter 4, a larger database of primary consolidation parameters (C_c and C_r) enables the discretization of models for ranges of plasticity. Models for secondary plasticity parameters (C_v and C_α) were only created for generic soil groups of *clays*, *organics*, and *peat* (i.e., fibrous and OC >75%). The following models for each classification of soil are recommended by the authors and can be considered statistically accurate for geotechnical engineering standards by holding an $R^2 > 0.5$ or a RMSE value near zero. The comprehensive list of models and their accuracy (in terms of regression values) can be found in Section 4.4. Engineering judgment must always be used when performing calculations based on statistical correlations. These models are intended to suppleme nt but not eliminate a geotechnical sampling and testing program. An explanation for each of the possible input variables for the models is presented in Table 6-1.

Table 6-1. List of input variables for proposed correlations

Input Variable	Parameter Explanation	Units (*example*)
w	Soil moisture content (ASTM D2216)	percent %
G_s	Specific Gravity (ASTM D854)	*unitless*
LL	Liquid Limit (ASTM D4318)	%
PI	Plasticity Index (i.e., LL – PL) (ASTM D4318)	%
Fines	%passing No.200 Sieve (ASTM D1140)	%
σ_o'	In situ effective stress at depth of sample retrieval	kips/ft²
OC	Organic Content (ASTM D2974)	percent %
N	Average SPT automatic hammer blow count at sample depth (ASTM D1586)	average blows/ft
Stress Level	Post-construction (i.e., design) in situ stress	lb/ft²

6.1.1. High plasticity Clays (CH)

- *Compression Index:*

$$C_c = 1.405 + (0.016 \times w) + (0.0005 \times LL) + (0.398 \times G_s) - 0.00003$$
$$\times [(w - 68.837) \times (LL - 105.48)] - 0.00002$$
$$\times [(w - 68.837) \times (w - 68.837)]$$

- *Recompression (swell) index:*

$$C_r = -0.0136 - (0.0023 \times \sigma_o') + (0.0014 \times w) + (0.0001 \times LL) - 0.0004$$
$$\times [(\sigma_o' - 1.986) \times (w - 68.176)] + 0.0002$$
$$\times [(\sigma_o' - 1.986) \times (LL - 105.323)] + 0.000007$$
$$\times [(w - 68.175) \times (LL - 105.323)]$$

6.1.2. Low plasticity Clays (CL)

- *Compression Index:*

$$C_c = -1.6912 + (0.0118 \times w) + (0.5919 \times G_s)$$

- *Recompression (swell) index*:*

$$C_r = -0.05 + (0.0021 \times w) + (0.0018 \times N)$$

*Note: R^2 = 0.3 but RMSE = 0.05

6.1.3. High plasticity Silts (MH)

- *Compression Index:*

$$C_c = -8.442 + (0.0077 \times w) + (0.0085 \times fines) + (0.0143 \times PI) + (3.337 \times G_s)$$
$$+ (0.0828 \times [(w - 89.8) \times (G_s - 2.664)])$$

- *Recompression (swell) Index:*

$$C_r = -3.551 + (0.0014 \times w) - (0.009 \times N) + (0.0006 \times PI) + (1.324 \times G_s)$$
$$- 0.00002 \times [(w - 100.99) \times (PI - 48.034)] + 0.0254 \times [(w - 100.99)$$
$$\times (G_s - 2.656)]$$

6.1.4. High plasticity Organic soils (OH)

- *Compression Index:*

$$C_c = -0.480 + (0.076 \times \sigma_o') + (0.0098 \times w) + (0.0046 \times PI) + 0.0005 \\ \times [(\sigma_o' - 1.445) \times (w - 123.02)] + 0.0036 \times [(\sigma_o' - 1.445) \times (PI - 81.879)]$$

- *Recompression (swell) Index:*

$$C_r = 0.0667 + (0.0326 \times \sigma_o') + (0.002 \times w) - (0.0036 \times OC) + 0.029 \\ \times [(\sigma_o' - 1.486) \times (OC - 21.652)]$$

6.1.5. Low plasticity Organic Soils (OL)

- *Compression Index:*

$$C_c = 0.8164 + (0.0096 \times w) - (0.0145 \times fines)$$

- *Recompression (swell) Index:*

$$C_r = 2.365 + (0.0039 * \sigma_o') + (0.011 \times OC) - (0.1212 \times PI) + 0.0586 \\ \times [(\sigma_o' - 1.015) \times (PI - 20.297)] - 0.0167 \\ \times [(OC - 17.8) \times (PI - 20.297)] - 0.0264 \\ \times [(\sigma_o' - 1.015) \times (\sigma_o' - 1.015)] + 0.0009 \times (OC - 17.8)^2$$

6.1.6. Peat (Pt)

- *Compression Index:*

$$C_c = -10.774 + (0.0078 \times w) + (0.0772 \times OC) + (2.867 \times G_s) + 0.0074 \\ \times [(w - 481.673) \times (G_s - 1.5677)] - 0.2644 \times [(OC - 83.021) \\ \times (G_s - 1.5677)] + 0.0075 \times [(OC - 83.021)]^2$$

- *Recompression (swell) Index:*

$$C_r = -0.5938 + (0.0009 \times w) + (0.3356 \times G_s) + 0.5344 \\ \times [(G_s - 1.4373)^2] + 0.0017 \times [(w - 472.835) \\ \times (G_s - 1.4373)]$$

6.1.7. Secondary Consolidation (Clays)

- *Coefficient of secondary compression:*

$$C_\alpha = -0.0077 + (0.0001 \times w) + (2 * 10^{-6} \times PI)$$
$$+ (6 * 10^{-7} \times stress\ level) - (9 * 10^{-9})$$
$$\times [(w - 60.3376) \times (stress\ level - 10{,}084.8)]$$
$$+ (4 * 10^{-6}) \times [(PI - 70.5461)^2] - (2 * 10^{-12})$$
$$\times [(stress\ level - 10{,}084.8)^2]$$

6.1.8. Secondary Consolidation (Organics)

- *Coefficient of secondary compression:*

$$C_\alpha = -0.09 + (0.0001 \times w) + (0.002 * fines) + (0.0001 \times PI)$$
$$+ (0.0185 \times Gs) + [(2 * 10^{-6}) \times stress\ level]$$
$$+ (2 * 10^{-8})$$
$$\times [(w - 95.95) \times (stress\ level - 5{,}674.24)]$$
$$+ (3 * 10^{-8})$$
$$* [(fines - 60.061) \times (stress\ level - 5{,}674.24)]$$
$$+ (4 * 10^{-8}) \times [(PI - 92.4545)$$
$$\times (stress\ level - 5{,}674.24] + (8 * 10^{-6})$$
$$\times [(G_s - 2.4) \times (stress\ level - 5{,}674.24)]$$

6.1.9. Secondary Consolidation (Peat)

- *Coefficient of consolidation:*

$$C_v = 11.7596 + (0.0815 \times N) - (0.0762 \times fines) + (0.0317 \times OC) - (3.1765$$
$$\times G_s) - (0.0002 \times stress\ level) - 0.0024$$
$$\times [(fines - 56.918) \times (OC - 59.522)] - 0.1156$$
$$\times [(OC - 59.522) \times (G_s - 1.9426)] - 0.00001$$
$$\times [(OC - 59.522) \times (stress\ level - 2{,}391.88)] - 0.0005$$
$$\times [(G_s - 1.9426) \times (stress\ level - 2{,}391.88)] - 0.4487$$
$$\times [(N - 2.162)^2] - 0.0004 \times [(fines - 56.918)^2]$$

- *Coefficient of secondary compression:*

$$C_\alpha = -0.0660 + (0.00005 \times w) + (0.0006 \times OC) + [(8 * 10^{-6}) \times stress\ level]$$
$$+ (2 * 10^{-8}) \times [(w - 575.783) \times (stress\ level - 2{,}020.6)] + (4 * 10^{-7})$$
$$\times [(OC - 64.933) \times (stress\ level - 2{,}020.6)]$$

6.2. Recommendations

As with any empirically-based model, caution should be used when applying proposed correlations to actual design situations. For the most accurate representation of the in situ consolidation settlement, consolidation testing or field settlement testing is always recommended when high quality undisturbed soil samples are feasible or available. However, the authors believe the proposed correlations are still valuable assessment tools for preliminary design stages or for decision making when evaluating the severity of anticipated settlement due to consolidation. The authors stress, however, that the input soil parameters must be of sufficient quality to ensure the accuracy of the correlations. Since the majority of the input parameters are a function of soil moisture content (e.g., w, LL, PI, OC), it is imperative that soil samples be properly sealed after retrieval via split spoon, to ensure no loss of moisture during transportation or time between field retrieval and lab testing. Also, the soil samples must not contain any drilling fluid, such as bentonite slurry, which will greatly increase the measured moisture content if accidently included with the sample. All sampling and lab testing must be in strict accordance with international, and state standards, and adhere to the FDOT's Soils and Foundation Handbook.

6.3. Conclusions

The following conclusions can be made to summarize the findings presented in this report.

- Results from a statewide survey to geotechnical practitioners shows that correlations between soil lab index testing and consolidation parameters are used for preliminary design and estimating. However, the primary correlation used is one developed by Terzaghi and Peck (1967) and is not specific to Florida soils.

- The authors created a database of Florida soil laboratory testing with consolidation results, consisting of 551 datasets of clayey, silty, and organic soils. This dataset was used to create several statistical models, relating primary and secondary consolidation parameters to several soil index parameters. All input variables for the developed models can be obtain via disturbed methods (e.g., SPT and split-spoon sampling). By doing so, the consolidation parameters can be effectively estimated with accuracy, and minimizing the number of high-quality sampling and lengthy oedometer testing.

- Statistical regression modeling was used to formulate multi-variate models shown in the previous sections. These models are specific to the classification type of soil in which the input data was obtained (i.e., CH, CL, MH, OH, OL, Pt). The authors cannot guarantee accuracy of the models if the input soil variables are from a different soil classification (e.g., the models developed for CH soils are not validated for Peat soils).

- Correlations from Cone Penetration Test (CPT) outputs to consolidation parameters were inconclusive at the time of this study due to the limited data available. The strong correlation between moisture content and the compressibility index (C_c) for clayey soils, coupled with the ability to directly estimate soil moisture with high resolution of depth from the CPT, suggests that this testing procedure would yield a viable way to estimate consolidation parameters. However, future analysis and collection of high-quality CPT results and lab consolidation datasets would be necessary to create more accurate statistical models and draw further conclusions.

6.4. Recommended Future Work

Recommended future work is summarized below. Concepts and approaches based on valid reasoning are presented herein.

- Field validation of the developed soil compressibility models is recommended. The models are used to estimate settlement in the field with the equation below.

$$S_p = \frac{C_c H}{1+e_o} \log\left(\frac{\sigma_o' + \Delta\sigma'}{\sigma_o'}\right) \tag{6.1}$$

$$S_p = \frac{C_r H}{1+e_o} \log\left(\frac{\sigma_{pc}'}{\sigma_o'}\right) + \frac{C_c H}{1+e_o} \log\left(\frac{\sigma_o' + \Delta\sigma'}{\sigma_{pc}'}\right) \tag{6.2}$$

The validation can be accomplished through comparison of measured field settlement data to settlement predictions derived from measured compression indexes and the predicted compression indexes from the developed models. Instrumentation and settlement monitoring under controlled environment would be necessary for more accurate comparison. In order for this to be achieved with any level of confidence, sites must be chosen with a known soil stratigraphy, measured settlement from a known source, etc.

- The current study exhibits that CPT q_c does not have a strong correlation with C_c and C_r. The poor correlation is mainly due to poor "quality" data and no accurate depth information for consolidation test and CPT. It is important to note that the time difference between soil sampling and CPT sounding test is up to around 10-15 years, which cause varied surface elevation over time. This caused extremely high variability in digitizing the CPT q_c and f_s data for the matched consolidation data. The researchers strongly believe that the correlation should be much improved if the test data under controlled environment are obtained. Therefore, the researchers recommend conducting field experiments including the sampling (for consolidation test) and CPT with the same depth matched. CPTu and dissipation tests are encouraged to be performed because hydraulic properties of surrounding soils can be characterized, which will improve the accuracy of the prediction. Particularly, these hydraulic properties can estimate C_v.

- The researchers believe that the recompression index is more related to particle re-arrangement or particle densification while the compression index is more strongly related to water dissipation out of soil grains during consolidation test. This postulation is derived from the author's many discussions with experts of CPT and consolidation. Continuous profiling of water content along the depth during CPT sounding will provide a better estimate of soil compressibility. To accomplish this, di-electrical and conductivity module can be added to existing electric CPT cone.

Estimating the soil compressibility characteristics from CPT sounding tests is very attractive and beneficial to engineers. More in-depth studies under controlled environment will be able to improve the accuracy and enable the development of CPT-based prediction models of soil compressibility.

REFERENCES

Ahadiyan, J., Ebne, J. R., & Bajestan, M. S. (2008). Prediction determination of soil compression index, C_c, in Ahwaz Region. *J. Faculty Eng., 35*(3), 75-80.

Al-Khafaji, A., & Andersland, B. O. (1992). Equations for Compression Index Approximation. *Journal of Geotechnical Engineering, 118*(1), 148-153. doi:10.1061/(ASCE)0733-9410(1992)118:1(148)

Alam, M., Panagopoulos, A. A., Rogers, A., Jennings, N. R., & Scott, J. (2014). *Applying extended Kalman filters to adaptive thermal modelling in homes: poster abstract.* Paper presented at the Proceedings of the 1st ACM Conference on Embedded Systems for Energy-Efficient Buildings, Memphis, Tennessee.

Anagnostopoulos, A. C., & Grammatikopoulos, I. N. (2011). A new model for the prediction of secondary compression index of soft compressible soils. *Bulletin of Engineering Geology and the Environment, 70*(3), 423-427. doi:10.1007/s10064-010-0323-x

Anderson, J. R., Krafft, P. A., & Remington, C. (1981). *Environmental Geology.* Retrieved from The Florida Geographer:

Asma, T. Y., & Abbas, A. F. (2011). Estimation of relation between coefficient of consolidation and liquid limit of middle and south Iraqi soils. *Journal of Engineering, 17*(3), 430-440.

ASTM International. (2014). *ASTM D854-14 Standard Test Methods for Specific Gravity of Soil Solids by Water Pycnometer.* Retrieved from West Conshohocken, PA:

ASTM International. (2017a). *ASTM D1140-17 Standard Test Methods for Determining the Amount of Material Finer than 75-μm (No. 200) Sieve in Soils by Washing.* Retrieved from West Conshohocken, PA:

ASTM International. (2017b). *ASTM D4318-17e1 Standard Test Methods for Liquid Limit, Plastic Limit, and Plasticity Index of Soils.* Retrieved from West Conshohocken, PA:

ASTM International. (2018). *ASTM D1586-18 Standard Test Method for Standard Penetration Test (SPT) and Split-Barrel Sampling of Soils.* Retrieved from West Conshohocken, PA:

ASTM International. (2019). *ASTM D2216-19 Standard Test Methods for Laboratory Determination of Water (Moisture) Content of Soil and Rock by Mass.* Retrieved from West Conshohocken, PA:

Azzouz, S. A., Krizek, R., & Corotis, B. R. (1976). Regression analysis of soil compressibility. *Soils and foundation, 16*(2), 19-29. doi:10.3208/sandf1972.16.2_19

Bishop, C. M. (2006). *Pattern Recognition and Machine Learning.* Berlin, Germany: Springer-Verlag.

Bowles, J. E. (1989). *Physical and geotechnical properties of soils* (2nd ed.). New York, NY: McGraw-Hill.

Buisman, A. S. K. (1936). *Results of a long duration settlement test*. Paper presented at the International Conference of Soil Mechanics and Foundation Engineering, Cambridge.

Carrier, W. D. (1985). Consolidation parameters derived from index tests. *Geotechnique, 35*(2), 211-213. doi:10.1680/geot.1985.35.2.211

Casagrande, A. (1948). Classification and Identification of Soils. *Proceedings of the American Society of Civil Engineers, 113*(1), 901-930.

Cook, P. N. (1956). *Consolidation characteristics of organic soils*. Paper presented at the The Ninth Canadian Soil Mechanics Conference, Ottawa, Ontario, Canada.

Cozzolino, V. M. (1961). *Statistical forecasting of compression index*. Paper presented at the 5th International Conference on Soil Mechanics and Foundation Engineering, Dunod, Paris, France.

Das, B. M. (2002). *Principles of Geotechnical Engineering* (5, illustrated ed. Vol. 5). Boston, Massachusetts: Brooks Cole/Thompson Learning

Elnaggar, H. A., & Krizek, R. J. (1970). Statistical approximation for consolidation settlement. *Highway Res. Rec., 323*(1), 87-96.

Florida Department of Transportation. (2019). *Soils and Foundation Handbook*. Retrieved from Gainesville, Florida:

Herrero, A. M. (1983). Universal compression index equation. *J. Geotech. Eng., 109*(5), 755-761.

Hine, A. C. (2013). *Geologic History of Florida: Major Events that Formed the Sunshine State*. Gainesville, FL: University Press of Florida.

Hough, B. K. (1957). *Basic soil engineering*. New York: Ronald Press.

Kalantary, F., & Kordnaeij, A. (2012). Prediction of compression index using artificial neural network. *Scientific Research and Essays, 7*(31), 2835-2848. doi:10.5897/SRE12.297

Koppula, S. (1981). Statistical Estimation of Compression Index. *Geotechnical Testing Journal, 4*(2), 68-73. doi:10.1520/GTJ10768J

Kulhawy, F. H., & Mayne, P. W. (1990). *Manual on Estimating Soil Properties for Foundation Design.* (Project 1493-6). Retrieved from Palo Alto, California:

Leu, S. S., Chen, C. N., & Chang, S. L. (2001). Data Mining for Tunnel Support Stability: Neural Network Approach. *Automation in Construction, 10*(4), 429-441.

Mayne, P. (2006). *Invited overview paper: In-situ test calibrations for evaluating soil parameters* (Vol. 3). London: Taylor & Francis Group.

Mayne, P. W. (1980). Cam-clay predictions of undrained strength. *J. Geotech. Eng. Div., 106*(11), 1219-1242.

McClelland, B. (1967). *Progress of consolidation in delta front and pro delta clays on the Mississippi River*. Retrieved from Champaign, IL. :

Melhem, H. G., & Cheng, Y. (2003). Prediction of Remaining Service Life of Bridge Decks Using Machine Learning. *Journal of Computing in Civil Engineering, 17*(1), 1-9.

Mesri, G. (1986). Discussion of 'Post construction settlement of an expressway built on peat by precompression'. *Canadian Geotechnical Journal, 23*(3), 403-407.

Mesri, G., Feng, T. W., & Benak, J. M. (1990). Postdensification Penetration Resistance of Clean Sands. *Journal of Geotechnical Engineering, 116*(7), 1095-1115. doi:10.1061/(ASCE)0733-9410(1990)116:7(1095)

Mesri, G., & Godlewski, P. M. (1977). Time and stress-compressibility interrelationship. *ASCE J. Geotech Eng. Div., 103*(5), 417-430.

Miyakawa, I. (1960). *Some aspects of road construction in peaty or marshy areas in Hokkaido*. Sapporo, Japan (text in Japanese): Hokkaido Development Bureau, Civil Engineering Research Institute.

Nakase, A., Kamei, T., & Kusakabe, O. (1988). Constitutive Parameters Estimated by Plasticity Index. *Journal of Geotechnical Engineering, 114*(7). doi:10.1061/(ASCE)0733-9410(1988)114:7(844)

Narasimha, R. P., Pandian, N., & Nagaraj, T. (1995). Analysis and Estimation of the Coefficient of Consolidation. *Geotechnical Testing Journal, 18*(2), 252-258. doi:10.1520/GTJ10325J

NAVFAC. (1982). *Design Manual: Soil Mechanics, Foundations, and Earth Structures*. Retrieved from Washington, D.C.:

Nishida, Y. (1956). A brief note on compression index of soil. *J. Soil Mech. Found. Div., 82*(3), 1-14.

Ozer, M., Isik, N. S., & Orhan, M. (2008). Statistical and neural network assessment of the compression index of clay-bearing soils. *Bulletin of Engineering Geology and the Environment, 67*(4), 537-545. doi:10.1007/s10064-008-0168-8

Panagopoulos, A. A., Alam, M., Rogers, A., & Jennings, N. R. (2015). *AdaHeat: A General Adaptive Intelligent Agent for Domestic Heating Control*. Paper presented at the 2015 International Conference on Autonomous Agents and Multiagent Systems, Istanbul, Turkey.

Panagopoulos, A. A., Jennings, N. R., Maleki, S., Rogers, A., & Venanzi, M. (2017). Advanced Economic Control of Electricity-Based Space Heating Systems in Domestic Coalitions with Shared Intermittent Energy Resources. *ACM Transactions on Intelligent Systems and Technology (TIST), 8*(4), 1-27. doi:10.1145/3041216

Panagopoulos, O. P., Pappu, V., Xanthopoulos, P., & Pardalos, P. M. (2016). Constrained Subspace Classifier for High Dimensional Datasets. *Omega, 59*(A), 40-46.

Pappu, V., Panagopoulos, O. P., Xanthopoulos, P., & Pardalos, P. M. (2015). Sparse Proximal Support Vector Machines for Feature Selection in High Dimensional Datasets. *Expert systems with Applications, 42*(23), 9183-9191.

Park, H., & Seung, R. L. (2011). Evaluation of the compression index of soils using an artificial neural network. *Computers and Geotechnics, 38*(4), 472-481. doi:10.1016/j.compgeo.2011.02.011

Peck, R. B., & Reed, W. C. (1954). *Engineering properties of Chicago subsoils*. Urbana, IL.: Engineering Experiment Station, Univ. of Illinois.

Rendon-Herrero, O. (1980). Universal Compression Index Equation. *Journal of Geotechnical Engineering Division, ASCE, GT11*, 1179-1199.

Robertson, P. K. (1990). Soil classification using the cone penetration test. *Canadian Geotechnical Journal, 27*(1), 151-158. doi:10.1139/t90-014

Robertson, P. K. (2009). Interpretation of cone penetration tests — a unified approach. *Canadian Geotechnical Journal, 46*(11), 1337-1355. doi:10.1139/T09-065

Robertson, P. K., & Wride, C. E. (1998). Evaluating cyclic liquefaction potential using the cone penetration test. *Canadian Geotechnical Journal, 35*(3), 442-459. doi:10.1139/t98-017

Sabatini, P. J., Bachus, R. C., Mayne, P. W., Schneider, J. A., & T.E., Z. (2002). *Evaluation of Soil and Rock Properties* (FHWA-IF-02-034). Retrieved from Washington, DC:

Samtani, N. C., & Nowatzki, E. A. (2006). *Soils and Foundations Reference Manual - Volume II* (FHWA-NHI–06-089). Retrieved from

Sanglerat, G. (1972). *The Penetrometer and Soil Exploration: Interpretation of Penetration Diagrams - Theory and Practice*: Elsevier.

Simons, & Menzies. (2000). *A Short Course in Foundation Engineering* (2nd ed. Vol. 2nd). London: Thomas Telford

Solanki, A. (2011). A Study on Consolidation and Correlation with Index Properties of Different Soils in Surat City. *International Journal of Engineering Research and Development, 11*(5), 57-63.

Sou-Sen, L., & Hsien-Chuang, L. (2004). Neural-Network-Based Regression Model of Ground Surface Settlement Induced by Deep Excavation. *Automation in Construction, 13*(3), 279-289.

Sowers, G. F., & Sowers, G. B. (1979). *Introductory soil mechanics and foundations* (4th ed.). Macmillan: New York.

Sridharan, A., & Nagaraj, H. (2004). Coefficient of Consolidation and its Correlation with Index Properties of Remolded Soils. *Geotechnical Testing Journal, 27*(5). doi:10.1520/GTJ10784

Teng, W. C. (1962). *Foundation Design*. Englewood Cliffs, NJ: Prentice-Hall, Inc. .

Terzaghi, K. (1925). *Erdbaumechanik auf Bodenphysikalischer Grundlager*. Deuticke, Vienna: Leipzig u. Wien, F.

Terzaghi, K., & Peck, R. B. (1967). *Soil mechanics in engineering practice*: Wiley.

US Navy. (1971). *Soil Mechanics, Foundations, and Earth Structures*. Retrieved from

Vesić, A. (1972). Expansion of Cavities in Infinite Soil Mass. *Journal of the Soil Mechanics and Foundations Division, Vol. 98*(3), 265-290.

Wroth, C. P., & Wood, D. M. (1978). The Correlation of Index Properties with some Basic Engineering Properties of Soils. *Canadian Geotechnical Journal, 15*(2), 137-145.

Yoon, G. L., & Kim, B. T. (2006). Regression Analysis of Compression Index for Kwangyang Marine Clay. *KSCE Journal of Civil Engineering, 10*(6), 415-418.

APPENDIX A: CPTu AND DISSIPATION TEST RESULTS

SOUNDING

SOUNDING
CUSTOMER: State Materials Office
OPERATOR: tsb
CONE ID: DSA1184
LOCATION:

JOB NUMBER: Sr-100-A Starke
HOLE NUMBER: cpt# 1
TEST DATE: 5/29/2019 8:10:58 AM
COMMENT: Auto Enhance On
COMMENT: Filter On

COMMENT:
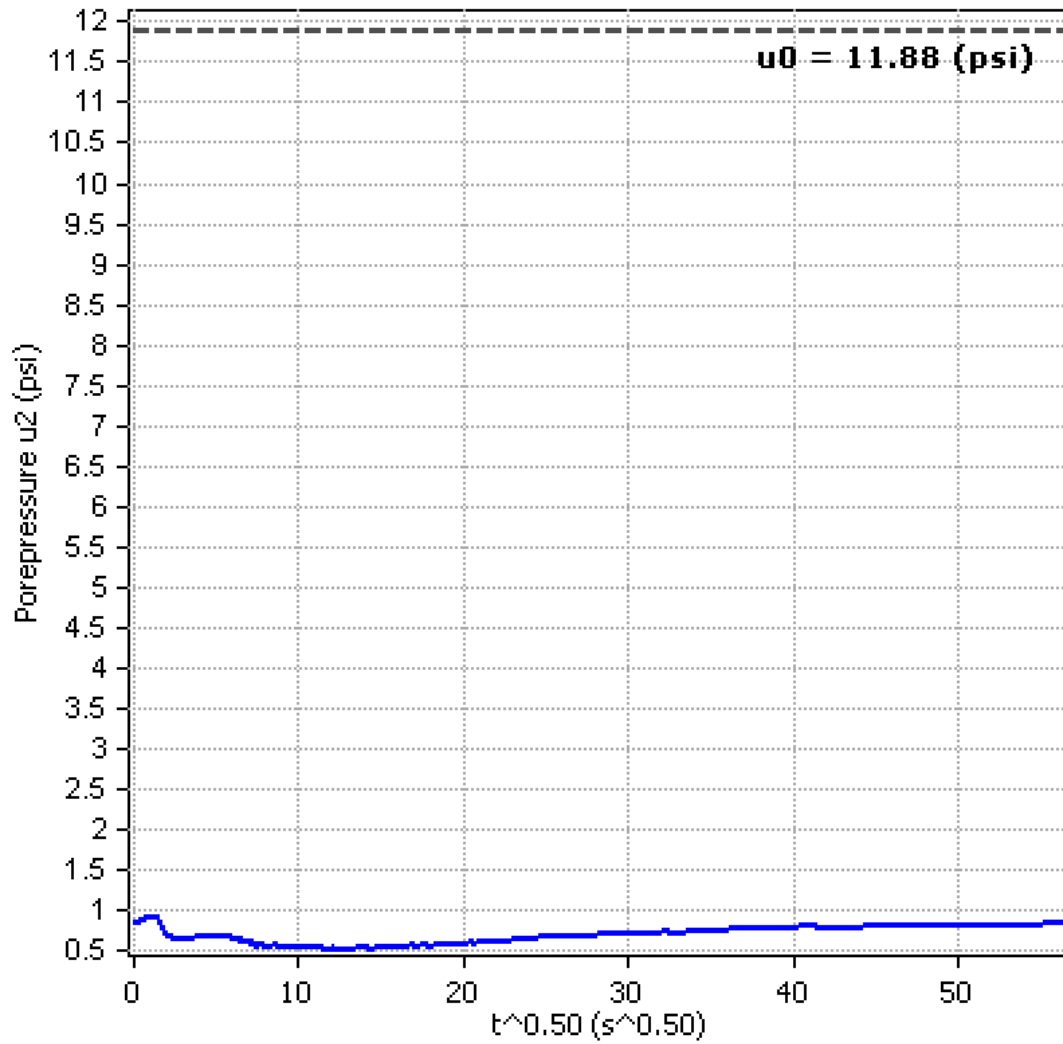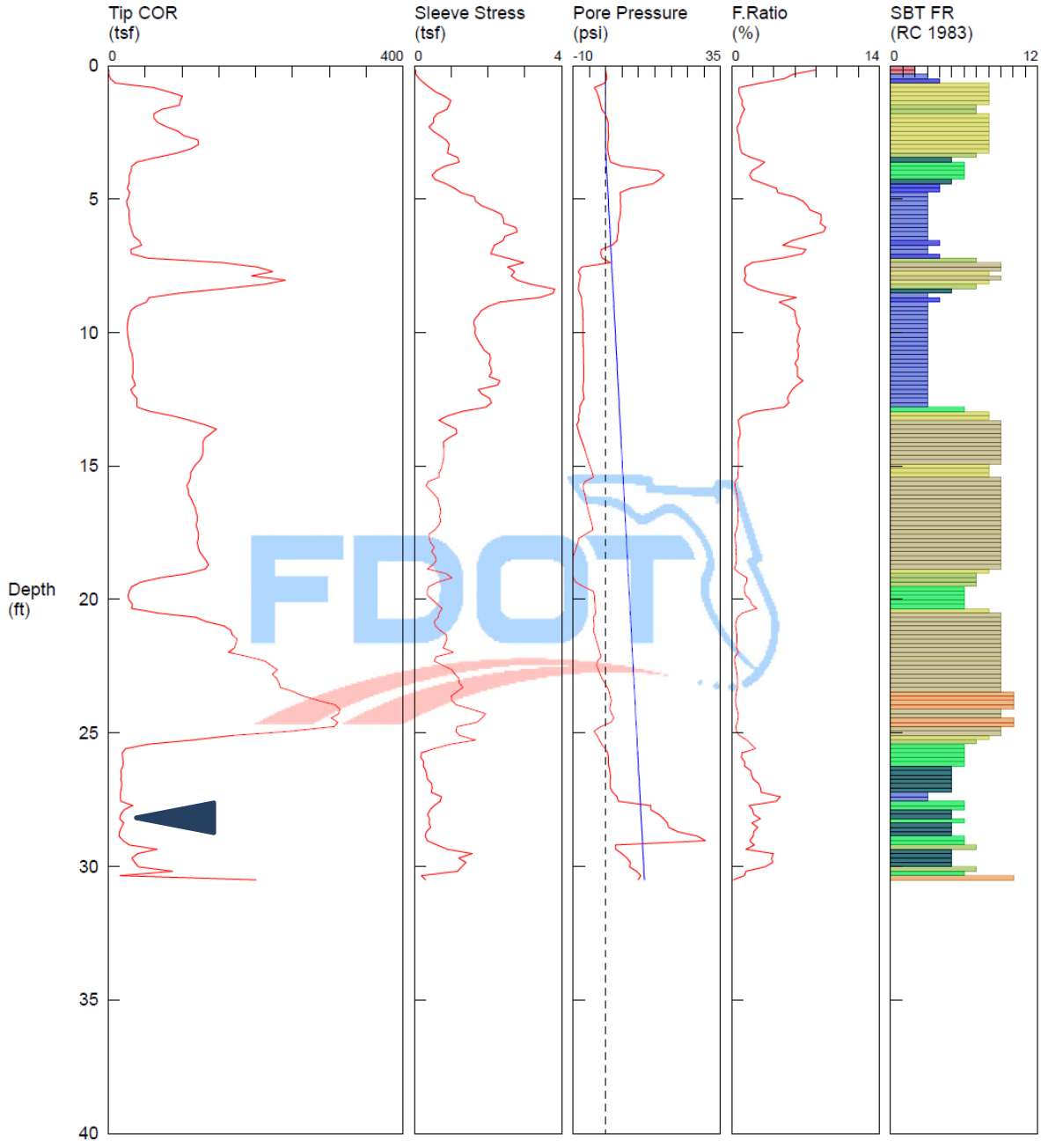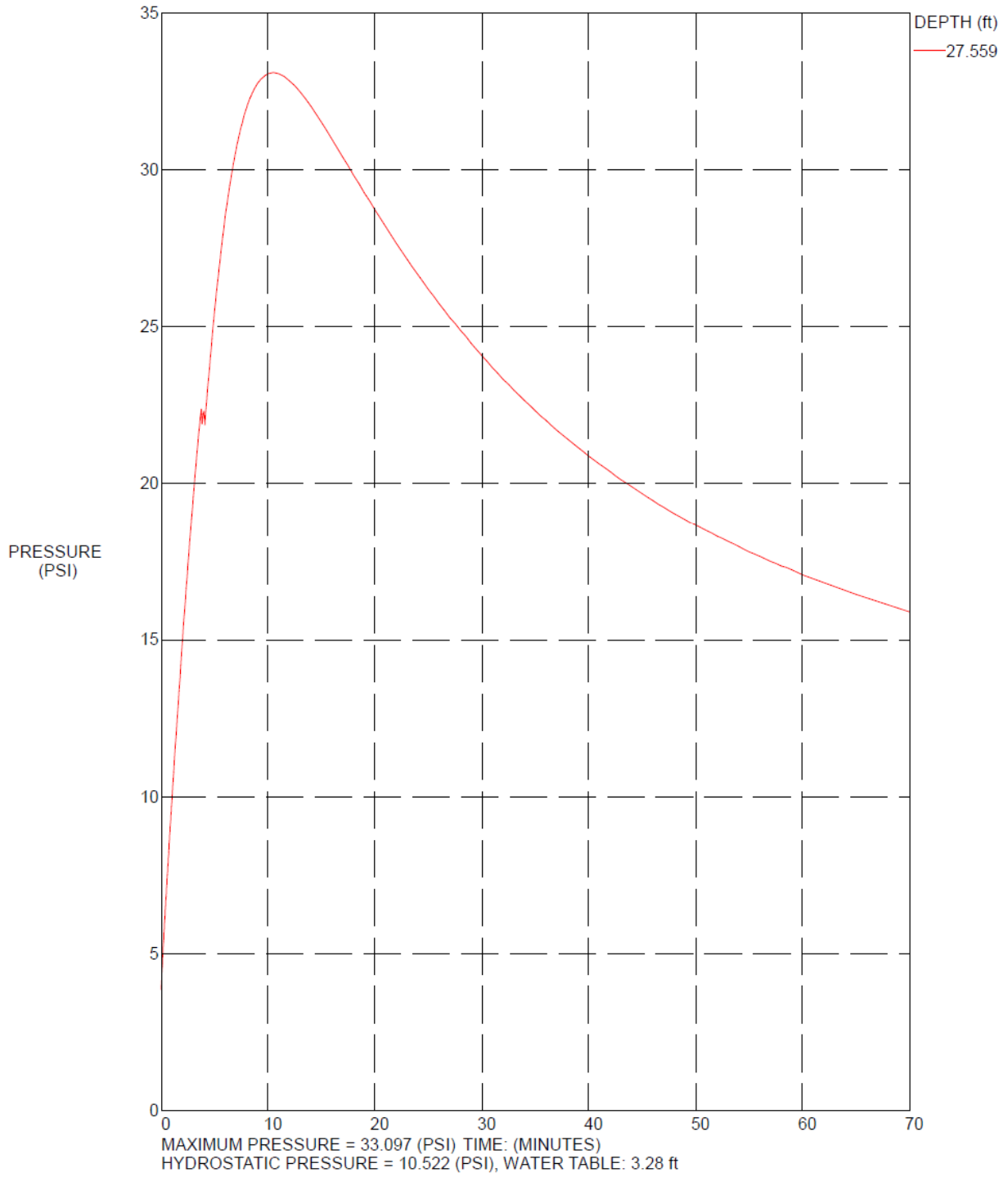GPS (LAT,LON,ALT): 0.00,0.00,0.0
LOCATION:
LOCATION:
LOCATION:
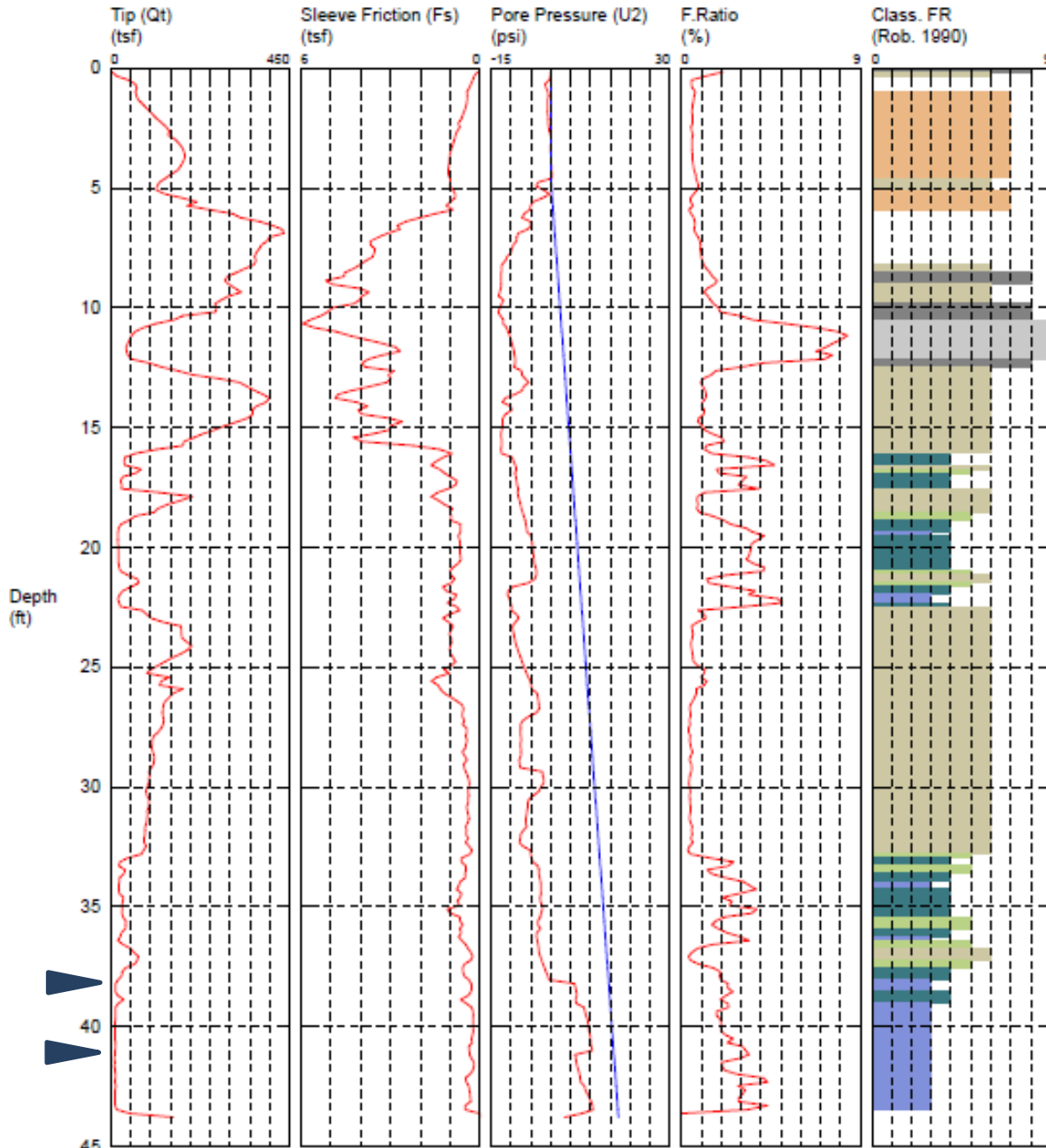
Depth of dissipation test

1 Sensitive, fine grained	**4** Silt mixtures - clayey silt to silty clay	**7** Gravelly sand to sand
2 Organic soils - peats	**5** Sand mixtures - silty sand to sandy silt	**8** Very stiff sand to clayey sand **
3 Clays - clay to silty clay	**6** Sands - clean sand to silty sand	**9** Very stiff, fine grained **

*SBT: Robertson 1990; **Overconsolidated or Cemented; *SBT/SPT CORRELATION: UBC-1983

MAXIMUM PRESSURE = 5.689 (PSI)   TIME: (MINUTES)
HYDROSTATIC PRESSURE = 14.503 (PSI), WATER TABLE: 4.59 ft
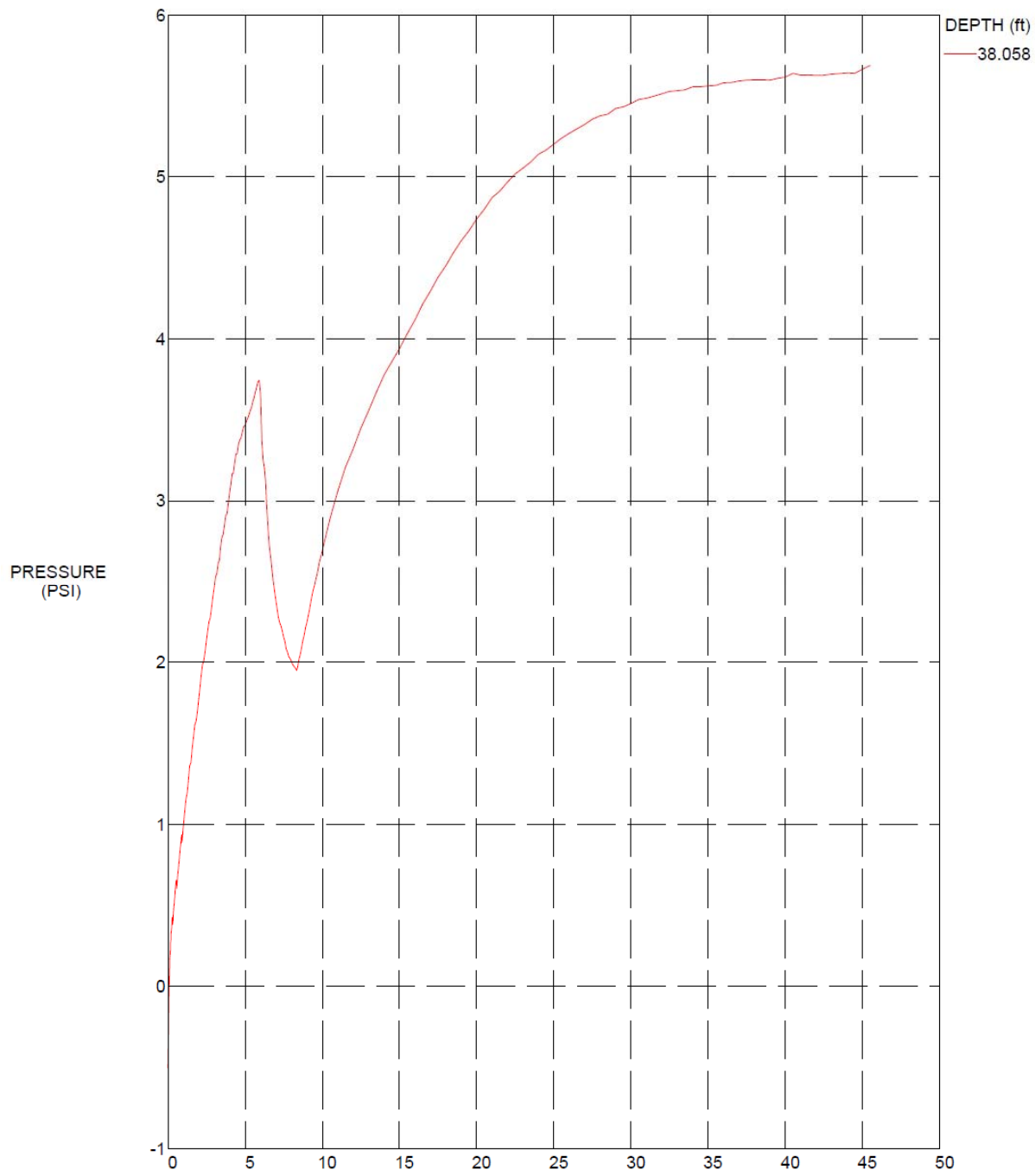
**SR-100A-Starke
CPT#1
Depth = 38ft**
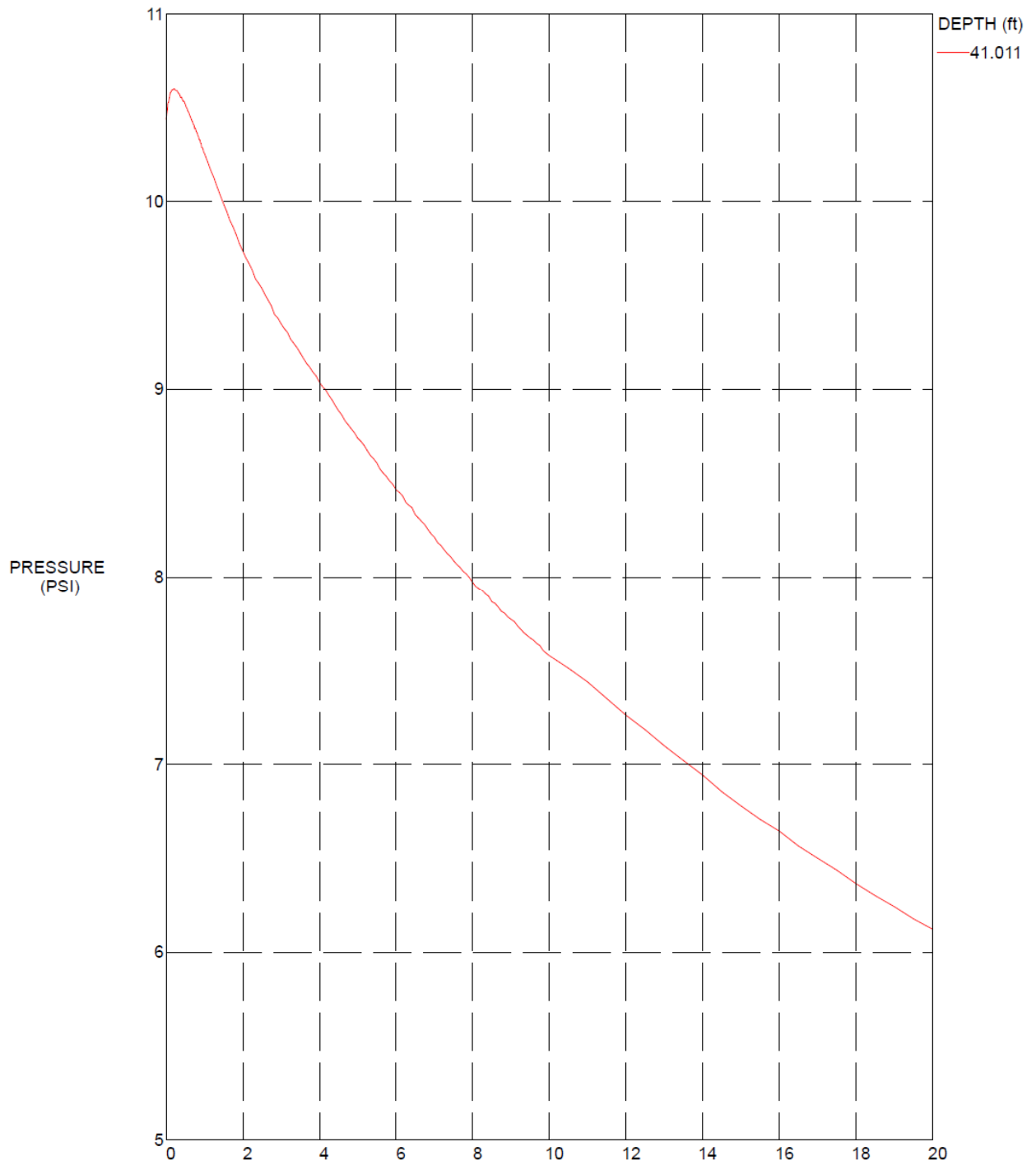
MAXIMUM PRESSURE = 10.601 (PSI) TIME: (MINUTES)
HYDROSTATIC PRESSURE = 15.783 (PSI), WATER TABLE: 4.59 ft

SR-100A-Starke
CPT#1
Depth = 41 ft

SOUNDING

▷ Depth of dissipation test

1 sensitive fine grained	4 silty clay to clay	7 silty sand to sandy silt	10 gravelly sand to sand
2 organic material	5 clayey silt to silty clay	8 sand to silty sand	11 very stiff fine grained (*)
3 clay	6 sandy silt to clayey silt	9 sand	12 sand to clayey sand (*)

*SBT/SPT CORRELATION: UBC-1983

86

Piezocone Dissipation Test: SR-100 PCPT2a data
Depth: 30.68 (ft)

u0 = 11.88 (psi)

Porepressure u2 (psi) vs *t^0.50 (s^0.50)*

SR-100A-Starke
CPT#2a
Depth = 30.68ft

SOUNDING

SOUNDING
CUSTOMER: State Materials Office
OPERATOR: tsb
CONE ID: DSA1184
LOCATION:

JOB NUMBER: SR-100
HOLE NUMBER: cpt# 3
TEST DATE: 9/27/2018 12:58:03 PM
COMMENT: Auto Enhance On
COMMENT: Filter On

COMMENT:
GPS (LAT,LON,ALT): 0.00,0.00,0.0
LOCATION:
LOCATION:
LOCATION:

▶ Depth of dissipation test

🟥 1	sensitive fine grained	🟦 4	silty clay to clay	🟩 7	silty sand to sandy silt	🟧 10	gravelly sand to sand
🟥 2	organic material	🟦 5	clayey silt to silty clay	🟨 8	sand to silty sand	⬜ 11	very stiff fine grained (*)
🟦 3	clay	🟩 6	sandy silt to clayey silt	🟨 9	sand	⬛ 12	sand to clayey sand (*)

*SBT/SPT CORRELATION: UBC-1983

MAXIMUM PRESSURE = 33.097 (PSI) TIME: (MINUTES)
HYDROSTATIC PRESSURE = 10.522 (PSI), WATER TABLE: 3.28 ft

SR100-Starke
CPT#3
Depth = 27.56 ft

Wekiva SR46 East
CPT#1 (TB10)

State Materials Office

Operator: tsb
Sounding: cpt# 1
Cone Used: DSA1173

CPT Date/Time: 2/19/2019 10:29:44 AM
Location: 30' west of bent 34
Job Number: WEKIVA

Depth of dissipation test

90
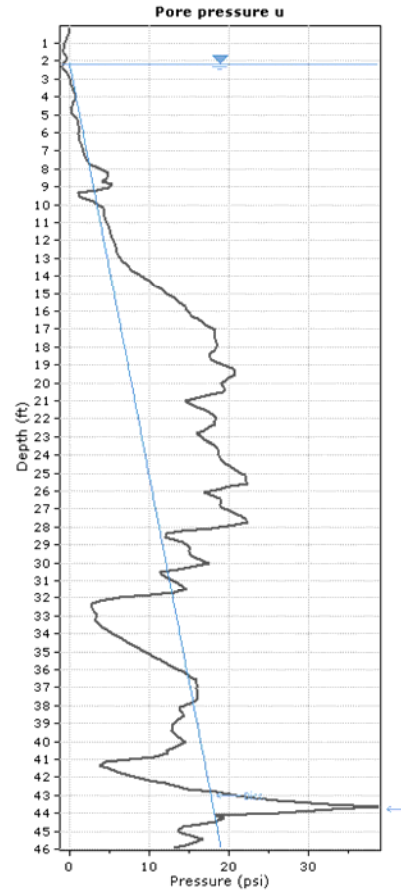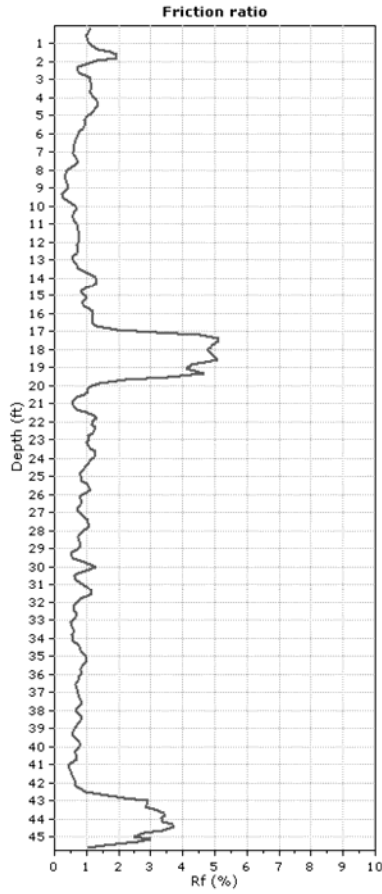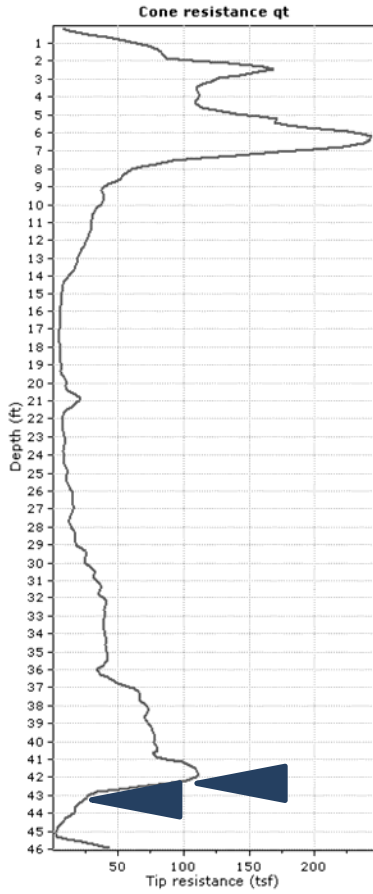
Piezocone Dissipation Test: CPT_TB-10_WekivaEAST
Depth: 42.98 (ft)

u0 = 17.68 (psi)
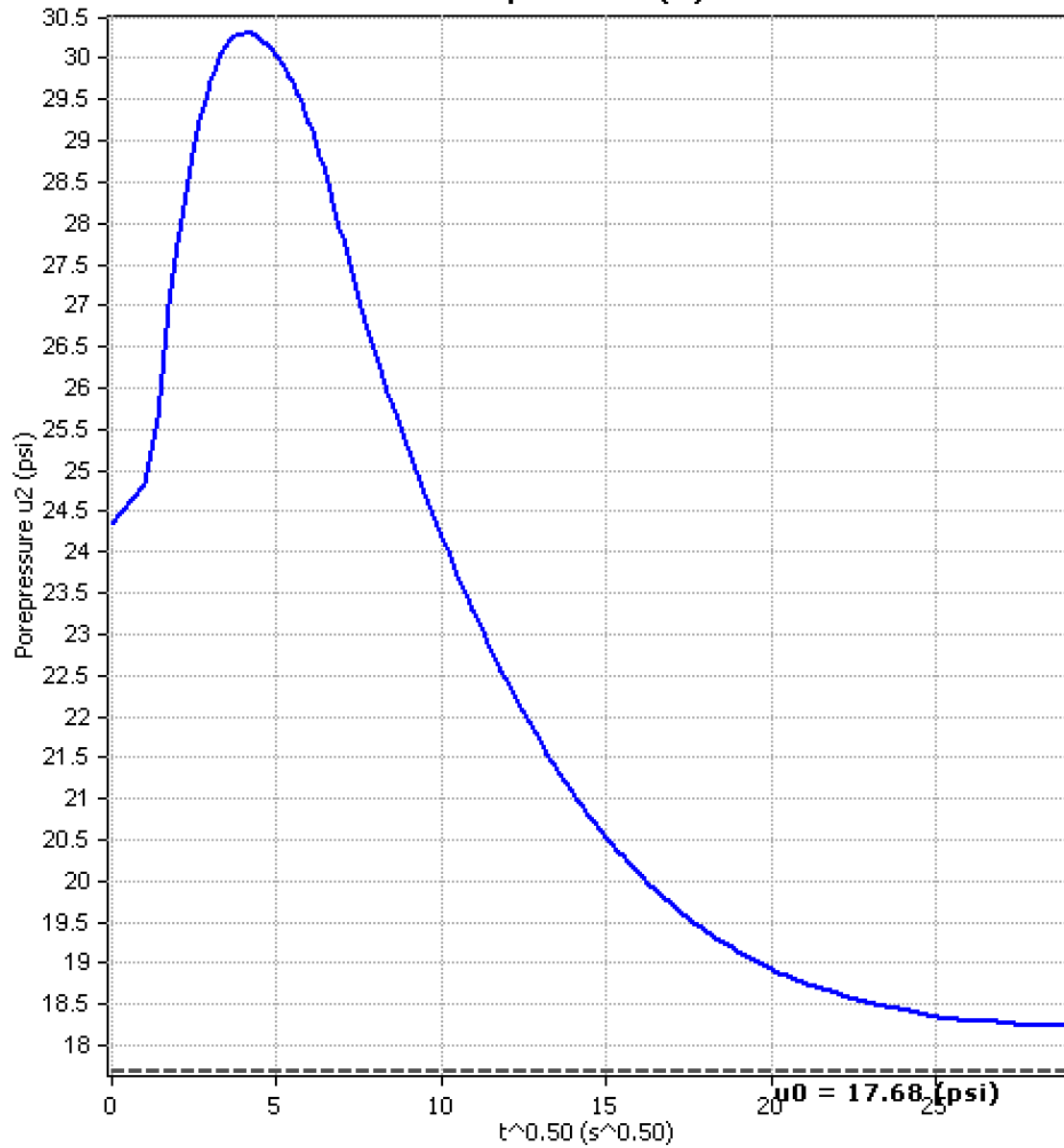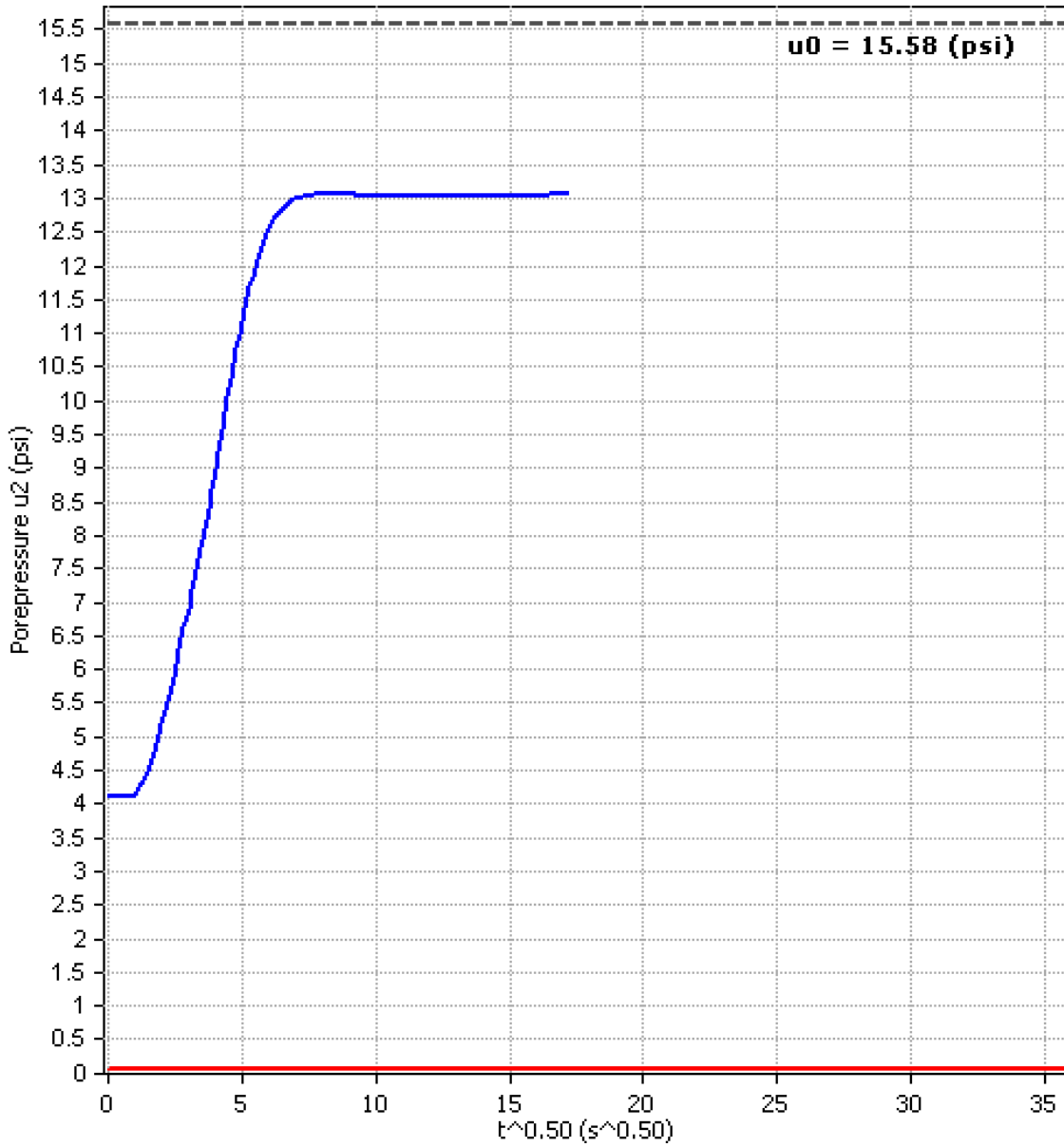
WekivaSR46 East
CPT#1 (TB-10)
Depth = 43.98 ft

Piezocone Dissipation Test: CPT_TB-10_WekivaEAST
Depth: 43.80 (ft)
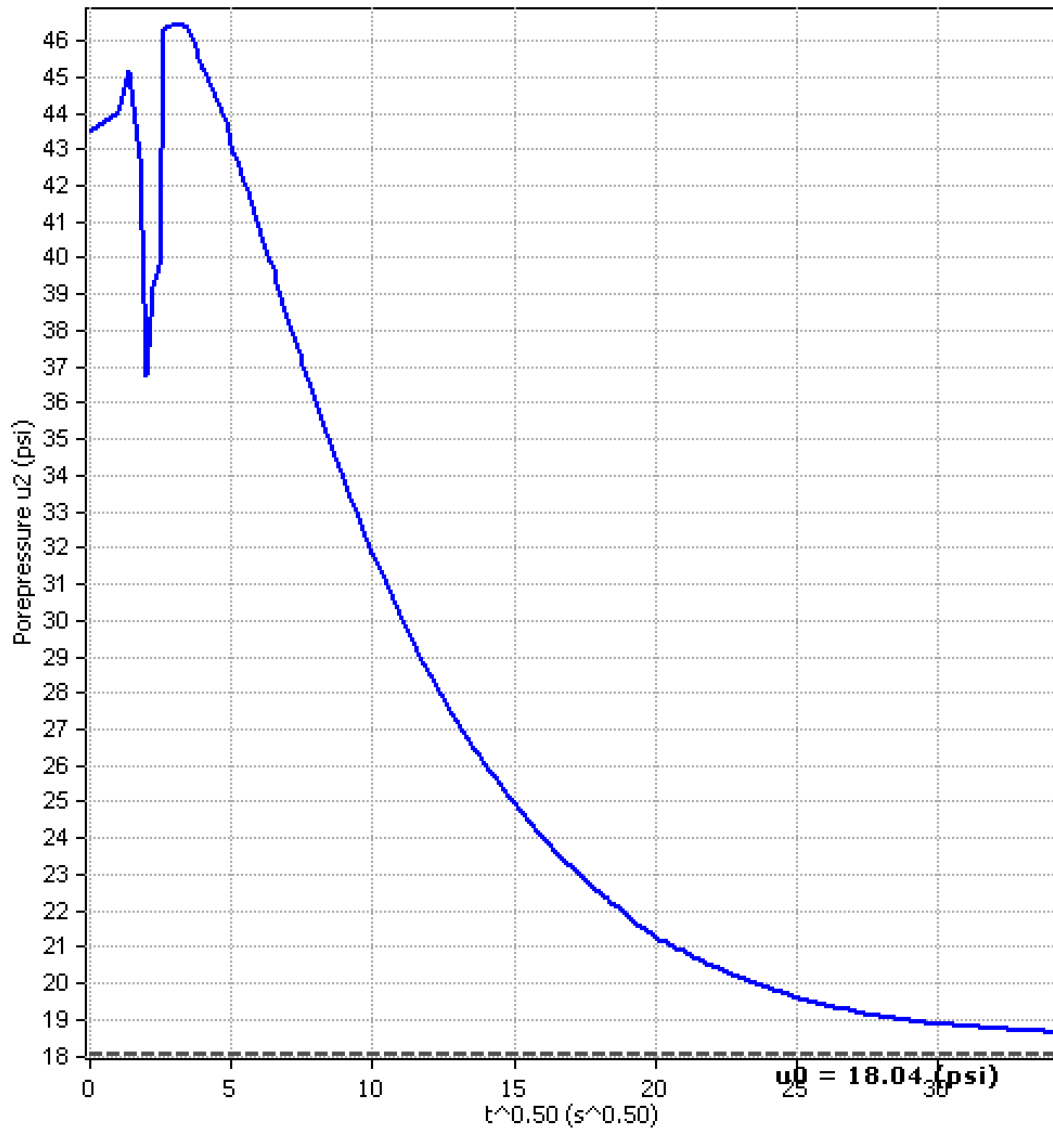
WekivaSR46 East
CPT#1 (TB-10)
Depth = 43.80 ft

**Wekiva SR46 East
CPT#2 (TB-12)**

State Materials Office

Operator: tsb
Sounding: cpt# 2
Cone Used: DSA1173

CPT Date/Time: 2/19/2019 12:22:57 PM
Location:
Job Number: WEKIVA

Tip Resistance	Local Friction	Pore Pressure	Friction Ratio	Soil Behavior Type*
Qt TSF	Fs TSF	Pw PSI	Fs/Qt (%)	Zone: UBC-1983
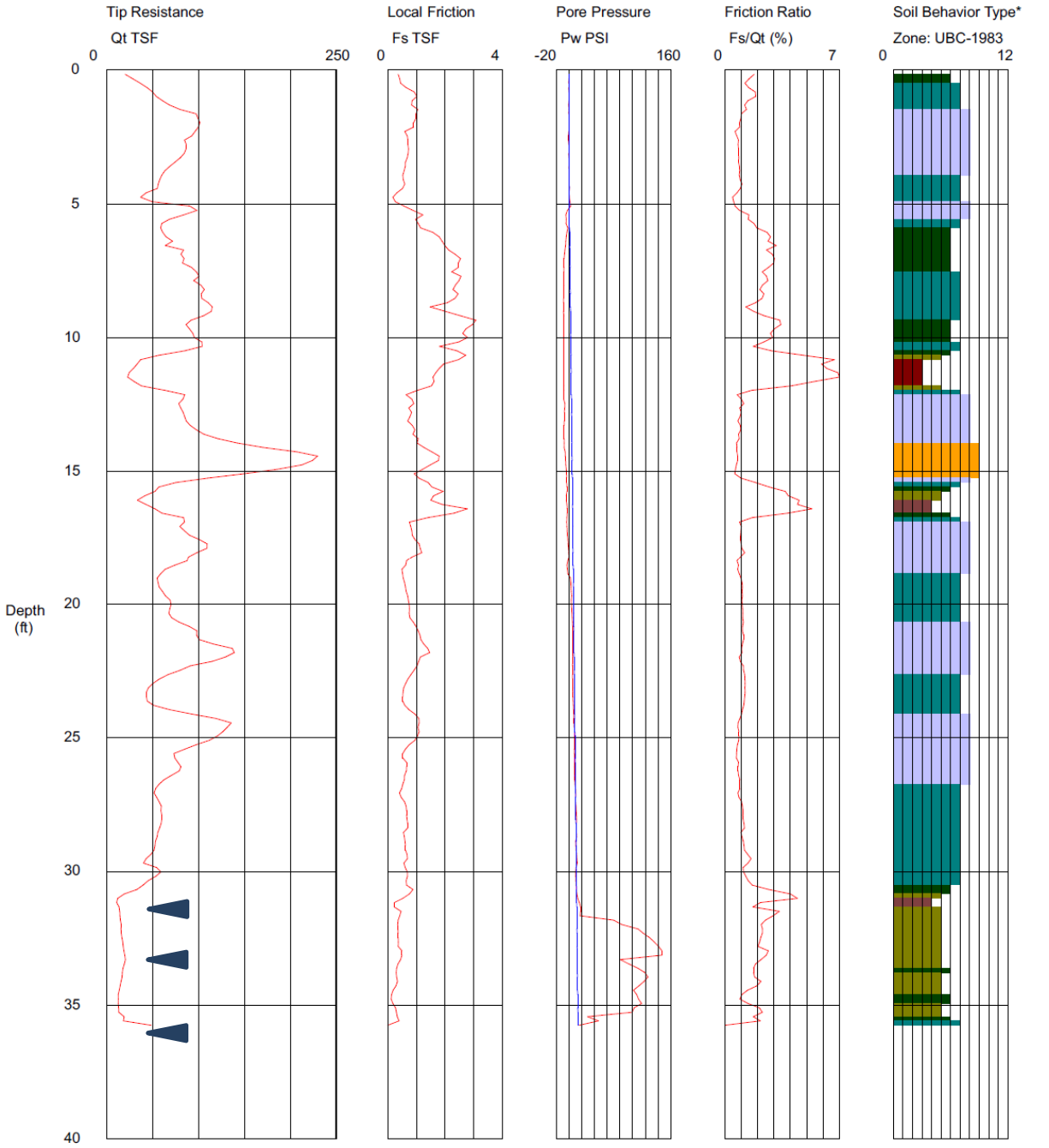
Maximum Depth = 35.76 feet

Depth Increment = 0.164 feet

▢ 1 sensitive fine grained	▢ 4 silty clay to clay	▢ 7 silty sand to sandy silt	▢ 10 gravelly sand to sand
▢ 2 organic material	▢ 5 clayey silt to silty clay	▢ 8 sand to silty sand	▢ 11 very stiff fine grained (*)
▢ 3 clay	▢ 6 sandy silt to clayey silt	▢ 9 sand	▢ 12 sand to clayey sand (*)

Filter On

Soil behavior type and SPT based on data from UBC-1983

► Depth of dissipation test

93
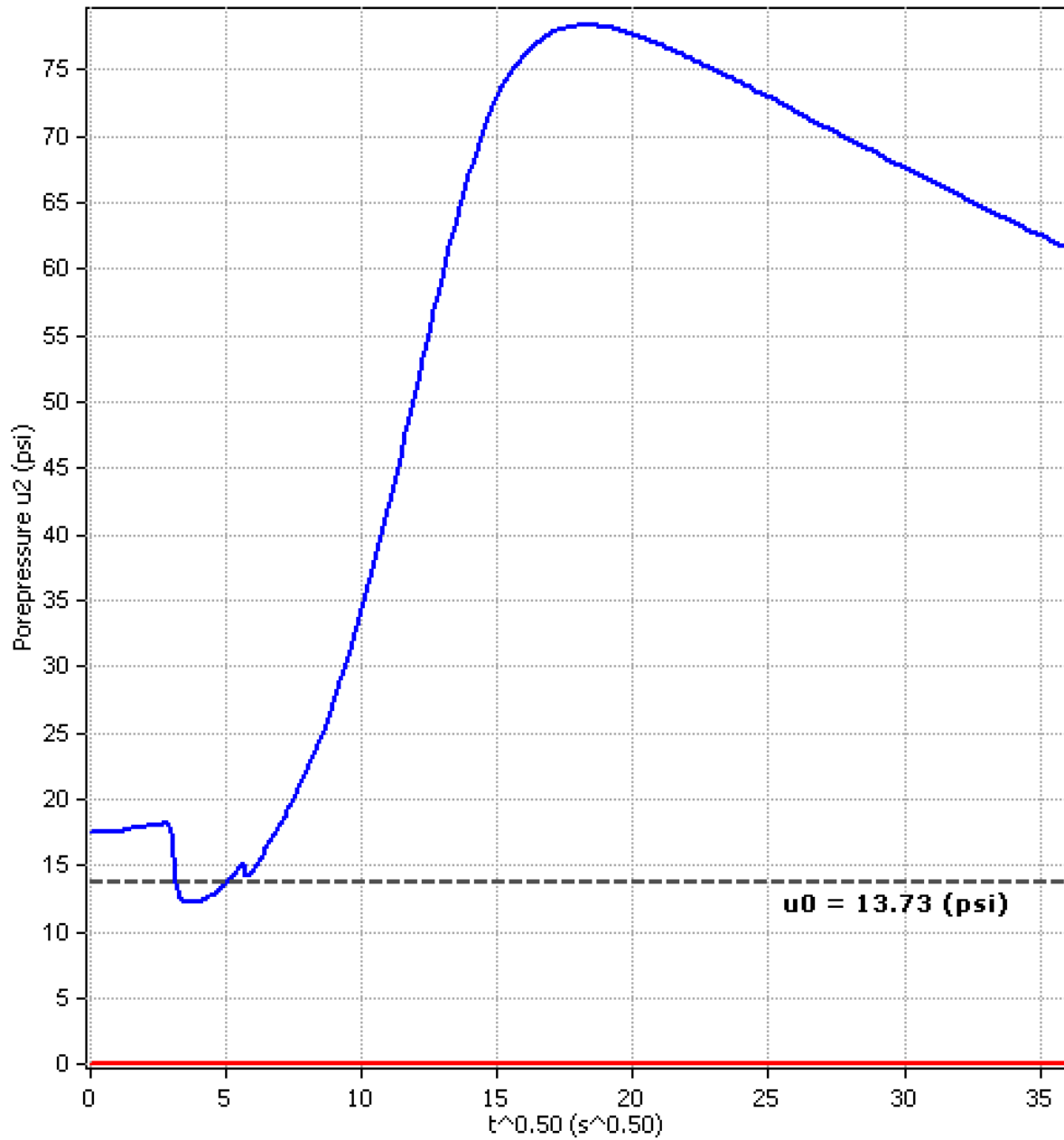
WekivaSR46 East
CPT#2 (TB-12)
Depth = 31.66 ft

Piezocone Dissipation Test: CPT_TB-12_WekivaEAST
Depth: 33.14 (ft)

u0 = 14.37 (psi)
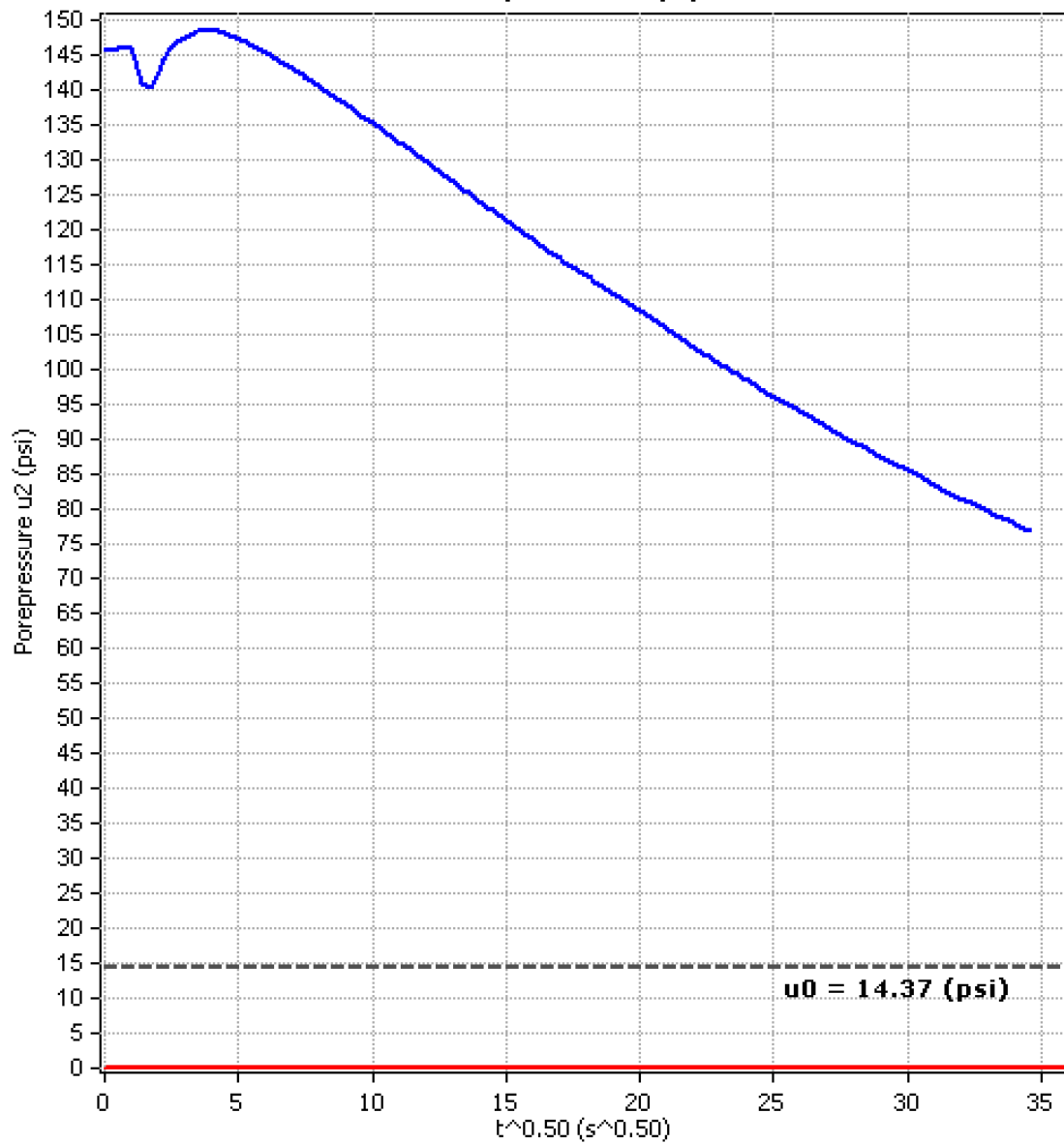
WekivaSR46 East
CPT#2 (TB-12)
Depth = 33.14 ft

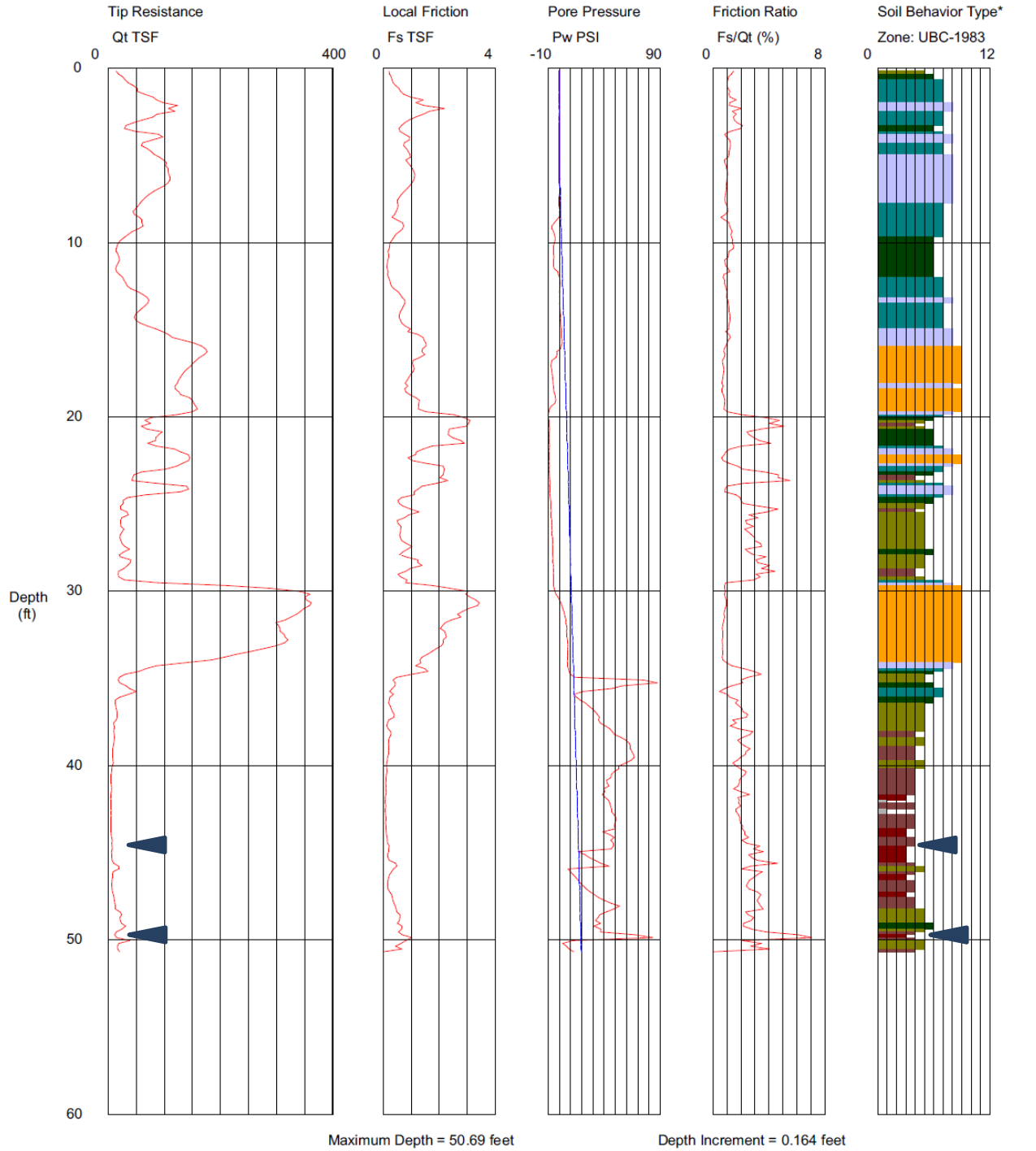**Piezocone Dissipation Test: CPT_TB-12_WekivaEAST**
Depth: 35.93 (ft)

u0 = 15.58 (psi)

Porepressure u2 (psi)

t^0.50 (s^0.50)

WekivaSR46 East
CPT#2 (TB-12)
Depth = 35.93ft

Wekiva SR46 East
CPT#3 (TB-1)

Operator: tsb
Sounding: cpt# 3
Cone Used: DSA1173

CPT Date/Time: 2/19/2019 2:11:40 PM
Location:
Job Number: WEKIVA

Tip Resistance	Local Friction	Pore Pressure	Friction Ratio	Soil Behavior Type*
Qt TSF	Fs TSF	Pw PSI	Fs/Qt (%)	Zone: UBC-1983

Maximum Depth = 50.69 feet

Depth Increment = 0.164 feet

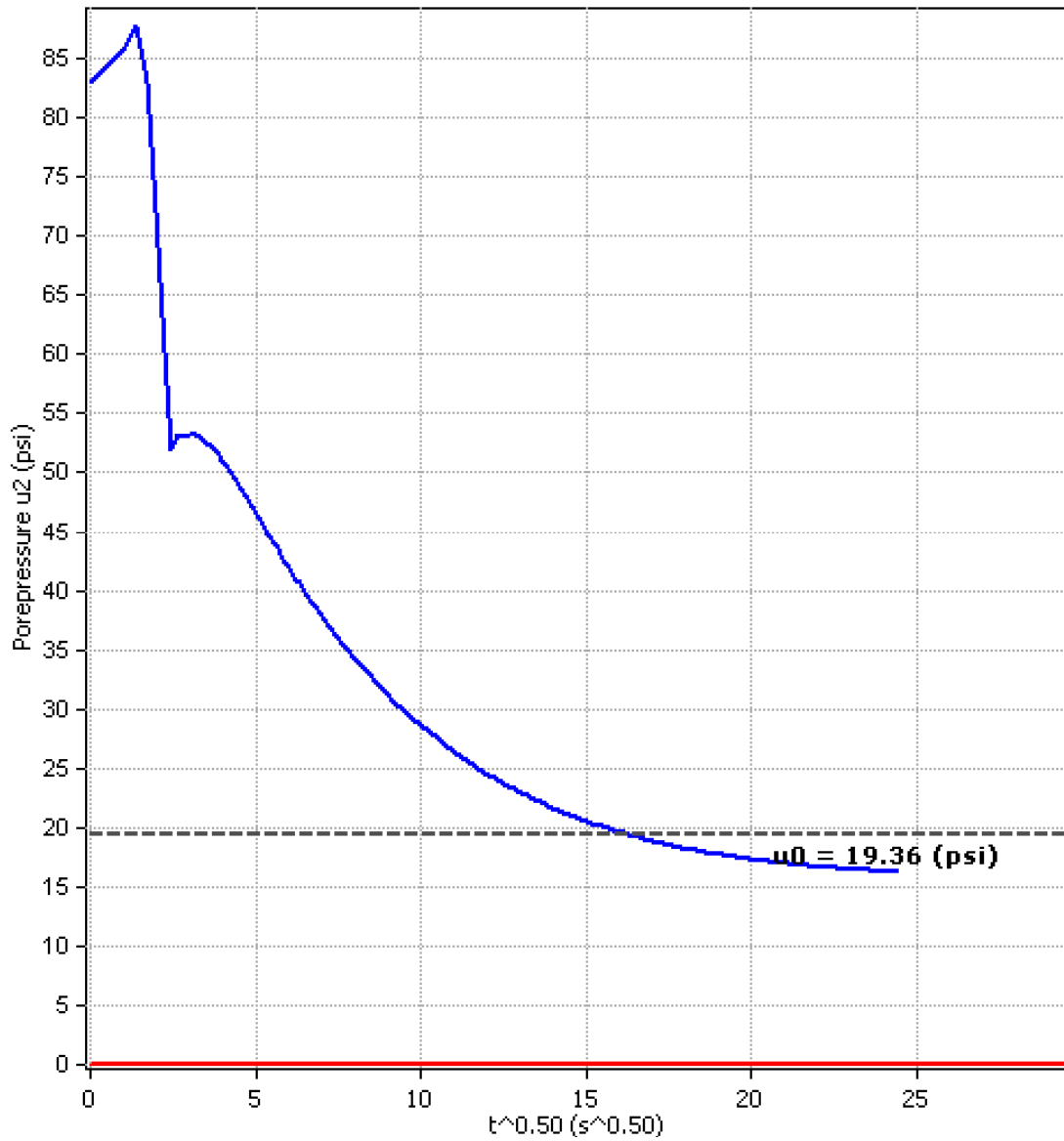|			
1 sensitive fine grained	4 silty clay to clay	7 silty sand to sandy silt	10 gravelly sand to sand
2 organic material	5 clayey silt to silty clay	8 sand to silty sand	11 very stiff fine grained (*)
3 clay	6 sandy silt to clayey silt	9 sand	12 sand to clayey sand (*)

Depth of dissipation test

97

Piezocone Dissipation Test: CPT_TB-1_WekivaEAST
Depth: 44.77 (ft)

u0 = 17.16 (psi)
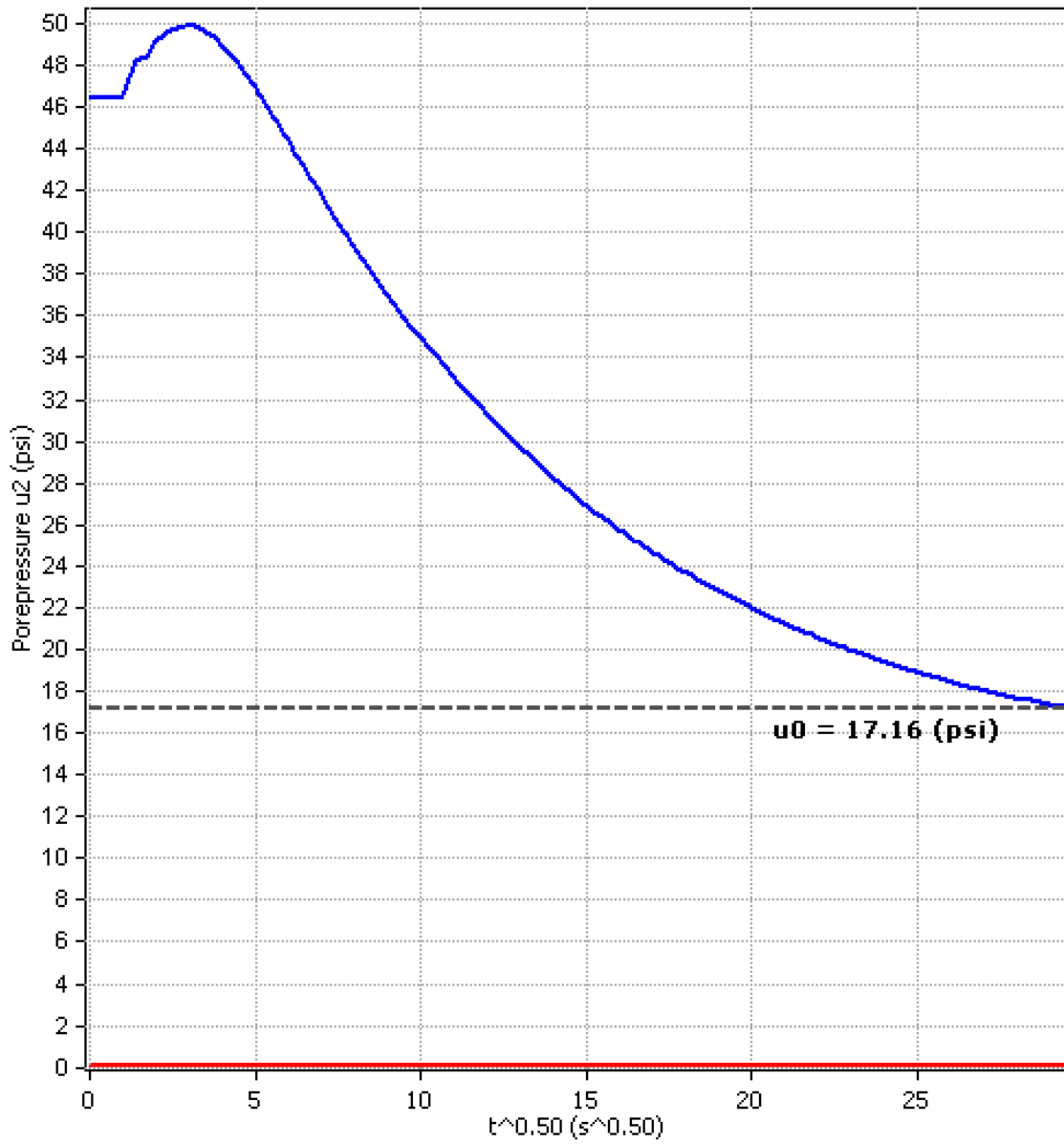
WekivaSR46 East
CPT#3 (TB-1)
Depth = 44.77 ft

Piezocone Dissipation Test: CPT_TB-1_WekivaEAST
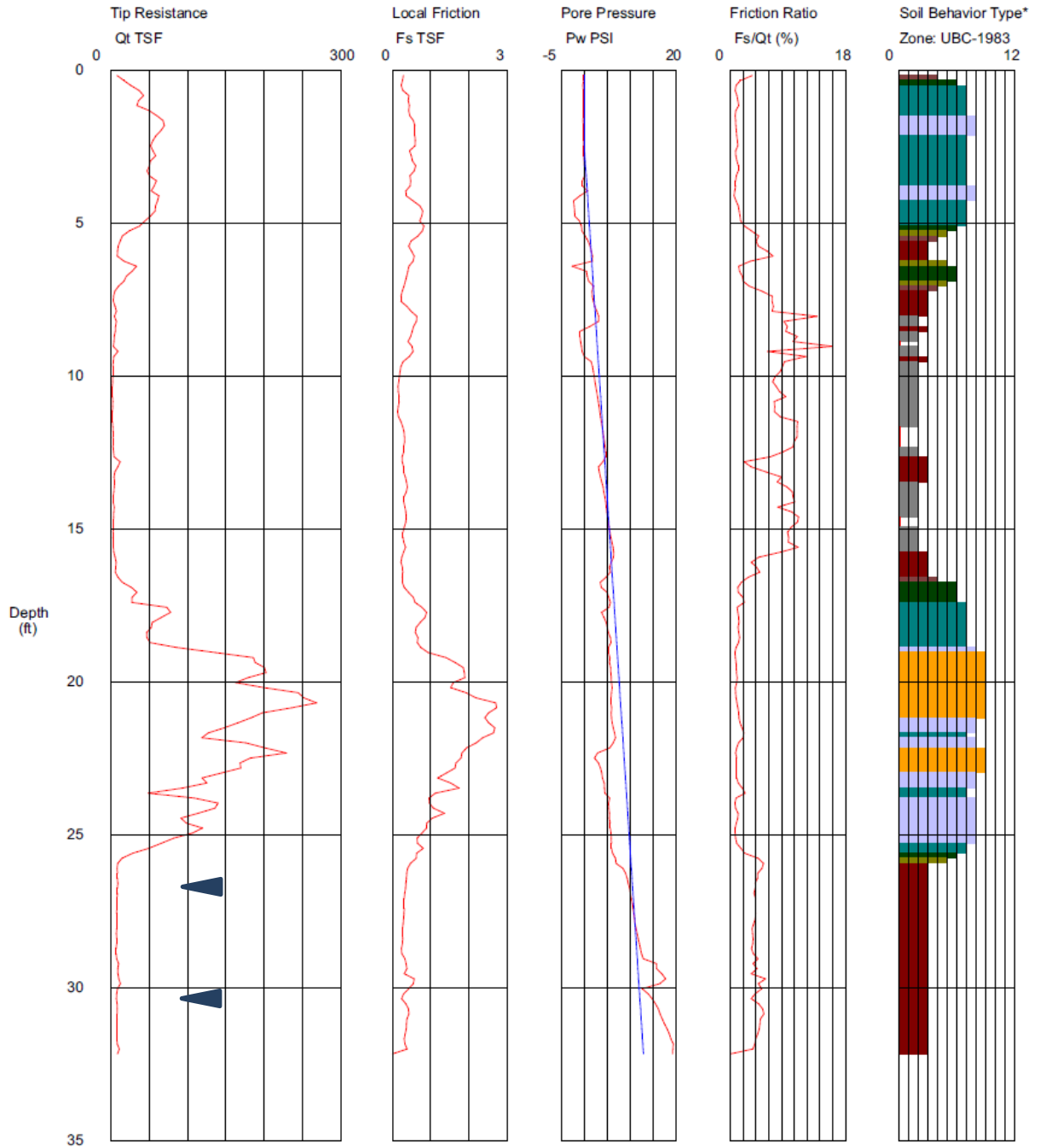Depth: 49.86 (ft)

WekivaSR46 East
CPT#3 (TB-1)
Depth = 49.86 ft

SR44 Near SJR
CPT#4 (WB-5)

State Materials Office

Operator: tsb
Sounding: cpt# 4
Cone Used: DSA1173

CPT Date/Time: 2/20/2019 9:00:38 AM
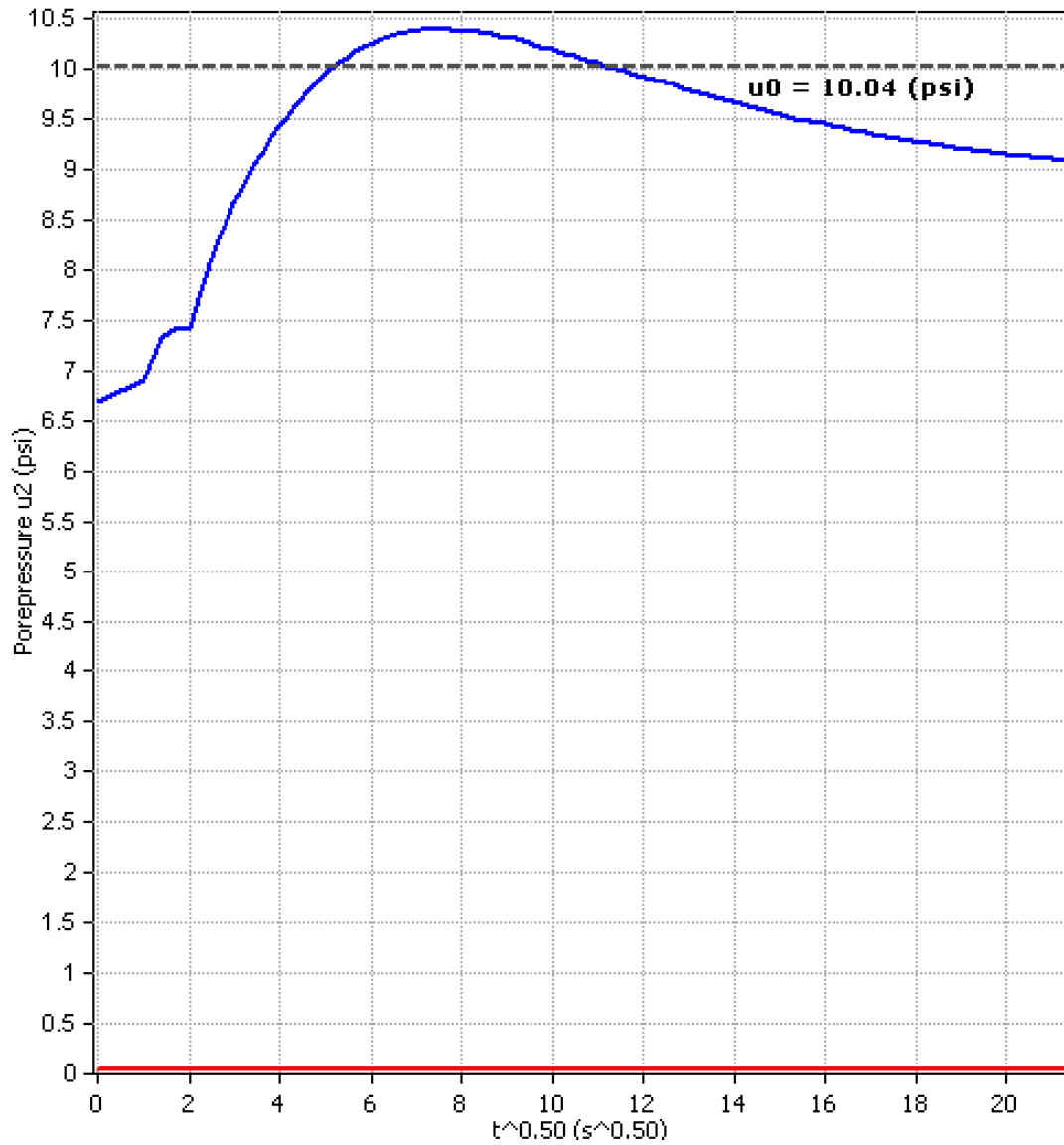Location:
Job Number: SR-44

Tip Resistance	Local Friction	Pore Pressure	Friction Ratio	Soil Behavior Type*
Qt TSF	Fs TSF	Pw PSI	Fs/Qt (%)	Zone: UBC-1983

Depth
(ft)

Maximum Depth = 32.15 feet   Depth Increment = 0.164 feet

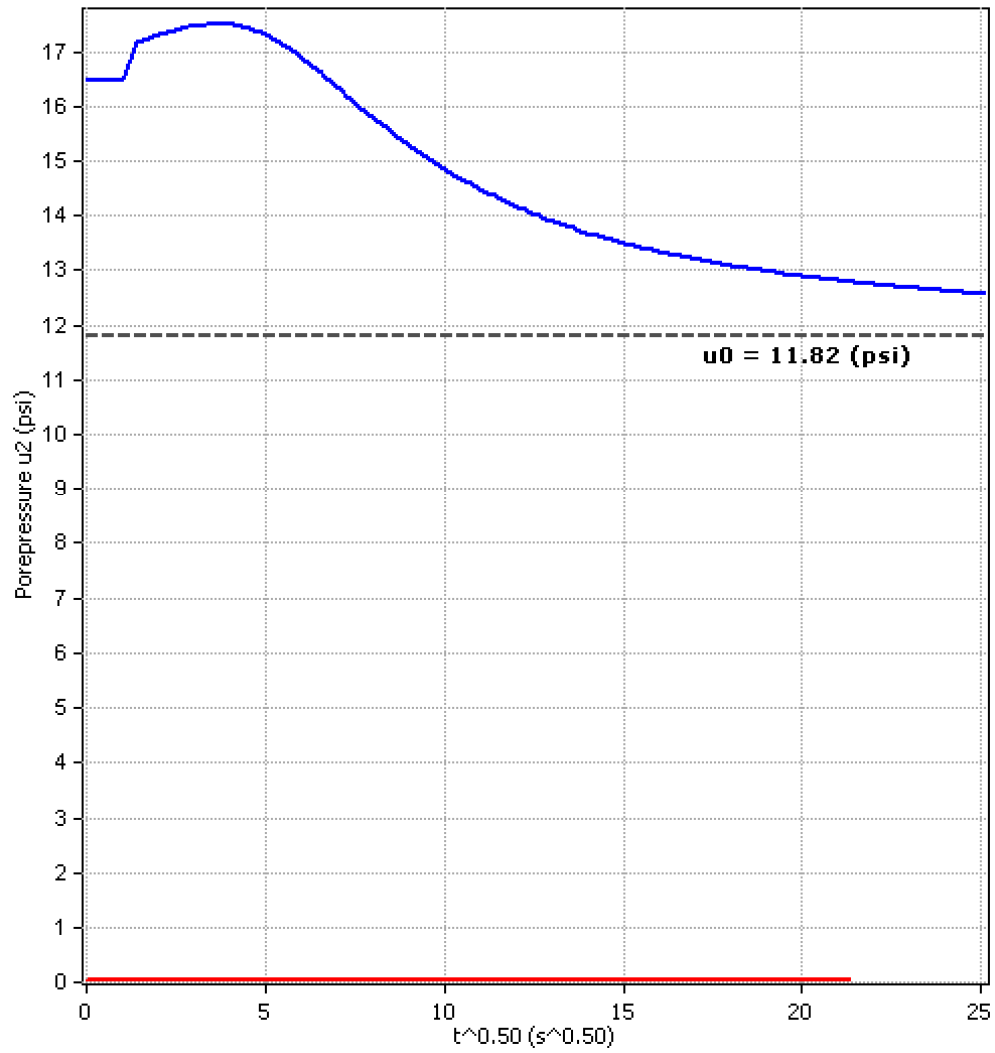|		
1 sensitive fine grained	4 silty clay to clay	7 silty sand to sandy silt	10 gravelly sand to sand
2 organic material	5 clayey silt to silty clay	8 sand to silty sand	11 very stiff fine grained (*)
3 clay	6 sandy silt to clayey silt	9 sand	12 sand to clayey sand (*)

Filter On

▶ Depth of dissipation test

100

Piezocone Dissipation Test: CPT_WB-5_SR44
Depth: 25.75 (ft)

u0 = 10.04 (psi)

Porepressure u2 (psi)

t^0.50 (s^0.50)

SR44 Near SJR
CPT#4 (WB-5)
Depth = 25.75 ft

Piezocone Dissipation Test: CPT_WB-5_SR44
Depth: 29.85 (ft)

u0 = 11.82 (psi)

SR44 Near SJR
CPT#4 (WB-5)
Depth = 29.85 ft